Non-centrosomal microtubule nucleation and organization in mitosis

Nicolas Lecland

Tesi doctoral UPF/2014

Director de la tesi**: Jens Lüders**, PhD

Cell & Developmental Biology Programme

Institute for Research in Biomedicine Barcelona

Department of Experimental and Health Sciences

Acknowledgment

I would like to thank Isabelle Vernos, Andreas Merdes, Helder Maiato, Manuel Mendoza and Travis Stracker for accepting to read and evaluate my work.

I am deeply thankful to Jens Lüders for his guidance, availability, patience and support along the years of my PhD. His great mind, scientific reflection and passion for science have been a motor for the progression of this work. Thank you for the critical reading and editions of this manuscript. I am very debt-full for everything I learnt from you scientifically and beyond the bench.

I would like to thank La Caixa that financially supported me and gave me the opportunity to work in a great environment in IRB.

I would like to thank the members of my TAC: Berta Alsina, Jordi Casanova and Joan Roig for our annual meetings, their useful comments and advices contributed to the development of this work. A special thanks to Joan, for extending his supervision beyond the TAC meetings and attending our lab meetings. I also would like to thank Francisco Real Arribas, for being my UPF tutor.

A special thank to the entire Microtubule Organization Group for the great atmosphere in the lab, the scientific discussion, the critics, comments and ideas about my work. I had great time every single day in the or out lab and this is thank to all of you. Thank you for all the parties, pétanque games, trips etc. To Cristina for the early treatments and agreeing every time I complained. To SabRosa (Sabine and Rosa) for the weekend or super late help, the ice-fights, the bad music and the gossiping. To Carlos my office mate, for his advises, the exchange of all these stupid links and information, for almost listening my non-sense discussion. To Lord Francisco, for all these non-scientific discussion, only you and I understood the joy of the robe-life! To Marko for his support, always understanding me and giving great advises about the life in general. Also for his almost as bad

jokes as mine. Susana and Paula, the two girls from upstairs for their good mood. To past or new members of the lab: Artur, Adrian, Roberta and Florian, we didn't have so much time together but it was always good time. To Marco and Neus the best postdocs ever! You welcomed me the very first day and became real friends, I was so sad when you left the lab; it was never the same without you. And finally to Martha, who also shared the office space and had to deal with my talks and music. I would like to NOT acknowledge the same persons for making fun of my French accent and also apologize to all of you for my bad jokes, complaints and everything else, but you'll miss all of these for sure!

I would like to thank the complete ADM facility, Julien, Anna, Lidia and Seb, I spent lot of time at the microscopes and you were always around when I needed help for images acquisition or processing.

Thank to my friends out of the lab, mostly from the "Spartans" football team (Rodrigo, Chiara, Victor, Manuel, Radek, Victor and all the others). I had great time on the field but also off side for lunches, drinks and discussions… By the way, we were the best! Also thank to the French community in Barcelona from the Paris Taxi (Pat!!) and to Arnaud a real friend and a great person.

A big thank to everybody in IRB administration and Natalia Ras from UPF who made everything easy when I arrived in Barcelona, for the paperwork, university registration etc.

I would thank my parents, my sister Magalie, almost-brother Nacim and all my family and friends from France for the support, their regular visits and help. I have the best family I could ever dream off, you're all amaizing.

Finally nothing could have been done without Manue, ma Copinette. Thank you for sharing my life, for your support, for your understanding, for turning bad days into good days, for trusting in me, for living with me, for your love, for everything!!

Abstract

During mitotic spindle assembly, γ-tubulin ring complexes (γTuRCs) nucleate microtubules at the centrosome, around mitotic chromatin and, by augmin-dependent recruitment, from pre-existing microtubules. The analysis of these distinct pathways in somatic cells is challenging due to the predominance of centrosomal nucleation. It is also unknown how microtubules derived from different nucleation pathways are organized into the bipolar spindle structure. Due to their intrinsic polarity, microtubules have so-called plus ends and minus ends. Using plus end-tracking proteins, such as EB1, previous work has revealed the dynamics of microtubule plus ends. Minus ends were shown to be present throughout the spindle with a higher concentration near the poles. However, the analysis of minus end dynamics has been prevented by lack of a suitable probe.

In the first part of this work I have identified the γ-tubulin ring complex (γTuRC), which is the main microtubule nucleator, as a reliable marker for non-centrosomal microtubule minus ends in the spindle and have confirmed the accumulation of minus ends in the pole-proximal region. Using human cells stably expressing γ-tubulin fused to photoactivatable GFP and mutants of γTuRC subunits, I have demonstrated that the γTuRC is recruited preferentially in the pole-distal spindle region, where it associates with microtubule minus ends and then moves poleward along the mitotic spindle. Poleward transport of γTuRC at minus ends depends on the molecular motors dynein, KIFC1 and KIF11. I also discovered that some of the γTuRC that reaches the poles is stably incorporated at the centrosomes, complementing the microtubule-independent centrosome targeting previously described.

In the second part, using laser ablation of centrosomes, I studied non-centrosomal spindle assembly in pig LLC-PK cells. At mitotic entry, in the absence of

centrosomes, these cells could nucleate microtubules from the nuclear area. These microtubules formed multipolar spindles but cells eventually divided into two daughter cells. However, cells derived from these abnormal mitoses were typically not viable.

In summary, by revealing the dynamics of the minus ends of non-centrosomal microtubules, I have provided novel insight into assembly and architecture of the mitotic spindle. In addition, I have shown that centrosomes, even though not essential for somatic cell division, play an important role in the fidelity of spindle assembly and function.

Resumen

Durante la formación del huso mitótico, los complejos anulares de γ-tubulina (γTuRCs, del ingles *γ-tubulin ring complexes*) nuclean microtúbulos alrededor de la cromatina mitótica y, mediante la interacción con el complejo de la Augmina, a partir de otros microtúbulos ya existentes. El estudio de estos mecanismos en células somáticas es complejo, debido a la predominancia de la nucleación centrosomal de los microtúbulos en estas células. En la actualidad, aun no se sabe como microtúbulos procedentes de distintas vías de nucleación se organizan en la estructura bipolar del huso mitótico.

Debido a su intrínseca bipolaridad, los microtúbulos tienen un extremo (+) y un extremo (-). Usando proteínas marcadoras propias del extremo (+), como EB1, investigaciones previas han revelado la dinámica de este extremo de los microtúbulos. Por otro lado, se ha observado que los extremos (-) están presentes a lo largo del huso, detectándose una mayor concentración cerca de los polos. A pesar de esto, no se conocen estudios detallados acerca de la dinámica del extremo (-) debido a la ausencia de marcadores adecuados.

En la primera parte de este trabajo he observado que el complejo anular de γ-tubulina (γTuRC), el principal nucleador de microtúbulos, es un marcador fiable de los extremos (-) en los microtúbulos acentrosomales presentes en el huso mitótico. Además, he confirmado la acumulación de estos extremos (-) en la región próxima a los polos del huso.

Utilizando líneas celulares humanas que expresan de forma estable γ-tubulina fusionada a un GFP foto-activable, y que además han sido transfectadas con isoformas mutantes de subunidades del γTuRC, he demostrado que el γTuRC se recluta preferentemente en regiones del huso alejadas de los polos. Allí el γTuRC

se asocia con los extremos (-) de los microtúbulos, para ser transportado a lo largo del huso mitótico en dirección a los polos.

El transporte del γTuRC presente en los extremos (-) en dirección a los polos lo realizan los motores moleculares Dineina, KIFC1 y KIF11. También he descubierto que una parte de las moléculas de γTuRC que alcanzan los polos del huso se integran de forma estable en los centrosomas, complementando la vía de incorporación al centrosoma independiente de microtúbulos que ha sido previamente descrita.

En la segunda parte, usando la técnica de ablación de centrosomas con laser, he estudiado la formación acentrosomal del huso en la línea celular porcina LLC-PK. Cuando estas células entran en mitosis en ausencia de centrosomas, pueden nuclear microtúbulos desde el área nuclear. Estos microtúbulos forman husos multipolares, aunque las células finalmente se dividen en dos células hijas. Las células procedentes de estas mitosis anormales no suelen ser viables.

En conclusión, mediante el revelado la dinámica de los extremos (-) de los microtúbulos no centrosomales, he proporcionado nueva información acerca del ensamblaje y arquitectura del huso mitótico. Además, he demostrado que los centrosomas, aunque no son esenciales para la división celular somática, juegan un papel importante en el correcto ensamblaje y función del huso mitótico.

Abbreviations

4A: D176A, E177A, S179A, D180A mutant of γ-tubulin

γTuRC: γ-tubulin ring complex

γTuSC: γ-tubulin small complex

APC: Anaphase promoting complex

ATP: Adenosine triphosphate

DNA: deoxyribonucleic acid

CDK: Cyclin-dependent kinases

CDK5RAP2: CDK5 regulatory subunit associated protein 2

ch-TOG: colonic and hepatic tumor-overexpressed gene

CLAP: Clathrin associated protein

CLIP: Class II-associated invariant chain peptide

EB: End-binding protein

EHNA: erythro-9-(2-hydroxy-3-nonyl)adenine

ER: endoplasmic reticulum

FRAP: Fluorescence recovery after photobleaching

GDP: guanosine diphosphate

GTP: guanosine triphosphate

G1 phase: Gap 1 phase

G2 phase: Gap 2 phase

GCP: gamma-tubulin complex protein

GFP: Green fluorescent protein

HAUS: Human augmin complex

HURP: hepatoma up-regulated protein

KIF11: Kinesin family member11

KIFC1: Kinesin family member 1C

M phase: Mitosis phase

MAP: Microtubule associated proteins

MCAF: monocyte chemotactic and activating factor

MCAK: Mitotic centromere-associated kinesin

mRNA: Messenger RNA

MTOC: Microtubule-organizing center

n.s.: not significant

NEB: Nuclear envelope breakdown

NEDD1: Neural precursor cell expressed developmentally down-regulated protein 1

NuMA: Nuclear mitotic apparatus protein

paGFP: photoactivitable GFP

PCM: Pericentriolar material

Ran: RAs-related Nuclear protein

Ran-GAP: Ran GTPase activating protein

RCC1: Regulator of chromosome condensation 1

RNA: Ribonucleic acid

RNAi: RNA interference

S phase: synthesis phase

SAC: Spindle assembly checkpoint

shRNA: small hairpin

SPB: Spindle pole body

SEM: Standard error to the mean

SD: Standard deviation

STLC: S-trityl-L-cysteine

TOG: tumor-overexpressed gene

TPX2: Targeting protein for Xklp2

+TIP: Microtubule plus-end tracking proteins

Table of Contents

List of figures

Introduction

1. Microtubule cytoskeleton

The cytoskeleton is required for cell shape, architecture, movement, internal transport, and division. In eukaryotes the cytoskeleton is composed of three different type of filaments: actin filaments, intermediate filaments and microtubules.

Actin filaments are polymers made of actin subunits. Actin is very dynamic and is involved in a range of processes including muscle contraction, cell migration, and cell division. The myosin family of molecular motors is able to use actin filaments as tracks to exert force or transport cargo.

Intermediate filaments are heterogeneous. Many different proteins can assemble different types of intermediate filaments. They are very stable and provide three-dimensional mechanical support to cells. They are also used as scaffold for organelle anchoring and for cell-cell interaction.

Microtubules are polymers made of heterodimers of α and β-tubulin. They are highly dynamic and have many functions such as intracellular transport, formation of centrioles and cilia, and, through the formation of a specific structure called mitotic spindle, the proper segregation of the chromosomes during cell division. A major organizer of microtubules in animal cells is the centrosome.

1.1 Tubulin

The Tubulin super family includes several families: alpha (α), beta (β), gamma (γ), delta (δ), epsilon (ε), zeta (ζ), eta (η), iota (ι) and kappa (κ) tubulins. The most common tubulins are α and β-tubulin, the highly conserved subunits of microtubules, and γ-tubulin, which is required to nucleate the polymerization of microtubules. The functions of others tubulins are poorly understood, but roles in centriole duplication, morphology and maintenance as well as in basal body biogenesis have been suggested (Dutcher 2003).

1.1.1 α and β-Tubulins

Both α- and β-tubulin have a mass of about 55 kDa and share a high similarity in their amino acid sequence (50%); they are formed by a core of two β-sheets surrounded by α-helices. One molecule each of α– and β-tubulin interact non-covalently to form a very stable 8 nm long and 4 nm wide heterodimer (Figure 1) that can interact longitudinally and laterally with other heterodimers to assemble microtubules (Nogales et al. 1998). Each tubulin monomer has a GTP-binding site, termed N-site for α-tubulin and E-site for β-tubulin. The GTP bound to α-tubulin is non-exchangeable and the N-site is buried at the intradimer surface; in contrast, the E-site of β-tubulin is exposed at the surface of the dimer and can hydrolyze GTP into GDP (Mitchison 1993) (Desai & Mitchison 1997) (Desai & Mitchison 1998) (Löwe et al. 2001). GTP hydrolysis affects the dimer conformation and controls assembly and dynamics of the microtubule. GTP bound tubulin is thought to have a “straight” conformation while the GDP bound state has a “curved”

conformation. The GDP bound form is forced into “straight” conformation by contacts within the microtubule (Downing & Nogales 1998).

Unicellular organisms tend to have only one or two genes coding for α and β-tubulins. In most eukaryotes, several isoforms are found; each differs slightly in its amino acid sequence and/or in the tissue/temporal/subcellular distribution.

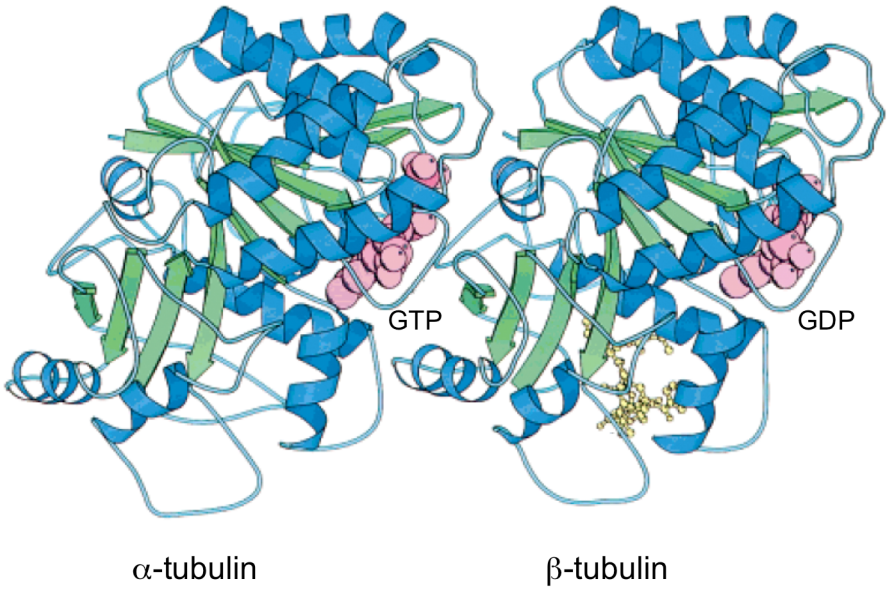

Figure 1. Structure of the tubulin dimer.

α and β-tubulins are formed of two β-sheets surrounded by α-helices. They interact to form a dimer. The GTP of α-tubulin is at the interface with β-tubulin. β-tubulin hydrolyzes the GTP into GDP that is present at the surface of the dimer. Adapted from (Desai & Mitchison 1998).

1.1.2 Microtubule structure

Microtubules are cylindrical protein filaments made of α and β-Tubulin heterodimers. Heterodimers are arranged in a head to tail fashion to form protofilaments (Figure 2a). Lateral α-α tubulin and β–β tubulin interactions between

protofilaments create a helical pattern. The helical arrangement generates a lattice discontinuity called the seam (Figure 2b). Microtubule formation can happen spontaneously *in vitro* but is tightly controlled in cells. *In vivo*, microtubules are generally made of 13 protofilaments that interact laterally to form a 25 nm diameter hollow tube, with a lumen of 17nm (Tilney et al. 1973). *In vitro*, the number of protofilaments in spontaneously assembled microtubules varies from 9 to 17, even within the same microtubule. Because lateral interactions are weaker, microtubules are thought to grow as sheets and then zip into a closed tube (Chrétien et al. 1995).

In vivo microtubule assembly is initiated by nucleation followed by polymerization to allow elongation of the microtubule (Figure 2c). Microtubules display an intrinsic polarity due to the head to tail assembly of α–β-tubulin heterodimers. The more dynamic so-called “plus end” displays the β-tubulin subunit, while α-tubulin is exposed at the “minus end”. In cells the minus ends of microtubules are usually less dynamic and are anchored at cellular structures from where microtubules grow (Allen & Borisy 1974).

Since GTP hydrolysis by β-tubulin accompanies microtubule growth, microtubules are mostly composed of GDP-β-tubulins with a cap of GTP-β-tubulin at the growing plus end. The change from the GTP-bound to GDP-bound form may be responsible for the sheet to cylinder transition, or could be a consequence of this conformation change (Rice et al. 2008).

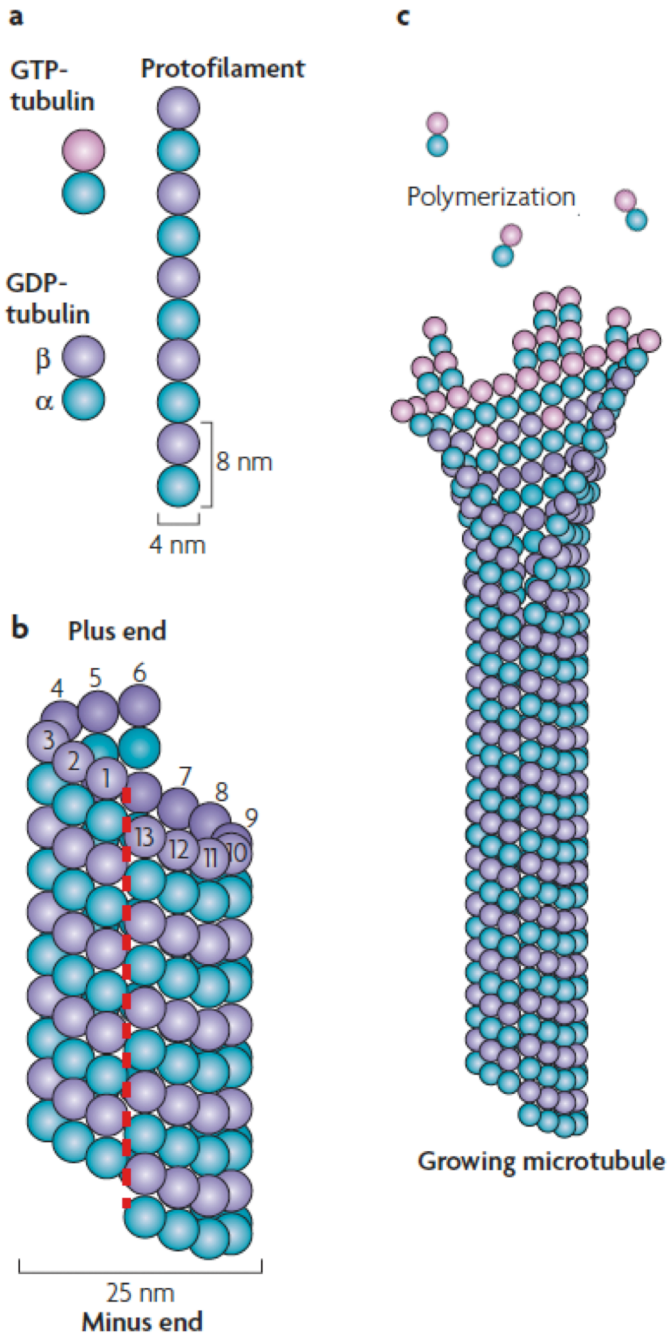

Figure 2. The microtubule structure and growth.

(**a).** α and β-tubulins form heterodimers that are the structural base of protofilaments **(b).** Microtubules are made of 13 protofilaments; the helical structure induced by lateral interactions between heterodimers leads to discontinuity along the lattice, the seam **(c).** Microtubules are growing at the plus end through addition of heterodimers in a sheet form, that will then be zipped to form the hollow tube. Modified from (Akhmanova & Steinmetz 2008).

1.2 Microtubule nucleation and dynamics

1.2.1 γ-Tubulin

γ-Tubulin, a ~50 kDa protein that shares around 30% identity with α/β-tubulins, was first discovered in *Aspergillus nidulans* in 1989 (C. Oakley & B. Oakley 1989). Like α– and β-tubulin, γ-tubulin has a GTP binding pocket. The crystal structure of γ-tubulin with bound GTPγS showed a structure comparable to the curved conformation of α and β-tubulins (Aldaz et al. 2005). Its amino acid sequence is highly conserved, for example human γ-tubulin is 98% and 78% identical to γ-tubulin from *Xenopus laevis* and *Drosophila melanogaster*, respectively. Despite the high degree of sequence conservation, γ-tubulin function is also well conserved; human γ-tubulin can rescue the deletion of the γ-tubulin gene in the fission yeast *Schizosaccharomyces pombe* (Horio & B. R. Oakley 1994). Humans have two isoforms of γ-tubulin (TUBG1 and TUBG2). TUBG1 is ubiquitinously expressed while TUBG2 is expressed in specific tissues, preferentially in brain.

γ-Tubulin is required for microtubule nucleation and localizes at microtubule organizing centers (MTOCs). In some cases γ-tubulin can also be observed to localize along microtubules and is suspected to influence the dynamics (Bouissou et al. 2009). In addition, most cells also contain a large amount of soluble γ-tubulin. It is not clear whether soluble γ-tubulin has a specific function or simply serves as a reservoir from which it can be recruited to nucleation sites. Whereas γ-tubulin is the main microtubule nucleator, it may not be the only one; indeed Drosophila interphase cells depleted for γ-tubulin can still nucleate and properly organize microtubules (Rogers et al. 2008).

1.2.2 γ-Tubulin complexes

γ-Tubulin is mainly found associated with other proteins. Two distinct complexes have been described: the γ-tubulin small complex (γTuSC) and the γ-tubulin ring complex (γTuRC) (Oegema et al. 1999). Each of these complexes contains several γ-tubulin molecules and additional proteins termed γ-tubulin complex proteins (GCPs) (Figure 3).

Early work in *Saccharomyces cerevisiae* indentified a heterotetrameric Y-shaped complex containing two molecules of γ-tubulin and one molecule each of GCP2 and GCP3, the only two GCPs present in the budding yeast (Kollman et al. 2008). This complex is now referred to as the γTuSC. In the γTuSC GCP2 and GCP3 each interact with one γ-tubulin molecule through their C-terminal domains and with each other through their N-terminal domains.

In higher organisms, γ-tubulin is also found in larger complexes termed γTuRCs. In the γTuRC multiple γTuSCs associate laterally to form a lock washer-type of structure, in which ~13 γ-tubulin molecules are coordinated in a helical arrangement. Depletion of γ-tubulin or any of the GCPs 2-6 leads to the disruption of the complex, suggesting structural roles for all of these proteins. However, the exact functions of GCP4, GCP5, and GCP6 in the γTuRC structure are poorly understood (Xiong & B. R. Oakley 2009). Based on the recently solved crystal structure of GCP4 (Guillet et al. 2011), it has been proposed that the GCPs 2-6 share a conserved core fold and that GCP4, GCP5 and GCP6 might assemble γTuSC-like subcomplexes that integrate into and stabilize the γTuRC (Figure 3), for example at the beginning or the end of the open ring-like structure (Kollman et al. 2011) (Teixidó-Travesa et al. 2012).

Apart from GCPs 2-6, additional, unrelated γTuRC subunits have been described. The NEDD1 (GCP-WD; GCP7) subunit contains a WD repeat domain that is

required to target the γTuRC to MTOCs (Gunawardane et al. 2003) (Lüders et al. 2006) (Haren et al. 2006). Mozart2 (GCP8) has recently been demonstrated to play a role in microtubule organization in interphase but not in mitosis (Teixidó-Travesa et al. 2010), (Hutchins et al. 2010), and Mozart1 is required in mitosis for γ-tubulin recruitment to centrosomes and for spindle assembly (Hutchins et al. 2010) (Janski et al. 2012) (Nakamura et al. 2012).

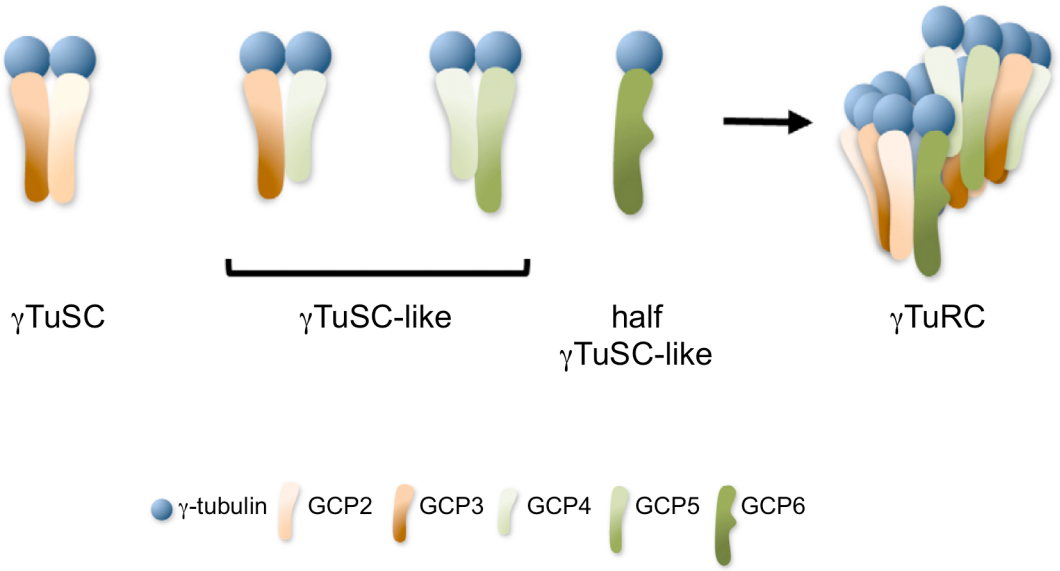

Figure 3. The γ-tubulin complexes.

γTuSC is made of one subunit of each GCP2 and GCP3 and two molecules of γ-tubulin. γTuSC-like complexes could be formed by replacement of GCP2 and/or GCP3 by GCP4,5 or 6. All these complex participate to the formation of the larger ring shaped γTuRC. Adapted from (Teixidó-Travesa et al. 2012).

1.2.3 Microtubule nucleation

The main nucleator of microtubule polymerization in cells is the γTuRC. Its ring-shaped structure most likely templates microtubule formation (Moritz et al. 2000), (Zheng et al. 1995). The helically arranged 13 γ-tubulins on one side of the γTuRC

interact with the α-tubulin subunits of α/β-tubulin dimers to initiate polymerization (Figure 4). Subsequently γTuRC may also act as a stabilizing cap at the minus end of the microtubule while microtubule growth continues by polymerization at the plus end (Wiese & Zheng 2000), (Anders & Sawin 2011).

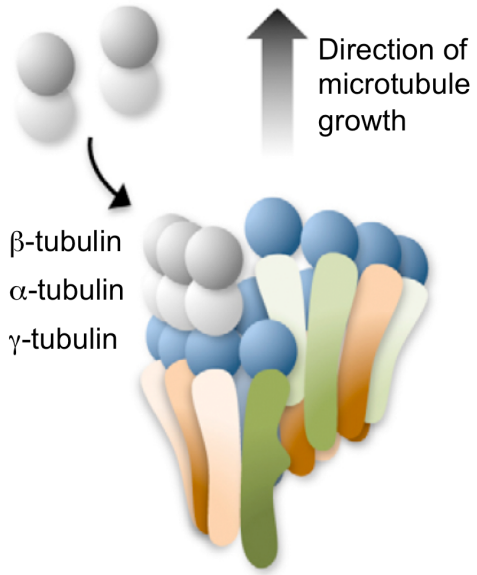

Figure 4. Microtubule nucleation, the template model.

The open ring γTuRC is used as a matrix for microtubule nucleation. Longitudinal interactions of α–β-tubulins dimer with γ-tubulin lead to the generation of a microtubule. Adapted from (Teixidó-Travesa et al. 2012).

1.2.4 Microtubule dynamics

In particular the microtubule plus end is highly dynamic. It oscillates between polymerization and depolymerization phases, a property also known as dynamic instability (Figure 5). The transition from growth phase to shortening is called catastrophe and the transition from shrinkage to growth is called rescue. Between

catastrophe and rescue microtubule plus ends frequently display pause phases, in which neither growth nor shrinkage occur (Desai & Mitchison 1997), (Mitchison & Kirschner 1984).

Even though the plus end is more dynamic, addition or removal of tubulin dimers can occur at both ends of the microtubule. The incorporation of dimers at one end coupled to the removal of dimers at the other end leads to treadmilling. During treadmilling unidirectional flux of subunits from one end to the other occurs, while microtubule length and position can remain relatively constant (Margolis & Wilson 1978). Poleward microtubule flux is observed, for example, in a subset of microtubules in the mitotic spindle.

In addition to GTP binding and hydrolysis, a large number of factors controls the dynamics of microtubules including posttranscriptional modifications such as phosphorylation, acetylation, polyglycylation, polyglutamylation, methylation, tyrosinylation, and polmytoylation. While the complex modification patterns of microtubule are still poorly understood, detyrosinylation, acetylation and polyglutamylation, for example, are suspected to stabilize microtubules. In addition, some modifications seem to be involved in regulating the binding of proteins (Janke & Bulinski 2011).

Apart from various well-established microtubule binding proteins that regulate microtubule dynamics and will be described in the following paragraphs, recent work suggests that γTuRC can also regulate microtubule dynamics by lateral binding to microtubules, independently of its role as microtubule nucleator (Bouissou et al. 2009).

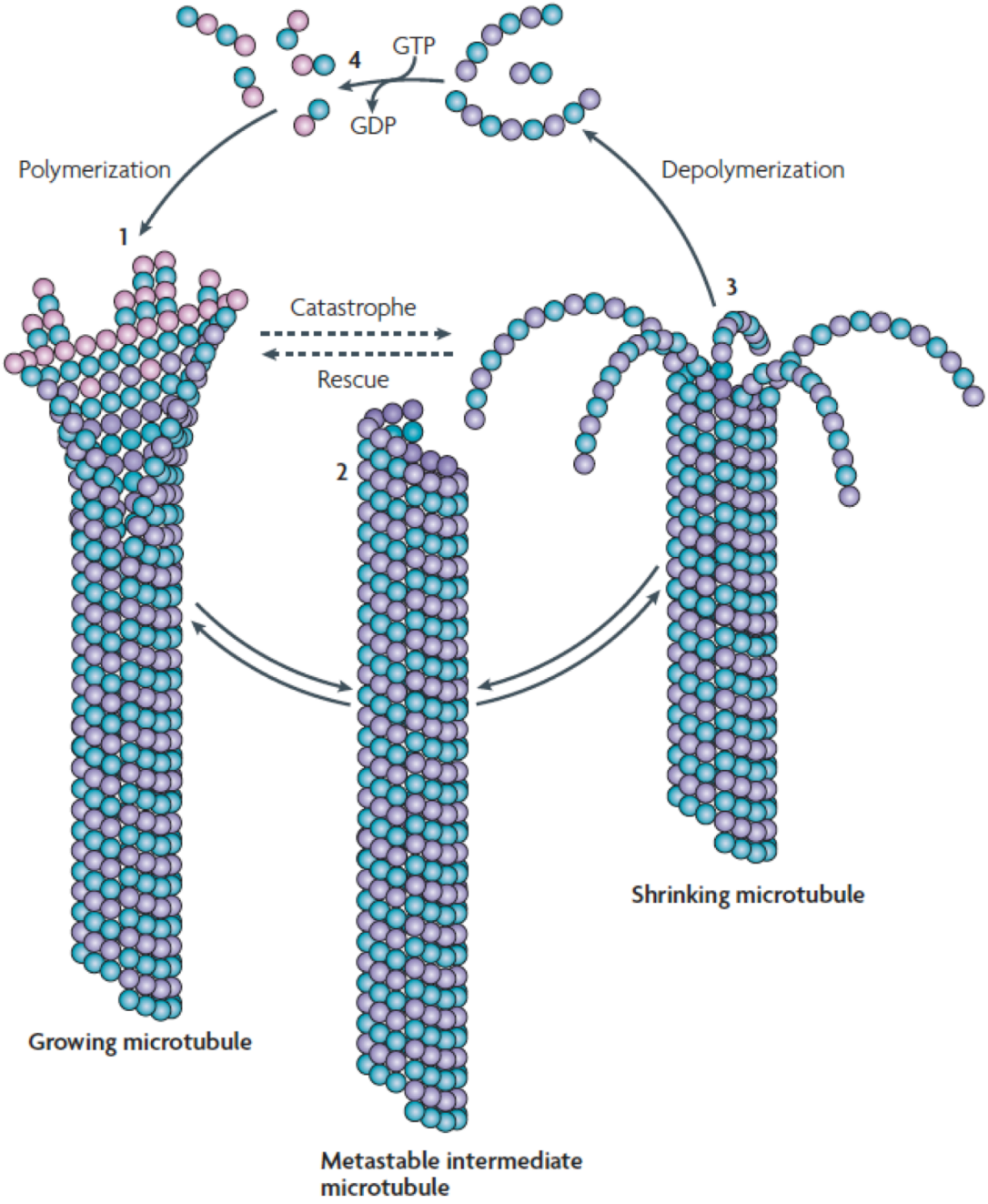

Figure 5. Microtubule dynamic instability.

A catastrophe event on a growing microtubule leads to shrinkage that is characterized by fountain-like curved protofilaments. The depolymerization leads to the release of heterodimers that can exchange the GDP by a GTP and be incorporated into growing microtubules. The end of a shrinkage phase is called rescue. When a microtubule is not growing or shrinking it is said to be in a pause phase. Modified from(Akhmanova & Steinmetz 2008).

1.3 Microtubule associated proteins

A multitude of microtubule-associated proteins (MAPs) regulate microtubules. These proteins can function as stabilizers, destabilizers, molecular motors, bundlers, or severing enzymes.

1.3.1 Stabilizing and destabilizing proteins MAPs

Stabilization of microtubules can be done through several actions: reducing catastrophes, rescuing depolymerizing microtubules, or decreasing shrinkage velocity. Some proteins such as Tau, MAP2 and MAP4 (Drechsel et al. 1992), (Ookata et al. 1995), which are abundant in neurons, are able to stabilize microtubules simply by binding to the microtubule lattice. This prevents dissociation of tubulin dimers leading to an increase in rescue events and a decrease in catastrophe events.

Proteins that induce catastrophe, prevent rescue or increase the shrinkage rate promote an overall destabilization of microtubules. Stathmin, for example, can interact with microtubules and trigger a catastrophe event by forcing GTP hydrolysis by β-tubulin at the plus end (Howell et al. 1999). Some kinesin motors such as MCAK, Kip3p or Kar3 function as depolymerazes. MCAK acts through an interaction with tubulin subunits at microtubule plus ends, hydrolysis of the ATP bound to the “motor domain” leads to a conformation change of the bound tubulin, which induces catastrophe (Hunter et al. 2003).

Other proteins have microtubule severing activity (katanin, fidgetin, spastin). These proteins use energy from ATP to cut microtubules, which can lead to

destabilization (D. Zhang et al. 2007). However, the severing mechanism might also be used to generate additional microtubules in the absence of nucleation.

1.3.2 Molecular motors

The molecular motors are molecules that can “walk” along the microtubule lattice, they are divided in two classes: the minus end-directed and the plus end-directed motors according to the direction of their movement (Figure 6). These proteins hydrolyze an ATP molecule, leading to a conformation change that is reflected by the movement of the motor along the microtubule.

The superfamily of kinesin gathers 14 families. Most of these molecules are plus end directed motors and allow the transport of cargos (vesicles, organelles, chromosomes) along the microtubule. Some of the kinesins also play a role in microtubule dynamics. The kinesin KIF11 is able to oligomerize, crosslink anti-parallel microtubules (Kapitein et al. 2005) and induce an outward sliding through the action of its motor domains. This process is required in mitosis for centrosome separation, bipolarity maintenance and chromosomes separation (Ferenz et al. 2010).

Kinesins with a motor domain at their C-terminus are minus end-directed motors. One example is the motor KIFC1 (McDonald et al. 1990), which can regulate spindle length by crosslinking and sliding of microtubules (Cai et al. 2009).

Dynein is a minus end-directed motor that is involve in many biological processes such as transport of vesicles, transport and anchoring of organelles, subcellular localization of proteins and complexes, movement of cilia and flagella, and mitotic spindle assembly and function. Dynein is a protein complex composed of several heavy, intermediate and light chains. The main structure is always similar and

consists of two globular heads at the end of the small arms of a Y-shaped complex. Hydrolysis of ATP allows the two heads to alternatively take a step, resulting in a walking-like movement on the microtubule (Cho & Vale 2012). Dynein is found in complex with dynactin, its regulator. In mitosis, dynein was described to be involved in centrosomes separation, the spindle positioning and the movement of chromosomes (Raaijmakers et al. 2012), (Kotak et al. 2012), (Starr et al. 1998).

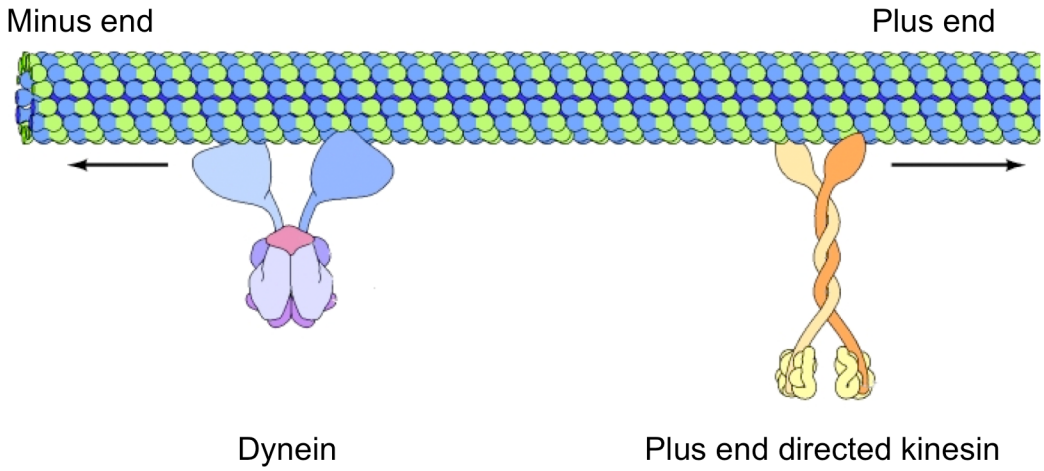

Figure 6. The molecular motors.

Two classes of motors are distinguishable, the kinesins mostly move toward the plus end. The dynein and few kinesins (including KIFC1) are directed toward the minus end. Modified from (Cooper 2000)

1.3.4 Others MAPs

Many other proteins interact with microtubules, one of the biggest superfamily is the plus end-associated proteins (+TIPs), it covers a wide range of families, differing in their size, function, structure, plus end recognition and microtubule

binding. These proteins preferentially bind the plus end of a microtubule and only poorly bind or are absent along the rest of the microtubule (Akhmanova & Hoogenraad 2005).

The EB family proteins are mostly found at growing microtubule plus ends. By controlling microtubule dynamics, they play roles in proper mitotic spindle organization, microtubule anchoring at the centrosome, assembly of cilia and microtubule interaction with the cell cortex.

Other +TIPS have been described to accelerate the recruitment of tubulin at the growing end (ch-TOG/XMAP215), regulate the dynein motor activity ($p150^{glued}$), stabilize microtubule-kinetochore (CLIPs) and microtubule-actin interactions.

More proteins interact with the microtubules that could not be classified in above categories, such as Lissencepahly 1 (Lis1). Lis1 has been reported to play a role in neuronal migration and in the brain development (Vallee et al. 2001), and has been implicated in barrier formation in epidermis cells (Sumigray et al. 2011). Lis1 is known to interact with CLIP170 and also the dynein/dynactin complex (Tai et al. 2002). This protein also plays a role in the mitotic division through spindle position and interaction with the kinetochores (Faulkner et al. 2000).

1.4 Microtubule organizing centers

In cells, most microtubules are nucleated and organized by specialized structures termed microtubule organizing centers (MTOCs). Analysis of MTOCs in different organisms and cell types revealed that despite differences in MTOC shape and distribution, a common feature is the ability to recruit γ-Tubulin complexes and nucleate microtubules. The minus ends of these microtubules are typically

anchored at the MTOC and the plus ends extend into the cytoplasm. Whereas budding yeast has only one MTOC, the spindle pole body, different types of MTOCs are found in animal cells. The main microtubule organizer is the centrosome, but other cellular structures have been shown to have microtubule-organizing activity in certain cell types or at specific cell cycle stages.

1.4.1 Spindle pole body

The main microtubule organizer in yeast is the spindle pole body (SPB). It is embedded in the nuclear envelope and divided in three plaques: the outer plaque that faces the cytoplasm, the inner plaque that faces the nucleoplasm, and the transmembrane central plaque. More recent studies by cryo-electron-microscopy and electron tomography revealed two intermediate layers between the outer and the central plaque called intermediates layers 1 and 2 (Figure 7) (Bullitt et al. 1997), (O'Toole et al. 1999).

To date, 17 proteins are known to compose the SPB (Jaspersen & Winey 2004). Apart from structural elements and proteins involved in the duplication, the SPB also contains γTuSC: Tub4 (yeast γ-tubulin), Spc97 and Spc98 (yeast GCP2 and GCP3, respectively). Spc72 (Knop & Schiebel 1998) and Spc110 (Knop & Schiebel 1997) have been demonstrated to recruit and attach γTuSC to the SPB (Figure 7). Since γTuSC is not an efficient nucleator (Oegema et al. 1999), it has been suggested that Spc110 promotes γTuSC oligomerization to form a γTuRC-like arrangement that can efficiently template microtubule nucleation (Kollman et al. 2008).

Facing both, the nucleoplasm and the cytoplasm, the SPB is able to nucleate microtubules in both compartments. In interphase, the SPB nucleates microtubules

on its cytoplasmic side. In mitosis, an intra-nuclear spindle is then assembled from microtubule nucleated at the inner plaque. Microtubule nucleation, spindle orientation and chromosome separation are controlled by the SPB.

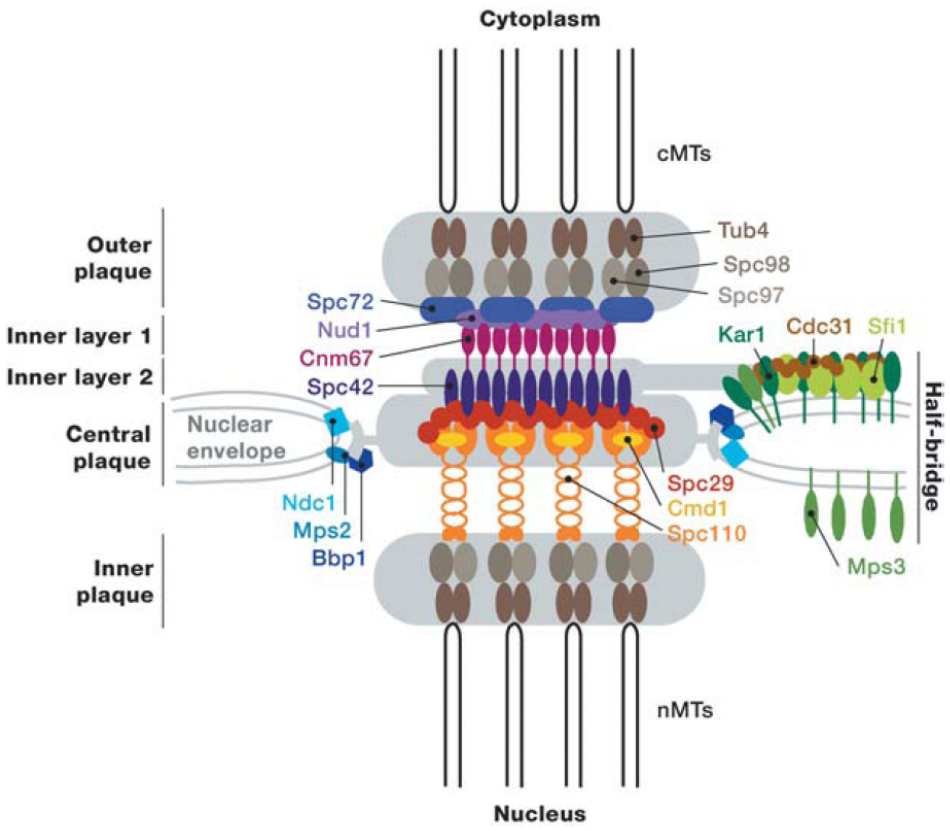

Figure 7. The yeast spindle body.

The SPB is composed of three plaques and two intermediate layers and embedded into the nuclear envelope. γ-Tubulin complexes are recruited at both sides by Spc72 and Spc110 and can nucleate microtubule in the cytoplasm and in the nucleus. Adapted from (Jaspersen & Winey 2004).

1.4.2 Centrioles and centrosomes

In most animal cells, the main MTOC is the centrosome. It is composed of a pair of centrioles surrounded by a dense protein matrix known as the pericentriolar material (PCM) (Figure 8).

Centrioles are microtubule-based cylindrical structures that present a 9-fold radial symmetry (Bornens 2002). The mother-daughter pair of centrioles present in a newly born cell is duplicated precisely once (in parallel to the replication of the DNA) and the resulting two pairs of centrioles (now composing two centrosomes) are then segregated into the two daughter cells by associating with one of the two spindle poles. The centriole number is strictly regulated and an abnormal number of centrioles is often found in cancer and other diseases (Cunha-Ferreira et al. 2009). To become fully functional centrosomes newly formed daughter centrioles require going through a maturation process. This process occurs during mitosis and enables centrioles to recruit PCM and nucleate microtubules in the subsequent cell cycle (La Terra et al. 2005), (Wang et al. 2011).

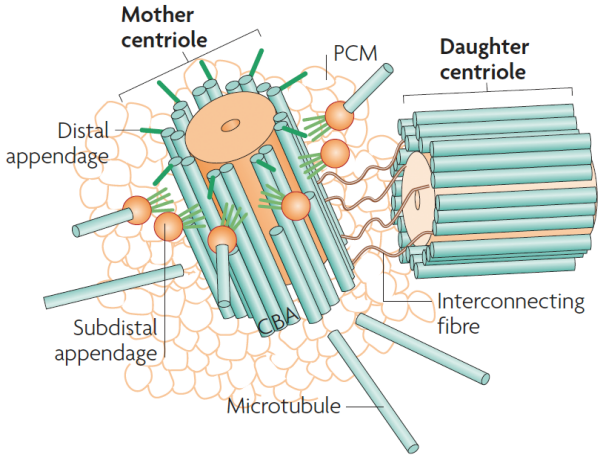

Figure 8. The centrosome.

Centrioles are cylinder composed of nine microtubules triplets. Every cell cycle they are duplicated and the mother centriole is used as a template to form the daughter centriole. Matured centrioles are surrounded by the PCM that contain γ-tubulin and nucleate microtubules. Adapted from (Bettencourt-Dias & Glover 2007).

Until recently, the PCM was thought to be a relatively unstructured "cloud" of proteins that have diverse functions. Thanks to several super-resolution microscopy studies it is now accepted that the PCM is organized in layers around the mother centriole (Lawo 2012), (Mennella et al. 2012), (Fu & Glover 2012), (Sonnen et al. 2012) (Figure 9). Several scaffold proteins including pericentrin (Zimmerman et al. 2004) and CDK5RAP2 (Fong et al. 2008) recruit and anchor γ-tubulin complexes at the surface and promote microtubule nucleation and organization. Microtubules grow radially from the centrosome with their plus ends exploring the cytoplasm.

Like the SPB, the centrosome also has functions that are independent of its role as microtubule organizer. The centrosome is a platform that integrates many signaling pathways and controls the regulation of the cell cycle and other processes.

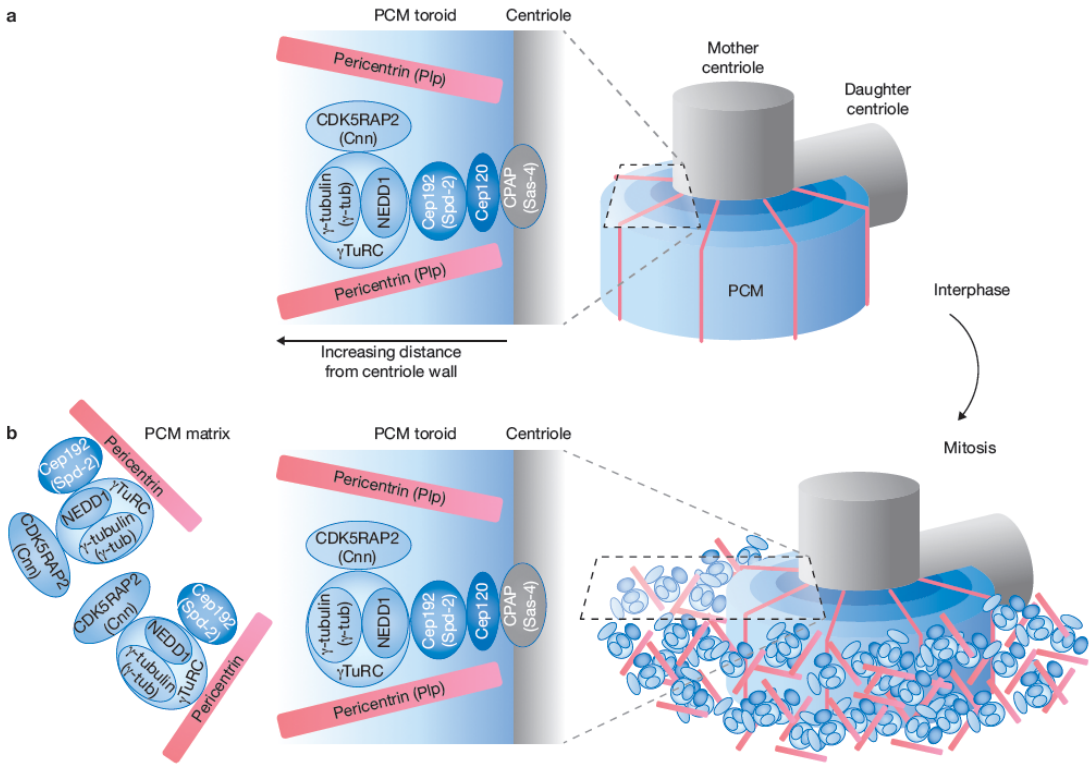

Figure 9. Organization of the centrosome.

In interphase **(a)** PCM proteins are organized in a donut-shape around the centriole. The proteins form several concentric layers with the microtubule nucleator at the outer layer. Some proteins such as Pericentrin organize radially with one end close to the centriole and the other end outward. In mitosis **(b)** centrosomes recruit a larger amount of PCM components that form an extended matrix outward. Adapted from (Lüders 2012).

1.4.3 Other MTOCs

Since its discovery the centrosome has been described as a major MTOC. However, some organisms or cell types do not have centrosomes but still present an organized microtubule array and are able form a mitotic spindle.

In higher plants, which lack centrioles and centrosomes, γ-Tubulin is found at the nuclear envelope and at the cell cortex and these structures can be considered MTOCs (Ehrhardt & Shaw 2006). γ-Tubulin is also present along the lattice of pre-

existing microtubules triggering microtubule-dependent, branching microtubule nucleation (Murata et al. 2005).

In animals, some specialized cells inactivate or disassemble their centrosome and form non-centrosomal MTOCs. For example, oocytes typically loose their centrosome during oogenesis (Szollosi et al. 1972). During meiotic divisions acentrosomal spindles assemble from microtubules nucleated by non-centrosomal mechanisms (Maro et al. 1985).

During muscle differentiation, myoblasts fuse to form a syncytial structure. Several PCM proteins including pericentrin, ninein and γ-tubulin relocalize to the surface of the multiple nuclear envelopes and organize a parallel microtubule array (Tassin et al. 1985), (Musa et al. 2003), (Bugnard et al. 2005), (Srsen et al. 2009).

A similar relocalization of PCM proteins occurs in epithelial cells, where an apico-basal microtubules network has been described. Several PCM proteins have been shown to be present at the apical region, colocalizing with the microtubule minus ends (Reilein & Nelson 2005). Epithelial cells also have a centrosome; the current view is that microtubules are generated from the centrosome, released and relocated with their minus ends anchored to the apical region (Mogensen 1999).

Neurons also have a centrosome but it has been shown to be inactivated during the differentiation process. In advanced stages of neuron maturation (Leask et al. 1997), γ-tubulin disappears from the centrosome (Stiess et al. 2010). One possibility is that soluble γ-tubulin nucleates microtubules in the cytoplasm or from Golgi membranes, as has been observed in other cell types (Chabin-Brion et al. 2001) (Rios et al. 2004) (Maia et al. 2013).

Work in animal cells has identified additional non-centrosomal nucleation sites that are specific to mitosis. These will be discussed in the following paragraphs.

2. Microtubule organization throughout the cell cycle

The cell cycle is divided into two principal phases: interphase and mitosis. Some cells can escape the cell cycle; they don't divide anymore and become differentiated. These cells are specialized to carry out particular functions. Mitosis is the process of cell division; the DNA, the two centrosomes and other organelles will be segregated equally into the two daughter cells. Cell divisions can be asymmetric and specifically segregate certain factors that will influence the fate of the daughter cells. A special structure made up of microtubules, the mitotic spindle, is responsible for proper DNA segregation. In eukaryotes, cell cycle progression is regulated by several checkpoints. Active checkpoints prevent the transition from one phase to the next if some requirements are not met.

2.1 Interphase

The interphase is the longest phase of the cell cycle, corresponding to 90% of total time for a cell cycle. It is divided in three phases: G1, S, and G2 phases.

G1 and G2 phases are growth phases, the cell is producing proteins and synthetizes mRNA at a high rate, grows in size and the number of organelles (mitochondria, ribosomes) increase. Cell cycle exit and the start of differentiation happen from G1. At S-phase DNA replication starts. The cell will double its amount of DNA by copying once all the DNA content in order to transmit the complete genetic information during cell division. Precise and accurate DNA replication is require to prevent genetic abnormalities that often lead to cell death or disease.

Coupled with the DNA replication, the centrosome will duplicate resulting in two centrosomes containing two centrioles each.

In animal interphase cycling cells, the microtubule network is mainly organized by the centrosome in a radial array. The centrosome is located near the nucleus and microtubules extended toward the cell periphery with their plus ends exploring the cytoplasm in a very dynamic manner. Microtubules play a role in the positioning, organization and maintenance of different organelles in the cellular space. Microtubules oscillate between growths and depolymerization phases as described in 1.2.4. Differentiation and polarization of specialized cells cannot be completed without a proper microtubule array. The microtubule network is also involved in cell migration.

2.2 The microtubule network in mitosis

Animal mitosis is divided into several phases: prophase, prometaphase, metaphase, anaphase and telophase (Figure 10). The ultimate step of cell division involves the physical separation of the two daughter cells and is called cytokinesis.

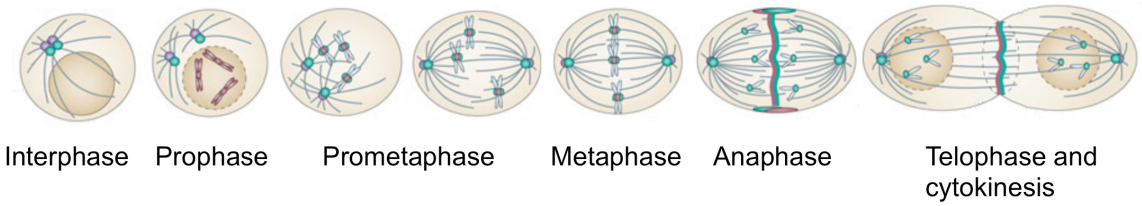

Figure 10. Microtubule organization during the cell cycle.

At the onset of mitosis, the interphase microtubule network is disassembled and centrosomes nucleate aster microtubules and migrate at opposite sides of the nucleus. At prometaphase, with NEB, microtubules invade the DNA area, attach the to chromosomes via their kinetochores and align them at the equatorial region in metaphase. When all sister chromatids are linked to the two poles, the cell enters anaphase and segregates the chromosomes. An acto-myosin network is set up at the center of the cell that will constrict the membrane until the physical separation of the two daughter cells during cytokinesis. Modified from (Rath & Kozielski 2012).

2.2.1. The mitotic spindle

At the onset of mitosis, the microtubule network is re-organized and the formation of the spindle takes place. Its assembly starts with the nucleation of microtubules at various sites (Duncan & Wakefield 2011) (Meunier & Vernos 2012).

Three populations of microtubules are distinguishable: kinetochore microtubules that are bundled in fibers and attach to the chromosomes by the kinetochores; interpolar microtubules that link the two opposite poles, and the astral microtubules which emerge from the centrosome toward the cell cortex (Meunier & Vernos 2012).

Several studies showed that the microtubules constituting the spindle have an identical orientation with the minus ends toward the centrosomes (Mastronarde et al. 1993) (Kamasaki et al. 2013).

2.2.2 Prophase

Prophase is the first part of mitosis during which DNA condensation and centrosome separation occur. During mitosis the cell needs to segregate its DNA content into the two daughter cells. To allow this, the interphase chromatin condenses into compact chromosomes. Since the DNA content has been replicated in S phase, the cell contains two copies of each chromosome called sister chromatids, which are connected by their centromeres.

The interphase microtubule network disassembles and the duplicated centrosomes, located near the nucleus, increase their microtubule nucleation capacity by recruitment of additional γTuRC (Khodjakov & Rieder 1999). Microtubules grow from both centrosomes and antiparallel microtubules emanating from the two centrosomes will be cross-linked by the KIF11 motor. Its plus end-directed motor activity will push the two centrosomes apart and position them at opposite sides of the nucleus (Ferenz et al. 2010). Dynein present at the surface of the nuclear envelope has also been proposed to contribute to centrosome separation (Raaijmakers et al. 2012).

2.2.3 Prometaphase

The prometaphase is sometimes not considered a separate phase but as a part of metaphase. Prometaphase is initiated by the disintegration of the nuclear envelope termed nuclear envelope breakdown (NEB), and the invasion of the nuclear space by microtubules. The chromosomes assemble a special proteinateous structure at their centromere termed kinetochore. Kinetochores are composed of many proteins and will serve as an interface for microtubule attachment and further mitosis progression) (DeLuca & Musacchio 2012).

2.2.4 Metaphase

At metaphase the condensation of chromosomes reaches its maximum, All chromosomes are connected to microtubules emanating from the two centrosomes and start migrating to the equator of the spindle. Pulling forces exerted by microtubules from both centrosomes result in the movement of the chromosomes to the exact center of the mitotic spindle. The proper attachment of sister kinetochores to microtubules emanating from opposite poles is called amphitelic attachment.

Improper attachment of microtubule at kinetochores will result in congression and alignment defects. Different types of attachment defects are observed: monotelic attachment, when only one kinetochore is bound to a spindle pole, syntelic attachment, when both sister kinetochores are connected to the same pole, and merotelic attachment, when one (or both) kinetochore is bound to the two poles instead of one (Guerrero et al. 2010) (Figure 11). The spindle assembly checkpoint (SAC) monitors the microtubule-kinetochore interactions and prevents the initiation of chromosome segregation until all attachments are corrected (Maiato et al. 2004), (Foley & Kapoor 2013).

Cell with super-numerous centrosomes often assemble a multipolar spindle. These additional poles eventually cluster by the action of several factors and form a bipolar spindle. Merotelic attachments are often observed in multipolar spindles and can lead to wrong chromosome distribution and genomic instability (Kramer et al. 2011).

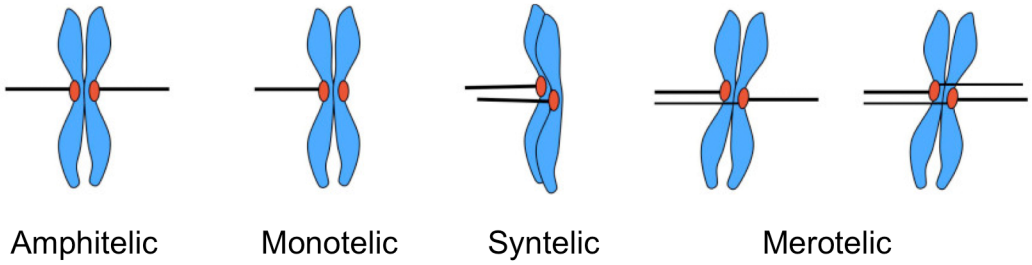

Figure 11.Kinetochores attachment errors.

In amphitelic attachment, the kinetochores from the sister chromatids are correctly connected to the two poles, resulting in a bi-oriented chromosome. If only one sister chromatid is attached to a single pole, the chromosome is mono-oriented and the attachment is called monotelic. In syntelic attachment, both sister chromatids are linked to the same pole and the chromosome is mono-oriented. If one or both sister kinetochores are connected to both poles the attachment is termed merotelic, in this case the chromosome is bi-oriented. Modified from (Guerrero et al. 2010).

2.2.5 Anaphase

Once the SAC is silenced, the anaphase-promoting complex (APC) gets activated, which leads to degradation of cyclin B and entry into anaphase. The APC also promotes the cleavage of the proteins that hold the chromatids together, which allows the physical separation of the sister chromatids. The released sister chromatids then migrate towards opposite poles, pulled by shortening kinetochore microtubules. Pushing forces exerted from KIF11 on interpolar microtubules and pulling forces on astral microtubules from the cortex increase the distance between the two poles and subsequently the associated chromosomes (Brust-Mascher & Scholey 2011).

New microtubules are generated within the spindle, or transported from the pole, to form the central spindle (Uehara & Goshima 2010).

2.2.6 Telophase and cytokinesis

When the two sets of chromosomes reach the opposite poles, cell division starts. Telophase is further defined by the reformation of the nuclear envelope and the decondensation of the chromosomes. DNA-bound microtubules depolymerize at this stage.

Cytokinesis involves formation of a contractile ring made of actin filaments and myosin that is set up at the cell cortex in the equatorial region. ATP hydrolysis by myosin triggers the contraction of the cell membrane, forming a cleavage furrow that will progress inward. Microtubules from the central spindle form bundles that are involved in the positioning of the contractile ring. When the progression of the contractile ring is maximal, it forms the midbody, which contains the bundles of microtubules. The final step of cytokinesis, abscission, consists of the cleavage of the midbody and therefore the physical separation of the two daughter cells (Green et al. 2012).

2.3 Microtubule nucleation in mitosis

2.3.1 Centrosomal nucleation

The best-characterized microtubule nucleation mechanism in animal mitosis is the centrosomal pathway. At the onset of mitosis, centrosomes increase in size and recruit additional γTuRC from the cytoplasm (Khodjakov & Rieder 1999) which increases their ability to nucleate microtubules (Piehl et al. 2004). At the beginning of prophase, two asters of microtubules emanate from the two centrosomes. At

NEB centrosomal microtubules invade the nuclear region and connect to kinetochores.

How this is achieved is not entirely clear, but according to the “search and capture” model (Kirschner & Mitchison 1986) (Figure 12), centrosomal microtubules explore the intracellular space in a random fashion until they find and “capture” a kinetochore. However, theoretical considerations suggest that this would be a rather inefficient mechanism that could not account for the efficiency of this process *in vivo* (Wollman et al. 2005). It was also shown that cells can assemble spindles and capture kinetochores without centrosomes. Higher plants, for example, do not have centrosomes and employ exclusively non-centrosomal nucleation pathways (H. Zhang & Dawe 2011). Furthermore, experimental removal (La Terra et al. 2005), destruction (Khodjakov et al. 2000) or inactivation (Bobinnec et al. 1998) of centrosomes does not disrupt mitotic spindle assembly and kinetochore capture by spindle microtubules.

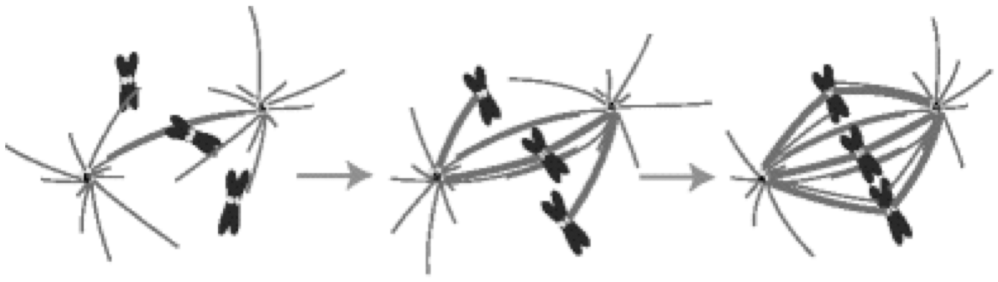

Figure 12. The search and capture model.

Centrosome-nucleated microtubules explore the cytoplasm until they attach to chromosomes by the kinetochores. When both sister kinetochores are connected to opposite poles, chromosomes are bi-oriented and align at the center of the spindle. Modified from (Heald & Walczak, 2008)

2.3.2 Chromosome-mediated nucleation

The first discovered non-centrosomal pathway for mitotic microtubule nucleation involves the chromatin (Witt et al. 1980), (Heald et al. 1996). During mitosis a Ran-GTP gradient is formed around the DNA by the action of the chromatin-bound guanine nucleotide exchange factor RCC-1 (Carazo-Salas et al. 1999), which converts Ran to the GTP-bound active form (Figure 13). In the vicinity of DNA, the level of Ran-GTP (Kaláb et al. 2002), (Kaláb et al. 2006) is high and triggers liberation of factors from importin, including TPX2 (Gruss et al. 2001), (Wittmann et al. 2000), NuMA (Wiese et al. 2001), (Nachury et al. 2001) and HURP (Sillje et al. 2006). These factors together with γTuRC and ch-Tog allow nucleation of short microtubules around the mitotic chromosomes (Groen et al. 2009) (Figure 13). The growth and organization of these microtubules by focusing factors (NuMA, KIFC1) leads to the formation of a bipolar mitotic spindle (Merdes et al. 1996), (Haren et al. 2009).

Early experiments revealed the capacity of kinetochores to organizes microtubules. Kinetochores have been suggested to nucleate microtubules through recruitment of γ-tubulin through the nuclear pore subcomplex Nup170-160 (Mishra et al. 2010). Nucleation of microtubules from the kinetochores seems to involve the RanGTP gradient (Tulu et al. 2006), (Torosantucci et al. 2008) and the chromosomal passenger complex (Tseng et al. 2010), (Sampath et al. 2004). I will refer to both chromatin and kinetochore-mediated nucleation as chromosome-mediated nucleation.

The discovery of chromosome-mediated microtubule assembly around mitotic DNA explained, how cells that naturally lack centrosomes or that had their centrosomal nucleation pathway inactivated experimentally, were still able to nucleate spindle microtubules. However, even in the presence of centrosomes, chromosome-dependent nucleation is involved in mitotic spindle assembly and microtubule attachment to kinetochores. Microtubules that grow from the DNA appear to

facilitate the “search and capture” of kinetochores by centrosomal microtubules (Maiato et al. 2004).

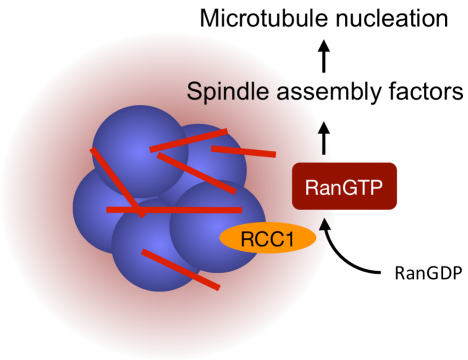

Figure 13. Ran-GTP mediated microtubule nucleation.

Chromatin bound RCC1 exchange the GDP bound to Ran into GTP forming a gradient surrounding the DNA. Close to the chromatin the high concentration of Ran-GTP activates several factors including NuMA, TPX2 and HURP. These factors trigger the nucleation of short microtubules in the vicinity of the DNA.

2.3.3 Nucleation form pre-existing microtubules

In 2008 Gohta Goshima described a protein complex termed augmin (or HAUS in humans) that allows microtubule nucleation from pre-existing microtubules in mitotic cells (Goshima et al. 2008) (Figure 14). This 8-subunit complex recruits γTuRC to pre-existing microtubules and its absence leads to a reduced microtubule density in the spindle, and, due to an imbalance of microtubule-dependent forces, to pole fragmentation and multi-polar spindles.

The exact roles of the eight HAUS subunits are not known, but HAUS8 (Hice1) seems to play a role in microtubule binding (Wu et al. 2008). HAUS6 was shown to recruit γTuRC by interacting with the γTuRC targeting subunit NEDD1 (Zhu et al.

2008). Serine 418 in NEDD1 is phosphorylated in mitosis and is crucial for γTuRC recruitment. Mutation of this residue to alanine (S418A) does not perturb centrosomal accumulation of γTuRC but impairs its recruitment along the spindle (Lüders et al. 2006), (Haren et al. 2006). Expression of this mutant in cells phenocopies depletion of HAUS. HAUS-dependent recruitment of γTuRC along pre-existing microtubules leads to “branching nucleation” of new microtubules and thus rapidly increases microtubule number in the forming mitotic spindle (Petry et al. 2013). Recently, the binding of HAUS to spindle microtubules was shown to be regulated by Plk1-dependent phosphorylation of HAUS8, which in turn is promoted by NEDD1-dependent Plk1 recruitment (Johmura et al. 2011).

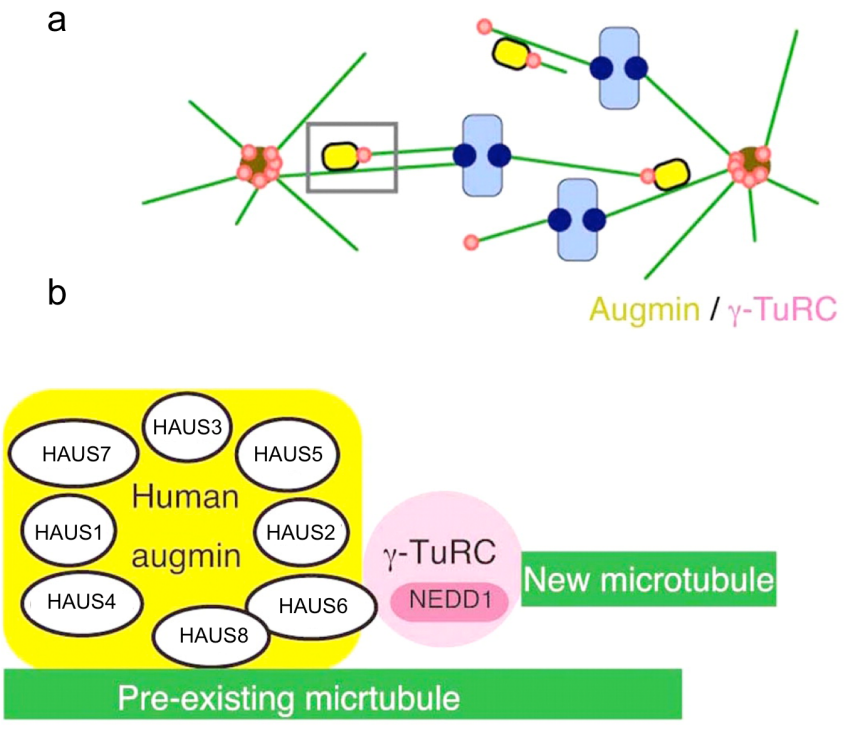

Figure 14. Microtubule generation from pre-existing microtubules.

(a) HAUS/γTuRC complexes are recruited along centrosomal microtubules and generate new microtubules increasing the microtubule density within the spindle. **(b)** HAUS8 subunit is thought to directly interact with the microtubule while HAUS6 recruits the γTuRC by interaction with the NEDD1 subunit. The roles of other HAUS subunits are not known to date. Modified from (Uehara et al. 2009).

2.3.4 Other pathways

The capacity of the nuclear envelope to nucleate and organize microtubules in differentiated cells is known and this could constitute an additional source of microtubules in mitosis. Indeed, studies in acentrosomal systems revealed the possibility of microtubule generation form remnant fragments of the nuclear envelope (Rebollo et al. 2004), (Schuh & Ellenberg 2007).

Microtubules have also been observed to be generated from no distinct region in the cytoplasm. In the presence of such microtubule in early mitosis, it has been shown that they are incorporated into the bipolar structure in a dynein-dependent manner (Tulu et al. 2003).

2.3.5 Spindle formation, a cooperative process

The observation of acentrosomal cells and organisms assembling a spindle through non-centrosomal mechanisms led to the discovery of additional microtubule nucleation pathways. Experimental disruption of the centrosome revealed the presence of these pathways even in centrosome-containing cells (Moutinho-Pereira et al. 2013) (Hayward et al. 2014) (Megraw et al. 2001).

Self-organization of a bipolar functional mitotic spindle from DNA-mediated nucleation raised the question of the necessity of the centrosome for cell division. The analysis of cell division after destruction of centrosomes (Khodjakov et al. 2000) (La Terra et al. 2005) (Bobinnec et al. 1998) and generation of adult flies without centrioles (Basto et al. 2006) showed that the centrosome is not strictly required for mitotic spindle formation and cell division. Increased genomic instability, difficulties to complete cytokinesis and impaired asymmetric division in

animal cells after centrosome disruption indicates that the centrosome might be an organelle that facilitates spindle assembly and ensures faithful chromosome segregation.

The simultaneous nucleation of microtubules from diverse pathways in animal cells is now accepted and the cooperation of these pathways is what drives the fast assembly of a robust bipolar spindle (Duncan & Wakefield 2011) (Meunier & Vernos 2012) (Figure 15).

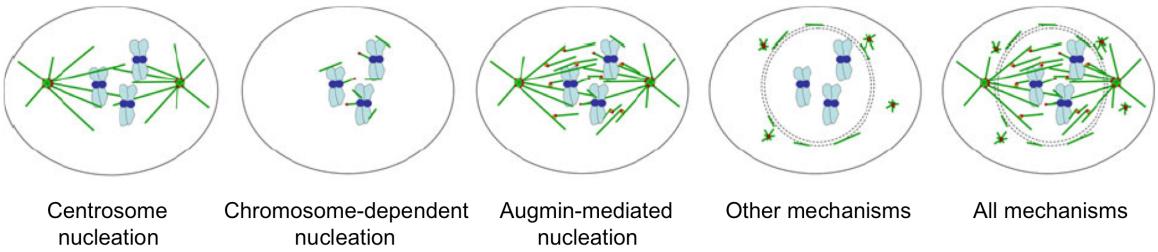

Figure 15. Microtubule nucleation in mitosis.

In centrosome containing cells, this organelle is the main source of microtubules. Additionally microtubules are nucleated in the vicinity of the DNA. HAUS recruits γTuRC at these microtubules and triggers new nucleation, increasing microtubule density. Other pathways can occur in some cells. All the pathways together ensure proper formation of the bipolar mitotic spindle and correct chromosome segregation. Adapted from (Duncan & Wakefield 2011).

2.3.6 γTuRC localization and dynamics in mitosis

As the complex in charge of microtubule nucleation, the localization of the γTuRC during mitosis has been investigated previously. Immunostaining directed against any element of the complex, shows the presence of the complex in a soluble form in the cytoplasm, in a concentrated form at the centrosomes and, more diffusely, along the spindle (Lajoie-Mazenc et al. 1994) (Moudjou et al. 1996).

In 1999, Khodjakov & Rieder studied the dynamics of γ-tubulin at the centrosome in mitosis (Khodjakov & Rieder 1999). They observed a sudden increase in the amount of γ-tubulin from the end of G2 to metaphase. This correlated with an increased microtubule nucleation ability of the centrosomes at these stages. At metaphase, the centrosomal amount of γ-tubulin reached a plateau before a reduction occured at anaphase onset. FRAP experiments directed at the centrosome in the absence of microtubules led to the recovery of the fluorescence (50% of recovery after 45min), suggesting that centrosomal γ-tubulin exchanges with the cytoplasmic pool and that recruitment at the centrosome is microtubule-independent.

The dynamics of spindle bound γ-tubulin are poorly understood. One study using FRAP in Drosophila S2 cells concluded that γ-tubulin only transiently interacted with microtubules, allowing fast nucleation followed by release of γTuRC (Hallen et al. 2008).

3. Objectives and strategies of the thesis

3.1 Analysis of microtubule minus end dynamics within the spindle

The generation of microtubules by three different pathways (centrosomal, RanGTP-mediated and HAUS-dependent) raises the question how these microtubules from different origins are organized to form a proper bipolar spindle. Due to their intrinsic polarity, microtubules present two distinct extremities, the plus-end and the minus-end. Information about distribution and dynamics of the two ends are essential for a better understanding of spindle assembly and architecture. For the plus ends, information can be obtained using the EB1 protein as a marker, which labels all growing plus ends. Understanding the orientation of centrosome-nucleated microtubules is straight forward; considering that the nucleator complex is present in the pericentriolar material, the minus ends will be attached to the pole and the plus ends exploring the cytoplasm. In the case of non-centrosomal microtubules, however, we lack a reliable probe for their minus ends. As previously discussed, we only know that at metaphase the minus ends of non-centrosomal microtubules are present throughout the spindle with a higher concentration near the poles. A model has been proposed where the microtubules generated away from the centrosome, would slide along centrosomal microtubules with the minus ends directed to the pole but there is no direct experimental evidence to support this model (Burbank et al. 2007).

My objectives were i) to identify and characterize a minus end marker for non-centrosomal microtubules in mitosis, and ii) to analyze the dynamics of these minus ends in the mitotic spindle. The overall goal was to better understand how microtubules generated away from the centrosome were integrated and organized to participate in the formation of a robust bipolar spindle.

To achieve this, I speculated that the nucleator complex γTuRC could be used as a probe for minus ends. I confirmed this hypothesis by analyzing its distribution along the spindle and by generating a γ-tubulin mutant that was unable to bind to microtubule minus ends. I then generated a fusion of γ-tubulin with photoactivatable GFP in order to analyze the dynamics of γTuRC within confined regions of mitotic cells.

3.2 Modalities of mitotic spindle formation in absence of centrosomes

Considering that at mitotic onset most animal cells possess highly active centrosomes, the analysis of the existence and contribution of additional nucleation pathways in the presence of centrosomes has been challenging. Several strategies have been developed to eliminate centrosomal microtubule generation and allow the analysis of alternative pathways. Most studies concluded that centrosomes are dispensable for mitotic spindle assembly and bipolar division and that these functions can be carried out by non-centrosomal mechanisms alone (Khodjakov et al. 2000) (Uetake & Sluder 2007) (Moutinho-Pereira et al. 2009) (Lecland et al. 2013). However, since such studies are more challenging in mammalian somatic cells, there is only limited data available on acentrosomal mitotic spindle assembly and division in this system.

My objectives were i) to establish a model that would allow elimination of centrosomes in mammalian somatic cells, and ii) to study acentrosomal mitosis in this model. The overall goal was to test if previous observations made in similar models are generally applicable or rather are cell type/model-specific.

To achive this I decided to use laser-directed centrosome ablation in pig LLC-PK cells. Laser ablation of centrosomes has been established previously to study acentrosomal mitoses in somatic animal cells (Khodjakov et al. 2000) (Uetake & Sluder 2007). Pig LLC-PK cells were chosen due to their flat morphology during both interphase and mitosis, which facilitates microscopic manipulation and imaging. Since the pig genome is almost completely sequenced this model would also make future RNAi-based functional studies straight forward.

Materials and methods

Molecular biology

The mCherry-α-tubulin plasmid was obtained from Addgene (Addgene 21043).

The Centrin2-GFP plasmid was a generous gift from Tim Stearns.

A plasmid expressing full length NEDD1-EGFP was constructed by inserting the NEDD1 sequence into pEGFP-N1 (Clontech). For simultaneous expression of shRNA from the same plasmid the NEDD1 shRNA expression cassette from pSUPER-NEDD1 was excised (EcoRI/KpnI), blunted and inserted into the DraIII site of pNEDD1-EGFP. Point mutations in the NEDD1 sequence to generate an RNAi resistant version and NEDD1 Y643A/S644A mutations were introduced by site-directed.

To obtain a plasmid coding for γ-tubulin tagged by photoactivitable GFP or mycHis, EGFP from pEGFP-N1 was cut out and replaced by paGFP or mycHis tag. Full-length γ-tubulin was then inserted on the N-terminus side of the tags. For simultaneous expression of shRNA from the same plasmid the γ-tubulin shRNA expression cassette from the plasmid p120194sh (Vinopal et al. 2012) was excised (NotI/EcoRI), blunted and inserted into the DraIII site of γ-tubulin-mycHis or γ-tubulin-paGFP plasmids. The shRNA targets the TUBG1 3'UTR so that expression of plasmid-encoded TUBG1 is not affected. γ-tubulin D176A, E177A, S179A, D180A mutants were obtained by site-directed mutation.

For depletion of KIFC1 I used previously described siRNA (5'-UCA GAA GCA GCC CUG UCA A-3') (Cai et al. 2009).

Cell Culture and treatments

LLC-PK, U2OS and Hela cell lines were grown in DMEM containing 10% fetal calf serum. Cells were transfected with plasmid or siRNA using Lipofectamine 2000 or Lipofectamine RNAiMAX (Invitrogen), respectively.

To generate a U2OS cell line stably expressing γ-tubulin-paGFP cells were transfected with γ-tubulin-paGFP and mCherry-α-tubulin expression plasmids and selected in the presence of 0.4 μg/ml geneticin and 20 μg/ml puromycin. Resistant clones were isolated and tested for expression of the tagged proteins.

To generate a LLC-PK cell line stably expressing Centrin-GFP and mCherry-α-tubulin, cells were transfected with corresponding plasmids and selected in presence of 0.4 μg/ml geneticin. Resistant clones were isolated and tested for expression of the tagged proteins.

For microtubule depolymerization and regrowth experiments, dishes containing coverslips with cells were incubated with 250 ng/ml nocodazole over night. Nocodazole was then washed out and coverslips were incubated for 30 min in an ice-water bath to depolymerize microtubules followed by -20°C methanol fixation. For mitotic microtubule regrowth experiments, coverslips were then incubated in medium at 37°C before -20°C methanol fixation. For fast microtubule depolymerization after γ-tubulin transport, nocodazole was added (5 μg/ml) during imaging. For microtubule depolymerization prior to imaging, cells were incubated with 1 μg/ml nocodazole for 1 hour.

For inhibition of dynein cells were incubated with 32 μM EHNA, or incubated at least two hours in MG132, to enrich bipolar mitotic cells, followed by addition of 50 μM Ciliobrevin D for 30 min. To inhibit KIF11 in bipolar spindles, cells were incubated with 5 μM MG132 to enrich mitotic cells with bipolar spindles followed by addition of 50 μM STLC for 30 min, for analysis of monopolar spindle, cells were

incubated with 50 μM without prior MG132 treatment. Inhibition of KIFC1 was done by RNAi-mediated depletion. Cells were analyzed 72 hours after transfection of siRNA.

Antibodies

The anti-HAUS6 antibody was generated prior to my arrival.

Other antibodies used in this study were: mouse anti-Myc (monoclonal 9E10); rabbit anti-Myc (c-Myc A14; Santa Cruz Biotechnology); mouse anti-γ-tubulin (GTU-88; Sigma); mouse anti-α-tubulin (DM1A; Sigma); rabbit anti-NEDD1; mouse anti-NEDD1 (7D10, Abnova), rabbit anti-pericentrin; rabbit anti-GFP (Torrey Pines Biolabs); mouse anti-GFP (3E6; Invitrogen); mouse anti-GAPDH (GAPDH 0411, Santa Cruz Biotechnology); rabbit anti-GCP3 (Proteintech group); rabbit anti-GCP6 (ab95172, abcam); rabbit anti-TPX2 (gift of Isabelle Vernos, CRG, Barcelona, Spain); rabbit anti-KIFC1 (orb101014, biorbyt).

Alexa dye-conjugated secondary antibodies used for immunofluorescence microscopy were from Invitrogen, and peroxidase-coupled secondary antibodies for western blotting were from Jackson Immunoresearch Laboratories.

Immunoprecipitation and western blotting

For immunoprecipitation of EGFP-tagged NEDD1 and myc-his tagged γ-tubulin transfected Hela cells were washed in PBS and lysed (50 mM HEPES, pH 7.5, 150 mM NaCl, 1 mM MgCl2, 1 mM EGTA, 0.5% NP-40, protease inhibitors) for 10 min on ice. After centrifugation for 15 min at 16,000g at 4°C cleared lysates were

incubated with anti-GFP or anti-myc antibodies for 2 hours at 4°C in presence of sepharose Protein G beads. The beads were pelleted and washed three times with lysis buffer. Samples were prepared for SDS-PAGE by boiling in sample buffer (0.5M Bis-Tris, 0.3M HCl, 20% glycerol, 8%SDS, 2mM EDTA, 0.06% bromophenol blue, 5%β-mercaptoethanol). Samples were loaded in an acrylamyde gel (4% for stacking and 8% for separation) and run at 120mV in MOPS buffer (2.5mM MOPS, 2.5mM Tris-base, 0.005% SDS, 0.05mM EDTA). Proteins were transferred to membranes for 1hour at 400mA in transfer buffer (2.5mM Tris-base, 192mM glycine, 20% methanol). Membranes were blocked in TBS-T (2.5mM Tris-base, 137mM NaCl, 2.7mM KCl, 0.1% tween20) + milk (5%) and probed with antibodies diluted in TBS-T + milk. Membranes were washed with TBS-T between each incubation.

Immunofluorescence Microscopy

Cells grown on coverslips were fixed in methanol at -20°C for at least 5 min and processed for immunofluorescence. Fixed cells were blocked in PBS-BT (1X PBS, 0.1% triton, 3% BSA) for 30 min, incubated with primary antibodies followed by secondary antibodies and finally with DAPI solution to stain the DNA. Coverslips were washed with PBS-BT between each incubation. Antibodies/DAPI solutions were diluted in PBS-BT to there working concentration. Images were acquired with an Orca AG camera (Hamamatsu, Bridgewater, NJ) on a Leica DMI6000B microscope equipped with 1.4 NA 100x oil immersion objective. AF6000 software (Leica, Wetzlar, Germany) was used for image acquisition and deconvolution.

Photoactivation and time lapse microscopy

For photoactivation experiments cells stably expressing γ-tubulin-paGFP and mCherry-α-tubulin or cells transiently transfected with plasmids for expression of γ-tubulin-paGFP/γ-tubulin shRNA and mCherry-α-tubulin or γ-tubulin 4A mutant-paGFP/γ-tubulin shRNA and mCherry-α-tubulin (3:1 ratio, respectively) were plated in glass bottom dishes. Cells were treated with drugs and/or KIFC1 siRNA and observed in an Olympus IX81 microscope equipped with an Yokogawa CSU-X1 spinning disc, a temperature-controlled CO_2 incubation chamber and a FRAPPA module for photoactivation. Images were acquired with 1.4 NA 100x oil immersion objective and an iXon EMCCD Andor DU-897 camera. iQ2 software was used for the acquisition. Photoactivation was performed by pulses from a 405nm laser directed on a selected area. For spindle transport and centrosome recruitment experiments stacks of five or fifteen images, respectively, were acquired every 5 or 15 seconds. For further image processing and quantification of fluorescence intensities ImageJ software was used.

Laser ablation and time lapse microscopy

Laser ablations were performed in a Zeiss microscope equipped with 1.2 NA 63x water immersion objective and a stage insert to control temperature and CO2 environment. Two 450Hz laser pulses at a wavelength of 355nm were applied to a 75 points region corresponding to the centrin-GFP labeling. The positions of the ablated cells were marked by drawing a square on the glass using laser shots. Cells were then fixed for immunofluorescence or moved to an Olympus ScanR microscope equipped with a 0.75 NA 40x objective and a temperature-controlled CO_2 incubation chamber for long term time-lapse imaging. Images were acquired with a Hamamatsu Orca-ER camera using Xcellence software. Stacks of 3 images were acquired every 5 minutes. For further image processing, ImageJ software was used.

Image processing and quantifications

For image processing and quantification of fluorescence intensities ImageJ software was used. Intensities were measured in images acquired with constant exposure settings.

To measure intensity distributions in half spindles a mask restricting the analysis to the spindle area was applied to maximum projection images. For individual half spindles mean intensities in 1-pixel line across the spindle width were measured along the entire length of half spindle axes excluding the centrosome area. This was automated using a custom-written macro. For centrosomes and microtubule asters, mean intensities were measured in a circular area around centrosomes (2 µM and 5 µM diameter, respectively). For background-correction the mean intensity measured in an adjacent area in the cytoplasm was subtracted.

To analyse changes in the distribution of photoactivation marks a mask restricting measurements to the spindle area was applied to maximum projection images of individual time points. Each time series of images was stacked and processed using the transformJ plugin of ImageJ. By projecting maximum intensities of the Y dimension (spindle width) kymographs were obtained. To calculate movement rates the slopes of marks in kymographs were determined using ImageJ software. Values were corrected for any centrosome movement that occurred during image acquisition.

Two-tailed, unpaired t-tests were performed for statistical analysis using Prism 6 software.

Results

1. The dynamics of microtubule minus ends in the mitotic spindle

1.1 γTuRC distribution along the mitotic spindle

1.1.1 γTuRC accumulates in pole-proximal spindle regions

In vertebrates, most of the minus ends are found near the poles in metaphase. To test if a similar distribution was observed for the nucleator complex γTuRC, I fixed Hela cells and stained them using antibodies directed against two subunit of the γTuRC: γ-tubulin and NEDD1. Antibody directed against α-tubulin was used in order to label the microtubules. Both γTuRC subunits showed a similar uneven distribution along the spindle axis, characterized by an enrichment close to the poles (Figure 16a). Since microtubule density was also higher near the poles, where microtubules converge, I decided to quantify the distribution of γTuRC subunits relative to α-tubulin staining. Even after normalization to the distribution of α-tubulin these quantifications revealed a clear accumulation of γTuRC complexes near the poles (Figure 16b). Using antibodies directed against an HAUS subunit (HAUS6) I observed that the HAUS complex was more evenly distributed along the microtubules lattice. Identical results were obtained in U2OS cells (Figure 16c, d). I concluded that the distribution of γTuRC subunits in the mitotic spindle is different from the distribution of HAUS, but matches the previously described distribution of microtubule minus ends in the spindle.

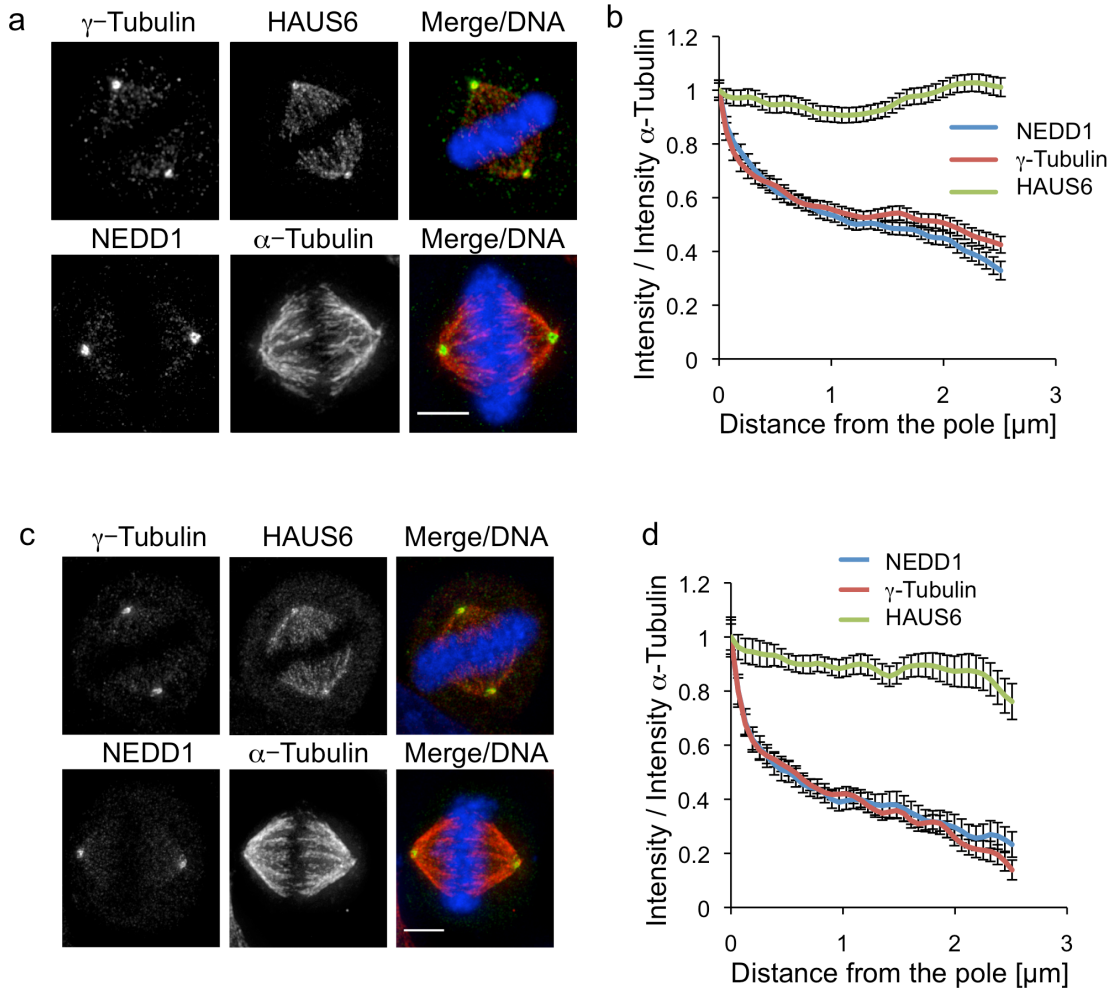

Figure 16. γTuRC pole-proximal accumulation.

(a) Immunofluorescence microscopy images of Hela cells fixed and stained with antibodies against γ-tubulin, NEDD1, HAUS6 and α-tubulin as indicated. DAPI was used to stain DNA. Scale bar, 5µm. **(b)** Fluorescence intensities in half-spindles of Hela cells prepared as in **a** were quantified along the spindle axis and plotted relative to the α-tubulin intensities as a function of distance from the spindle poles. For each protein the intensity closest to the pole was set to one. Values are means (error bars, SEM) of a total of 96 half-spindles from three independent experiments. **(c)** Immunofluorescence microscopy images of U2OS cells prepared as in **a**. Scale bar, 5µm. **(d)** Fluorescence intensities of U2OS cells prepared as in **c** and plotted as in **b**. Values are means (error bars (SEM) of a total of 30 half-spindles.

1.1.2 γ-Tubulin binding to microtubule minus ends is required for pole-proximal accumulation

To confirm that γTuRC was indeed associated with minus ends of non-centrosomal microtubules in the spindle I generated a mutant of the γ-tubulin subunit. It was known from previous work that within the microtubule protofilaments β-tubulin from one heterodimer interacts longitudinally with α-tubulin from the next heterodimer. It has been suggested that similar interactions occur between γ-tubulin in the γTuRC and α-tubulin that is exposed at the microtubule minus end. Mutation of four residues (D176A, E177A, S179A, D180A) in this interaction surface in human γ-tubulin was shown to cause cold-sensitivity or lethality in *Schizosaccharomyces pombe* depending on the presence or absence of endogenous γ-tubulin (Hendrickson et al. 2001).

I introduced the four mutations D176A, E177A, S179A, and D180A into human γ-tubulin (4A mutant) (Figure 17a) and expressed the mutant in cells partially depleted for endogenous γ-tubulin by co-expression of γ-tubulin shRNA (Figure 17b). The γ-tubulin shRNA was targeted at the 5'UTR of endogenous γ-tubulin and did not affect expression of the recombinant protein. The ability of the 4A mutant to assemble into γTuRC was verified by co-immunoprecipitation with other γTuRC subunits (Figure 17c). I also tested the recruitment of the mutant to the centrosome in both interphase and mitosis by immunostaining (Figure 17d, Figure 18c), and confirmed that it was similar to wild type γ-tubulin.

To test the ability of this mutant to interact with microtubule minus ends, I performed a microtubule nucleation assay. Cells were arrested in mitosis by nocodazole incubation followed by a cold treatment to completely depolymerize microtubules. Cells were then incubated at 37°C to allow microtubule regrowth. Cells depleted for endogenous γ-tubulin and expressing wild type γ-tubulin, showed normal microtubule nucleation ability illustrated by an aster of microtubules growing from the centrosome. In the case of γ-tubulin 4A expressing cells, microtubule

nucleation was strongly impaired and fluorescence intensity was decreased by 63% (Figure 18a, b). I also analyzed spindle assembly in mutant expressing cells. Treatment with γ-tubulin shRNA caused an increase in the number of mitotic cells with monopolar spindles (73% of the mitosis compare to 6.7% in control cells), but no significant increase in the total mitotic population (7.9% in cells depleted versus 6.2% in control cells), which was consistent with a partial depletion of γ-tubulin. Expression of wild type γ-tubulin fully rescued these defects.

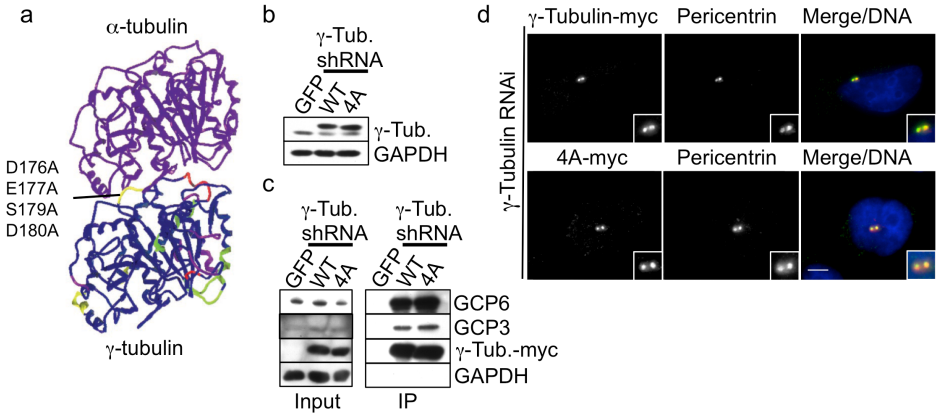

Figure 17. γ-tubulin 4A mutant forms γTuRC and localizes to centrosomes.

(a) Representation of the predicted longitudinal interaction of γ-tubulin with α-tubulin. Sites of mutations in the 4A-mutant are indicated. Modified from (Hendrickson et al. 2001). **(b)** Hela cells were transfected with plasmids expressing EGFP as a control, or expressing γ-tubulin shRNA in combination with myc-tagged γ-tubulin wild type, or myc-tagged γ-tubulin 4A mutant, respectively. After 72 hours lysates were prepared and probed by western blotting with antibodies against γ-tubulin and GAPDH as loading control. **(c)** Cells were transfected as in **b**. Lysates were prepared and immunoprecipitated with anti-myc antibody. Samples were probed with antibodies against the indicated proteins by western blotting. **(d)** Hela cells were transfected with plasmids expressing γ-tubulin shRNA in combination with myc-tagged γ-tubulin wild type or myc-tagged γ-tubulin 4A mutant. After 72 hours cells were fixed and stained with anti-myc and anti-pericentrin antibodies; DAPI was used to label DNA. Scale bar, 5 μm.

However, in cells expressing the 4A mutant a strong increase in the mitotic index was observed (18.5%). Moreover 73% of mitotic cells presented monopolar spindles (Figure 18d, e).

Together these results indicated a specific disruption of the interaction with α-tubulin at the interface of the γTuRC in cells expressing the γ-tubulin 4A mutant.

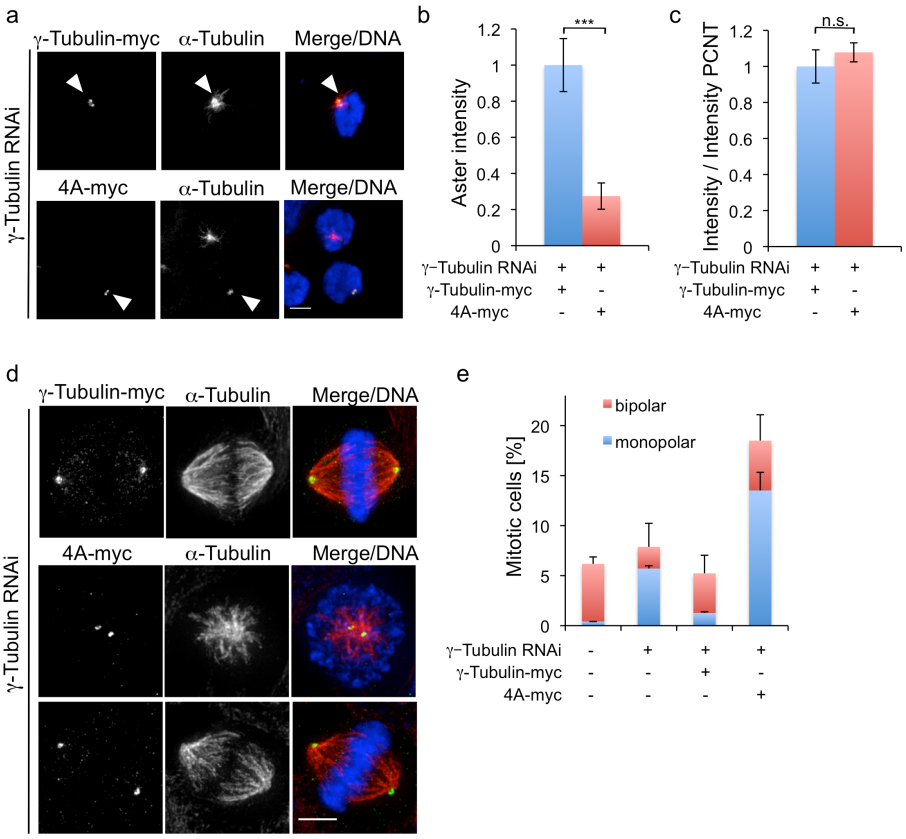

Figure 18. γ-tubulin 4A mutant present defects in minus end binding.

(a) Cells were transfected as in Figure 17**c**. After 60 hours cells were arrested in mitosis by incubation in nocodazole over night and a microtubule regrowth assay was performed. After one minute of regrowth cells were fixed and stained with anti-myc and anti-α-tubulin antibodies. DAPI was used to label DNA. Scale bar, 5 µm. **(b)** Fluorescence intensities of microtubule asters in the regrowth assay shown in **a**, were quantified. The mean aster intensity in cells expressing wild type γ-tubulin was set to one (error bars, SEM; at least 28 asters for each condition from two independent experiments; *** p<0.001). **(c)** Cells were transfected as in **a**. After 72 hours cells were arrested in mitosis by incubation with nocodazole for 5 hours and cold-treated to depolymerize microtubules. Cells were fixed and stained with antibodies against myc-tag and pericentrin. The fluorescence intensities of myc-tagged wild type and mutant γ-tubulin at mitotic centrosomes in the absence of microtubules were quantified relative to the intensity of pericentrin staining. The mean value obtained for cells expressing wild type γ-tubulin was set to one (error bars, SEM; at least 25 centrosomes per condition). **(d)** Cells transfected as in **a** were fixed and stained with anti-myc and anti-α-tubulin antibodies; DAPI was used to label DNA. Scale bar, 5 µm. **(e)** Cells were transfected with EGFP, EGFP and γ-tubulin shRNA expressing plasmid, or plasmid expressing γ-tubulin shRNA in combination with myc-tagged γ-tubulin wild type or myc-tagged γ-tubulin 4A mutant as indicated. After 72 hours cells were fixed and stained with anti-GFP or anti-myc antibodies and anti-α-tubulin antibodies. DAPI was used to label DNA. Mitotic figures in transfected cells were quantified by microscopic counting. For each of the indicated conditions the percentage of total mitotic cells, cells with bipolar spindles, and cells with monopolar spindles were determined and plotted. Values are means of two independent experiments (error bars, SD; in each experiment at least 250 cells per condition).

As commented, cells expressing the mutant form of γ-tubulin mainly presented monopolar spindles, but a fraction of mitotic cells still assembled bipolar spindles that allowed the analysis of protein distribution along the spindle axis. The distribution of wild type γ-tubulin was similar to the distribution of endogenous γ-tubulin (Figure 19a, b). In contrast, the 4A mutant showed a reduced recruitment along the spindle (68% of wild type intensity, Figure 19c). Importantly, the strongest reduction was observed in the pole-proximal region (Figure 19a, b). These results demonstrate that the γTuRC accumulates in pole-proximal spindle regions through interaction with microtubule minus ends.

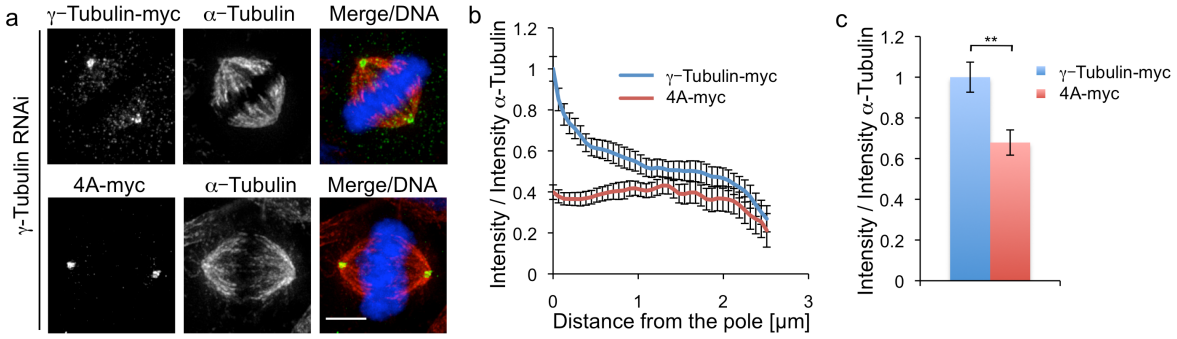

Figure 19. Microtubule minus end binding is necessary to properly distribute γTuRC along the spindle.

(a) Hela cells were transfected with plasmids expressing γ-tubulin shRNA and myc-tagged γ-tubulin wild type or 4A mutant. After 72 hours cells were fixed and stained with anti-myc and anti-α-tubulin antibodies, and DAPI to label DNA. Scale bar, 5 µm. **(b)** Fluorescence intensity distributions along the spindle axis of cells prepared as in **a** were quantified and plotted as in Figure 16**b**. The intensity of wild type γ-tubulin closest to the pole was set to one. Values are means (error bars, SEM) of a total of 56 half-spindles from three independent experiments. **(c)** Cells were prepared as in **a** and total fluorescence intensities of myc-tagged γ-tubulin wild type or 4A mutant in half-spindles along a length of 2.5 µm were quantified and plotted relative to the intensity of α-tubulin staining. The intensity obtained for wild type γ-tubulin was set to one. Values are means of a total of 56 half-spindles from three independent experiments (error bars, SEM; ** $p<0.01$).

1.1.3 Correct distribution of the HAUS complex and NEDD1 requires interaction with the γTuRC

Localization of the γTuRC has been demonstrated to be dependent on its NEDD1 subunit. Indeed NEDD1 targets the complex to the centrosome and, through interaction with HAUS, to the mitotic spindle. In this model the localization of NEDD1 and HAUS along the spindle may be independent of their binding to the γTuRC.

To test this I expressed several forms of the NEDD1 subunit in cells previously depleted for the endogenous protein: the S418A mutant previously described for its loss of interaction with HAUS and inability to target to spindle microtubules (Lüders et al. 2006), and the Y643A/S644A mutant (Manning et al. 2010). The Y643A/S644A mutant correctly localized to the centrosome but perturbed the recruitment of γ-tubulin at this site (Figure 20a, b). By immunoprecipitation, I further showed that the Y643A/S644A mutant is able to bind HAUS but not γTuRC (Figure 20c).

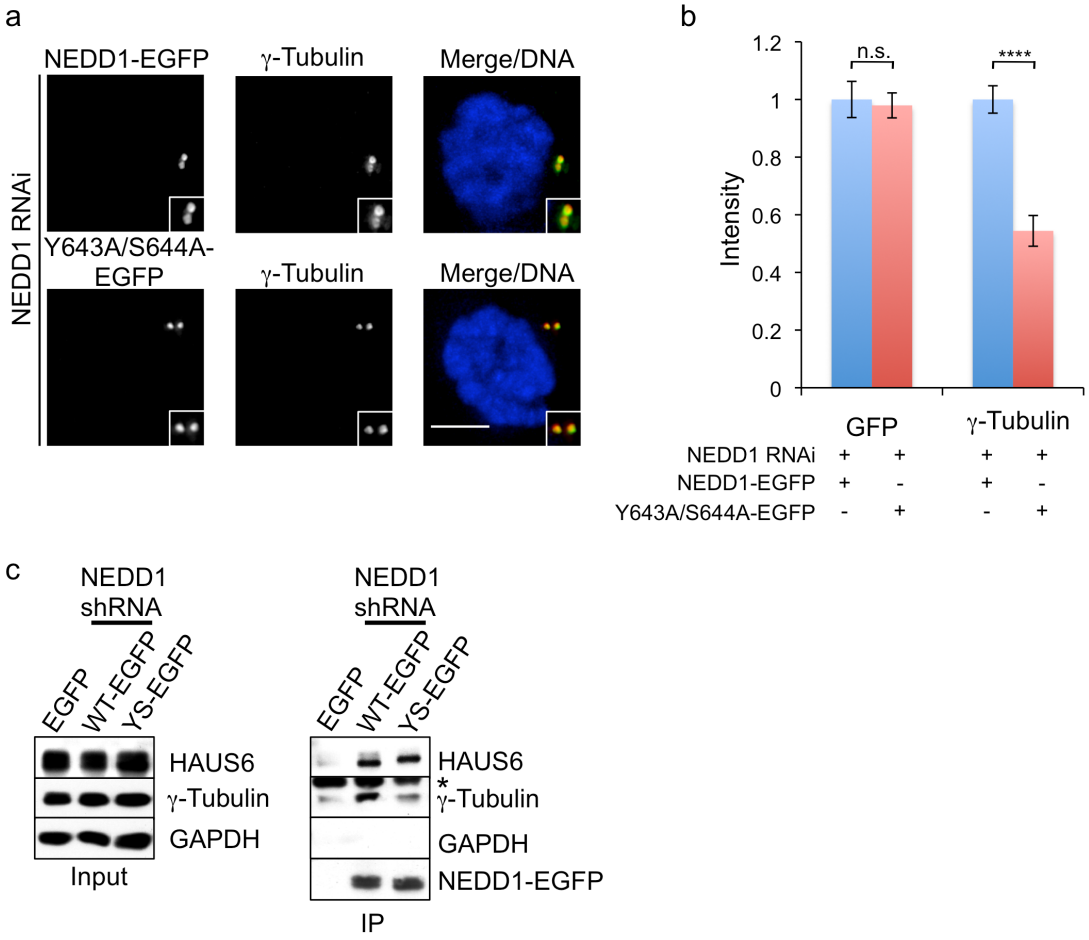

Figure 20. NEDD1 Y643A/S644A mutant binds to HAUS but not to γTuRC.

(a) Hela cells were transfected with plasmids expressing NEDD1 shRNA and EGFP-tagged NEDD1 wild type or Y643A/S644A mutant. After 48 hours cells were arrested in mitosis by incubation in nocodazole for 5 hours and cold treatment to depolymerize microtubules. Cells were fixed and stained with antibodies against GFP and γ-tubulin; DAPI was used to label DNA. Scale bar, 5 μm. **(b)** Cells were prepared as in **a** and for each condition the fluorescence intensities of the indicated proteins at centrosomes in the absence of microtubules were quantified. The mean intensities obtained for cells expressing wild type NEDD1-EGFP was set to one (error bars, SEM; at least 25 centrosomes per condition; **** $p<0.0001$). **(c)** Cells were transfected with plasmids expressing EGFP, or NEDD1 shRNA in combination with EGFP-tagged NEDD1 wild type or EGFP tagged NEDD1 Y643A/S644A mutant, respectively. After 48 hours cells were arrested in mitosis by incubation in nocodazole over night. Mitotic extracts were prepared and immunoprecipitated with anti-GFP antibody. Samples were probed with antibodies against the indicated proteins by western blotting. The asterisk indicates cross-reactivity with the IgG heavy chain derived from the anti-GFP antibody used for immunoprecipitation.

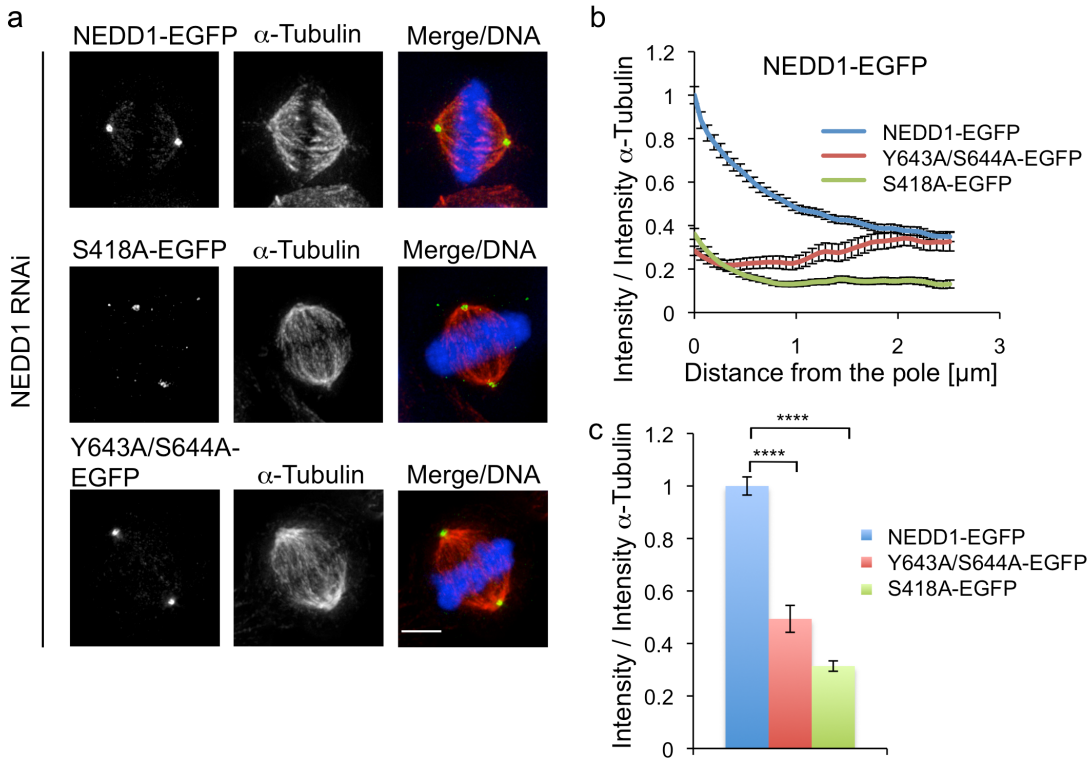

Figure 21. NEDD1 localization is dependent of its interaction with HAUS and the γTuRC.

(a) Hela cells transfected with plasmids expressing NEDD1 shRNA and EGFP-tagged NEDD1 wild type or Y643A/S644A and S418A mutants were fixed and stained after 48 hours with antibodies against GFP and α-tubulin, DNA was stained with DAPI. Scale bars, 5 µm. **(b)** Fluorescence intensity distributions of NEDD1-EGFP in half-spindles of cells prepared as in **a** quantified and plotted relative to α-tubulin as described in Figure 16**b**. The value closest to the pole obtained in cells expressing wild type NEDD1-EGFP was set to one. Values are means (error bars, SEM) of a total of 64 half-spindles from three independent experiments **(c)** Cells were prepared as in **a** and total fluorescence intensities of GFP-tagged NEDD1 wild type or Y643A/S644A and S418A mutant in half-spindles along a length of 2.5 µm were quantified and plotted relative to the intensity of α-tubulin staining. The intensity obtained for wild type NEDD1 was set to one. Values are means of a total of 64 half-spindles from three independent experiments (error bars, SEM; **** p<0.0001).

As expected expression of the wild type RNAi resistant form of NEDD1 presented a distribution similar to the endogenous protein. The S418A mutant was delocalized from the spindle lattice but strongly present at the centrosome (Figure 21a, c). The small amount of S418A protein observed on the spindle did not present any particular accumulation (Figure 21a, b) Surprisingly both the amount of NEDD1 Y643A/S644A and its distribution along the spindle were also strongly

perturbed (Figure 21a, b, c) indicating that not only interaction with HAUS but also binding to the γTuRC is required for targeting and correct distribution of NEDD1 along the spindle.

In untreated cells, HAUS complex was distributed in a different way than the γTuRC complex, presenting a more even distribution along the microtubule lattice. I repeated this analysis in cells expressing these two NEDD1 mutants in order to see if disturbing NEDD1/HAUS interaction or the ability of NEDD1 to bind γTuRC could influence the distribution of the HAUS complex. Expression of the NEDD1 mutants did not significantly reduce HAUS on the spindle microtubules (Figure 22a, c). In contrast, its distribution along the spindle was clearly affected; HAUS was reduced in the pole-proximal region and slightly increased in the center of the spindle (Figure 22a, b, c). Together these results demonstrate that HAUS does not need γTuRC interaction to bind the microtubules but for the proper distribution of along the spindle.

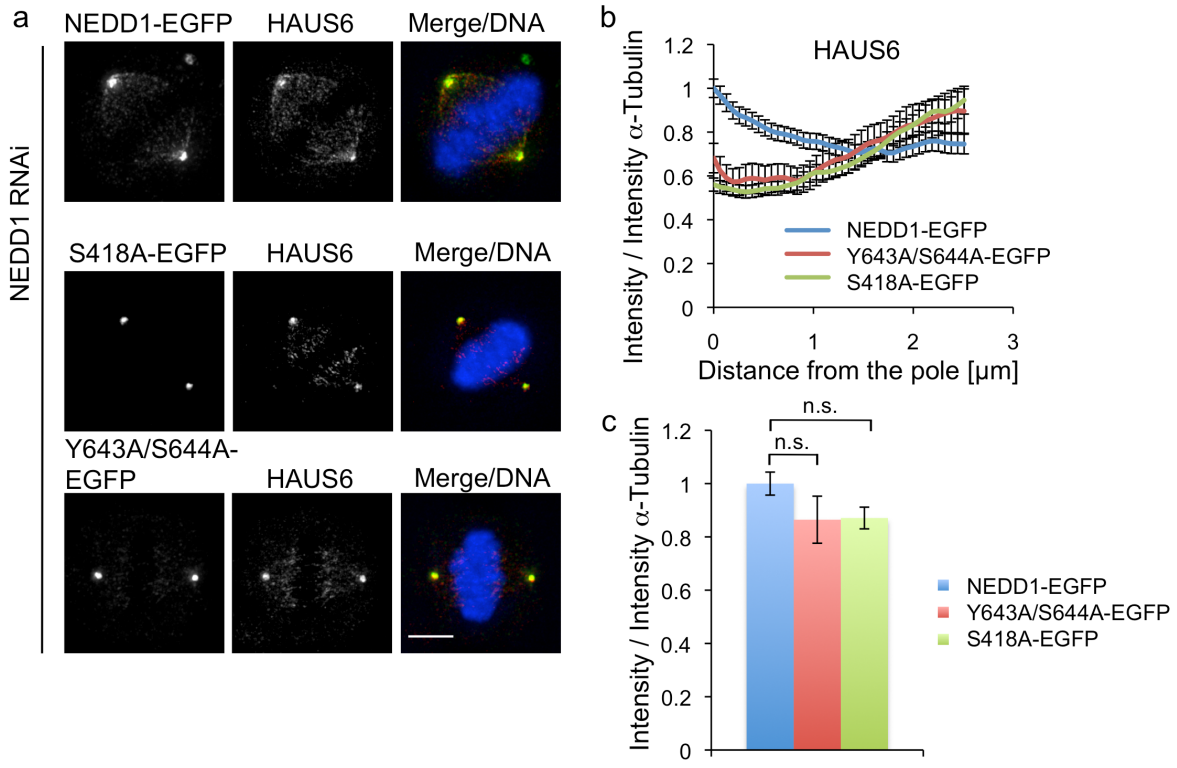

Figure 22. HAUS complex distribution requires functional γTuRC binding.

(a) Hela cells transfected with plasmids expressing NEDD1 shRNA and EGFP-tagged NEDD1 wild type or Y643A/S644A and S418A mutants were fixed and stained after 48 hours with antibodies against GFP and HAUS6, DNA was stained with DAPI. Scale bars, 5 µm. **(b)** Fluorescence intensity distributions of HAUS6 in half-spindles of cells prepared as in **a** quantified and plotted relative to α-tubulin as described in Figure 16**b**. The value closest to the pole obtained in cells expressing wild type NEDD1-EGFP was set to one. Values are means (error bars, SEM) of a total of 64 half-spindles from three independent experiments **(c)** Cells were prepared as in **a** and total fluorescence intensities of HAUS6 in half-spindles along a length of 2.5 µm were quantified and plotted relative to the intensity of α-tubulin staining. The intensity obtained for cells expressing wild type NEDD1 was set to one. Values are means of a total of 64 half-spindles from three independent experiments (error bars, SEM).

As a control I measured the distribution of the TPX2 protein. TPX2 has been described to be involved in non-centrosomal microtubule nucleation, and it accumulates close to the pole at metaphase. Expression of mutant forms of NEDD1 did not modify the amount or distribution of TPX2 present on the spindle and its distribution (Figure 23a, b, c).

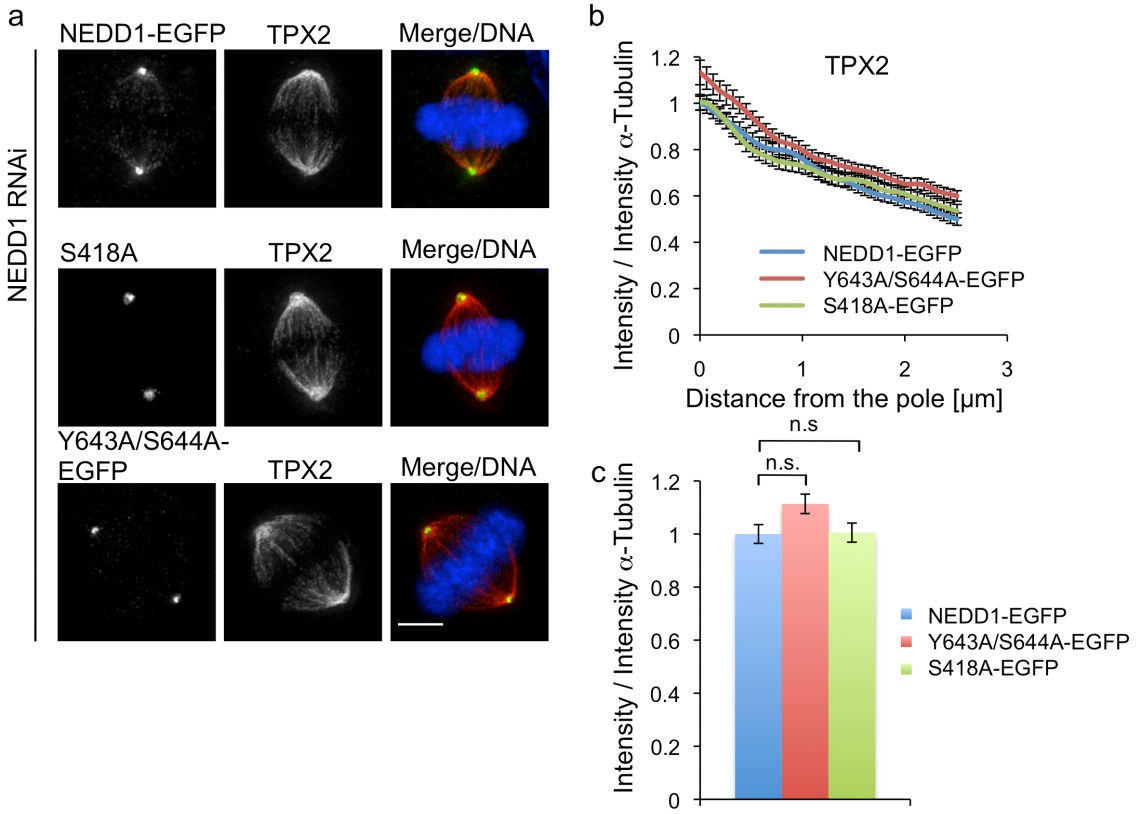

Figure 23. TPX2 distribution is not affected by NEDD1 mutants.

(a) Hela cells transfected with plasmids expressing NEDD1 shRNA and EGFP-tagged NEDD1 wild type or Y643A/S644A and S418A mutants were fixed and stained after 48 hours with antibodies against GFP and TPX2, DNA was stained with DAPI. Scale bars, 5 µm. **(b)** Fluorescence intensity distributions of TPX2 in half-spindles of cells prepared as in **a** quantified and plotted relative to α-tubulin as described in Figure 16**b**. The value closest to the pole obtained in cells expressing wild type NEDD1-EGFP was set to one. Values are means (error bars, SEM) of a total of 40 half-spindles from two independent experiments **(c)** Cells were prepared as in a and total fluorescence intensities of TPX2 in half-spindles along a length of 2.5 µm were quantified and plotted relative to the intensity of α-tubulin staining. The intensity obtained for cells expressing wild type NEDD1 was set to one. Values are means of a total of 40 half-spindles from two independent experiments (error bars, SEM).

1.2 γ-Tubulin dynamics at the centrosome

1.2.1 γ-Tubulin is recruited at the centrosome by two pathways

To study the dynamics of the γTuRC in mitosis, I generated a U2OS cell line stably expressing γ-tubulin fused to photoactivitable GFP (γ-tubulin-paGFP) and α-tubulin fused to mCherry (mCherry–α-tubulin). To validate the proper behavior of γ-tubulin-paGFP in these cells I analyzed its interaction with mitotic centrosomes. Previous work has demonstrated a sudden, microtubule-independent increase of centrosomal γ-tubulin at the onset of mitosis, and, using FRAP experiments, turnover of γ-tubulin at mitotic centrosomes with a half-life of 45 min (Khodjakov & Rieder 1999).

Direct photoactivation of γ-tubulin-paGFP at centrosomes in nocodazole-arrested cells led to the visualization of a bright centrosome whose intensity decreased progressively with kinetics similar to those observed by Khodjakov and Rieder using FRAP of γ-tubulin-GFP (Figure 24a). In order to control that the fluorescence decrease was due to γ-tubulin exchange and not due to photobleaching of the GFP, I also performed laser-activation of γ-tubulin-paGFP and acquired only two pictures, one at the beginning and one at the end of the time lapse experiment. The reduction in γ-tubulin-paGFP fluorescence at the 140 min time point was similar to cells that had been monitored continuously confirming that the decrease in fluorescence was indeed due to γ-tubulin exchange.

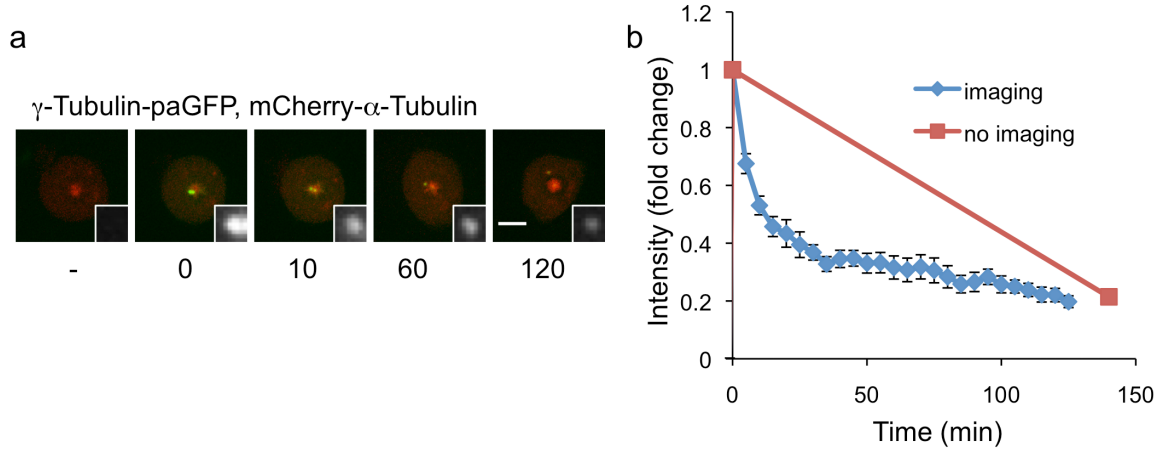

Figure 24. The γ-tubulin turnover at the centrosome.

(a) Still images of a time lapse recording of U2OS cells stably expressing γ-tubulin-paGFP and mCherry-α-tubulin before and after photoactivation. Shown is a merge of the channels for γ-tubulin-paGFP (green) and mCherry-α-tubulin (red). Numbers below images indicate time in minutes. Cells were incubated in presence of nocodazole before γ-tubulin-paGFP fluorescence was activated by a laser pulse on the centrosomal region. Scale bar, 5µm. **(b)** The fluorescence intensity of γ-tubulin-paGFP at centrosomes was quantified in series of still images obtained from time-lapse recordings of cells as in **a** or on a cell imaged right after the photoactivation and after 140min to minimize any photobleaching. The mean intensity after photoactivation was set to one and the fold change in intensity was plotted as a function of time (error bars, SEM; values are mean of 10 centrosomes).

To test whether centrosomal recruitment of γ-tubulin was microtubule-independent, I photoactivated γ-tubulin-paGFP in a restricted area of the cytoplasm and quantified the increase of fluorescence at centrosomes. A rapid accumulation of γ-tubulin at the centrosome was observed. Surprisingly, when I performed a similar experiment in cells treated with nocodazole to depolymerize microtubules, γ-tubulin recruitment occurred much more slowly (Figure 25a, b). This demonstrated that the rapid recruitment of γ-tubulin at mitotic centrosomes requires microtubules.

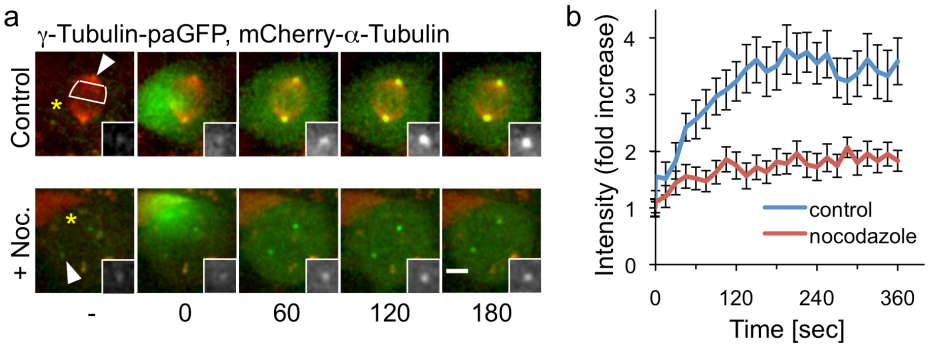

Figure 25. The fast recruitment of γ-tubulin at the pole is microtubule dependent.

(a) Still images of a time lapse recording of U2OS cells stably expressing γ-tubulin-paGFP and mCherry-α-tubulin before and after photoactivation. Shown is a merge of the channels for γ-tubulin-paGFP (green) and mCherry-α-tubulin (red). Numbers below images indicate time in seconds. Cells were incubated in the absence or presence of nocodazole before γ-tubulin-paGFP fluorescence was activated by a laser pulse in a confined region in the cytoplasm (yellow asterisk). The white arrowhead and the region outlined by a white line indicate centrosome and half spindle, respectively, where accumulation of fluorescence was measured. Scale bar, 5µm. **(b)** The fluorescence intensity of γ-tubulin-paGFP at centrosomes was quantified in series of still images obtained from time lapse recordings of cells incubated with or without nocodazole as in **a**. The mean intensity before photoactivation was set to one and the fold increase in intensity was plotted as a function of time (error bars, SEM; at least 28 centrosomes per condition from two independent experiments).

1.2.2 γ-Tubulin recruitment at the centrosome depends on its ability to bind minus ends

To test if γ-tubulin recruitment at the centrosome depends on minus end binding I repeated the cytoplasmic photoactivation experiment in cells transfected with the plasmid coding for γ-tubulin shRNA and expressing γ-tubulin wild type or 4A mutant. The accumulation of γ-tubulin 4A at the centrosome was strongly impaired compared to wild type (Figure 26a, b). Together these results demonstrate that the fast recruitment of γ-tubulin at the centrosome is mediated by minus end interaction.

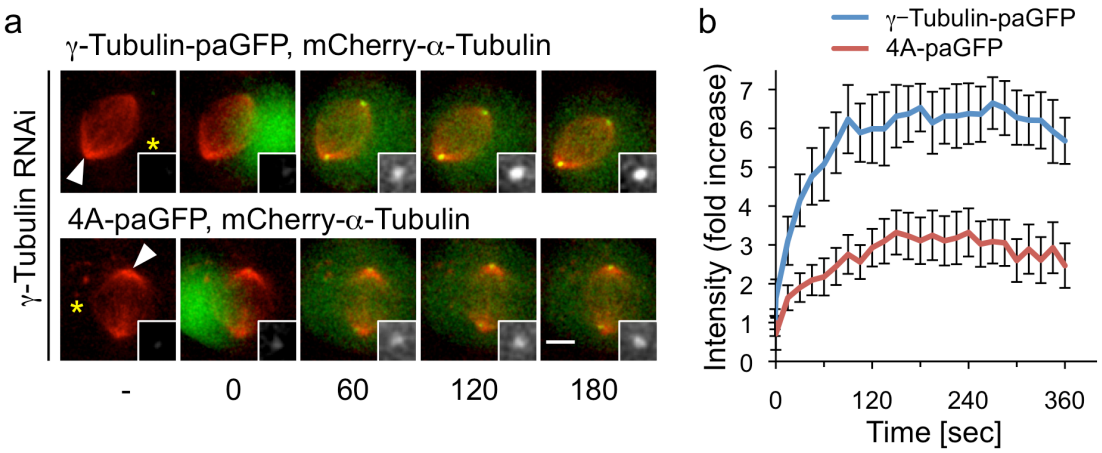

Figure 26. γ-tubulin recruitment at the centrosome depends on its ability to bind minus ends.

(a) Still images of a time lapse recording of U2OS cells transiently co-transfected with plasmid co-expressing γ-tubulin shRNA and γ-tubulin-paGFP wild type or 4A mutant, and plasmid expressing mCherry-α-tubulin. Shown is a merge of the channels for γ-tubulin-paGFP (green) and mCherry-α-tubulin (red). Numbers below images indicate time in seconds. γ-Tubulin-paGFP fluorescence was activated by a laser pulse in a confined region in the cytoplasm (yellow asterisk). The white arrowheads indicate centrosomes where accumulation of fluorescence was measured. Scale bar, 5µm. **(b)** Quantification of centrosomal fluorescence in series of still images from time lapse recordings of cells transfected as in **a**. The mean intensity before photoactivation was set to one and the fold increase in intensity was plotted as a function of time (error bars, SEM; at least 31 centrosomes per condition from 2 experiments).

1.3 Dynamics of the γTuRC along the spindle

1.3.1 Loading of γ-Tubulin on the spindle occurs preferentially at pole distal sites

The requirement for microtubule minus end binding in the fast recruitment of γ-tubulin to the centrosome raised the question whether γ-tubulin loading along the

spindle might be involved in centrosome recruitment. Indeed, quantification of γ-tubulin-paGFP intensity along the spindle after photoactivation in a confined region of the cytoplasm revealed a fast recruitment of the nucleator to spindle microtubules (Figure 27a).

At early time points, the distribution of the signal relative to the mCherry-α-tubulin intensity revealed a preferential binding of γ-tubulin-paGFP to pole-distal regions (Figure 27b). Interestingly, over time a redistribution of the signal towards the pole was observed suggesting active relocalization of the γTuRC to pole-proximal spindle regions.

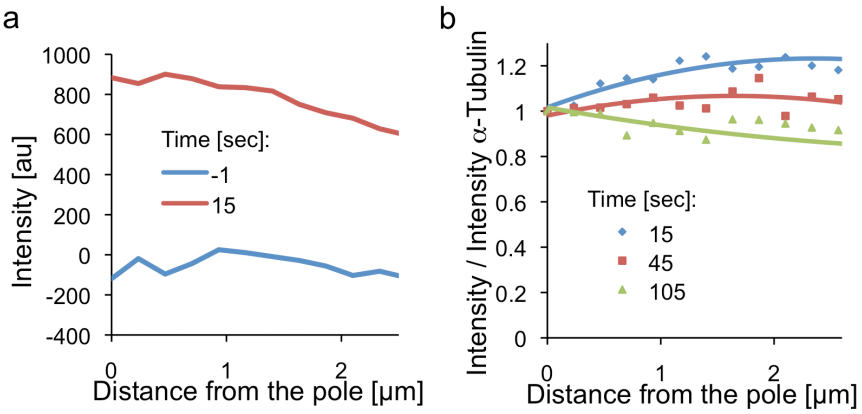

Figure 27. γ-Tubulin is preferentially recruited to pole distal regions and actively redistributes toward the poles.

(a) The fluorescence intensity distribution of γ-tubulin-paGFP along half-spindles was quantified in still images obtained from time-lapse recordings before (time point -1 sec) and after (time point 15 sec) photoactivation of γ-tubulin-paGFP in the cytoplasm as in Figure 25**a**. The mean fluorescence intensities along the spindle axes were plotted as a function of distance from the spindle poles (n=18 half-spindles). **(b)** The distribution of the mean fluorescence intensities of γ-tubulin-paGFP relative to α-tubulin were quantified for the indicated time points and plotted as a function of distance from the spindle poles (n=18 half spindles). For each time point the value closest to the pole was set to one.

1.3.2 Spindle-bound γ-Tubulin moves poleward along microtubules and slows down close to the pole

To address more directly the redistribution of the spindle fraction of γ-tubulin, I performed photoactivation of γ-tubulin-paGFP within the spindle, along a line across the width of the spindle, perpendicular to its axis. Within a few seconds I could observe rapid diffusion of some γ-tubulin from the activated area throughout the cytoplasm. However, a fraction of photo-activated γ-tubulin remained on the spindle, indicating a stable association with microtubules.

Time-lapse recording showed that the fluorescent line moved towards the pole and eventually accumulated at the pole and within the pole-proximal spindle region (Figure 28a). I measured the speed of this movement by determining the slope of fluorescent marks in the kymographs (Figure 30a). The average speed of the poleward movement of γ-tubulin was 2.12 μm/min (Figure 28b, Table 1). However, I found that the speed was dependent on the distance from the pole; in the central region of the spindle (>1.7 μm away from the centrosome) the measured speed was 2.47 μm/min. Close to the pole (< 1.7 μm away from the centrosome), movement slowed down to 0.39 μm/min (Figure 28b). The reduced speed close to the pole may be responsible for the accumulation of γTuRC in this area that I observed under steady state conditions in fixed samples (Figure 16).

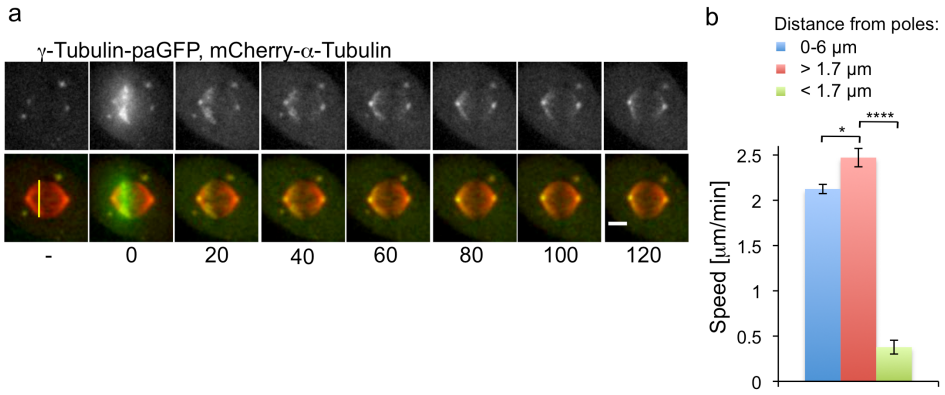

Figure 28. γ-tubulin stably binds microtubules, moves poleward and accumulates close to the centrosome.

(a) Metaphase spindles in U2OS cells stably expressing γ-tubulin-paGFP and mCherry-α-tubulin were subjected to laser-directed photoactivation in a line that was perpendicular to the spindle axis and positioned in pole-distal regions of half-spindles. Shown are still images of the channel for γ-tubulin-paGFP (grey scale) and a merge of the channels for γ-tubulin-paGFP (green) and mCherry-α-tubulin (red) before and after photoactivation. Numbers below images indicate time in seconds. The yellow line in the image before photoactivation indicates the area that was targeted by the laser. Scale bar, 5µm. **(b)** Using kymograph analysis the rates of poleward movement of γ-tubulin-paGFP fluorescence marks obtained as in **a** were quantified within the entire half-spindle region (0-6 µm), for the pole-proximal region (<1.7 µm), and for the pole-distal region (>1.7 µm) as indicated. Mean rates were calculated and plotted (error bars, SEM; n=22 half-spindles from four independent experiments, * $p<0.05$, **** $p<0.0001$).

1.3.3 γ-Tubulin interaction and transport on the mitotic spindle require minus end binding

Our analysis of fixed spindles revealed a requirement for microtubule minus end interactions for γTuRC to accumulate close to the pole. To confirm this I photoactivated spindles in cells transiently transfected with the plasmid expressing shRNA directed against endogenous γ-tubulin together with tagged wild type or mutant γ-tubulin. Wild type γ-tubulin showed stable interaction and poleward transport at a similar rate as endogenous γ-tubulin (Figure 29a, Table 1). In contrast, photoactivation of spindles in the γ-tubulin 4A expressing cells resulted in

a rapid diffusion of the fluorescence. No stable interaction and therefore no poleward transport could be visualized (Figure 29b).

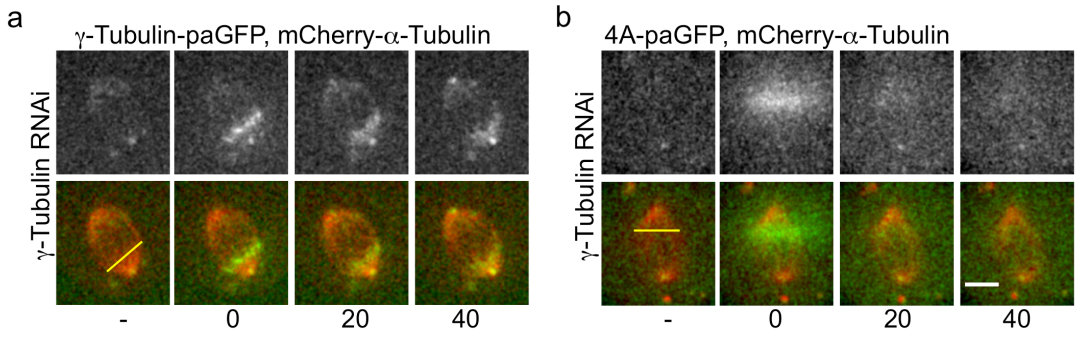

Figure 29. Microtubules minus end binding stabilizes γ-tublin-spindle interaction and allows the movement along the spindle.

(a, b) Still images of a time-lapse recording of U2OS cells transiently co-transfected with plasmid co-expressing γ-tubulin shRNA and γ-tubulin-paGFP wild type **(a)** or 4A mutant **(b)**, and plasmid expressing mCherry-α-tubulin. Shown are still images of the channel for γ-tubulin-paGFP (grey scale) and a merge of the channels for γ-tubulin-paGFP (green) and mCherry-α-tubulin (red) before and after photoactivation. Numbers below images indicate time in seconds. Activation of γ-Tubulin-paGFP fluorescence in the spindle was done as in Figure 28a. Scale bar, 5µm.

1.3.4 γ-Tubulin transport depends on molecular motors

To better understand the modalities of γ-tubulin movement I investigated the underlying forces. A poleward movement on microtubules reflects movement directed toward the minus ends of the centrosomal microtubules. One possibility was that movement occurred as a result of poleward microtubule flux. A protein bound to the lattice of fluxing microtubules would passively be transported. However the velocity that I measured for γ-tubulin movement was much faster than the flux rate previously reported for U2OS cells (~0.5-0.6 µm/min) (Ganem et al. 2005) (Maffini et al. 2009).

Another possibly was that minus end-bound γ-tubulin was actively transported along other microtubules with the help of molecular motors. Candidates were minus end-directed motors and the kinesin KIF11. Through crosslinking anti-parallel microtubules in the central spindle and exerting plus end-directed motor activity, KIF11 can push microtubules outwards and thus generate a poleward force. I performed photoactivation experiments after inhibition of various motor proteins; the minus end-directed motor dynein was inhibited by treatment with EHNA or ciliobrevine D; the minus end-directed kinesin KIFC1 was depleted by RNAi; the kinesin KIF11 was inhibited by treatment with STLC.

Inhibition of dynein with EHNA reduced the velocity of γ-tubulin transport to 1.42 μm/min (Figure 30b, Table 1). EHNA has been described as an inhibitor of dynein but may have other targets. In order to confirm that the slowing down of the transport was specific to dynein inhibition, I used the recently described specific dynein inhibitor ciliobrevine D (Firestone et al. 2012). The reduction of the speed could be reproduced confirming the implication of dynein in γ-tubulin transport (Table 1).

Similarly, RNAi depletion of KIFC1 showed a reduction in the rate of the movement to 1.30 μm/min (Figure 30b, Table 1). Surprisingly, the combined inhibition of dynein and KIFC1 did not have additive effects (1.48 μm/min) (Figure 30b, Table 1).

Inhibition of KIF11 by STLC leads to monopolar spindle formation. In such figures the measured rate for γ-tubulin movement was 1.45 μm/min (Figure 30c, Table 1). This result indicates a probable implication of the KIF11 motor in γ-tubulin transport. To confirm this in bipolar spindles, I arrested cells in metaphase using the MG132 compound. This proteasome inhibitor prevents entry into anaphase and blocks cells in a bipolar metaphase state. Addition of STLC to such MG132-pretreated cells resulted in a reduction of the transport rate that was similar to the rate in STLC-induced monopolar spindles (1.42 μm/min, Figure 30b and Table 1).

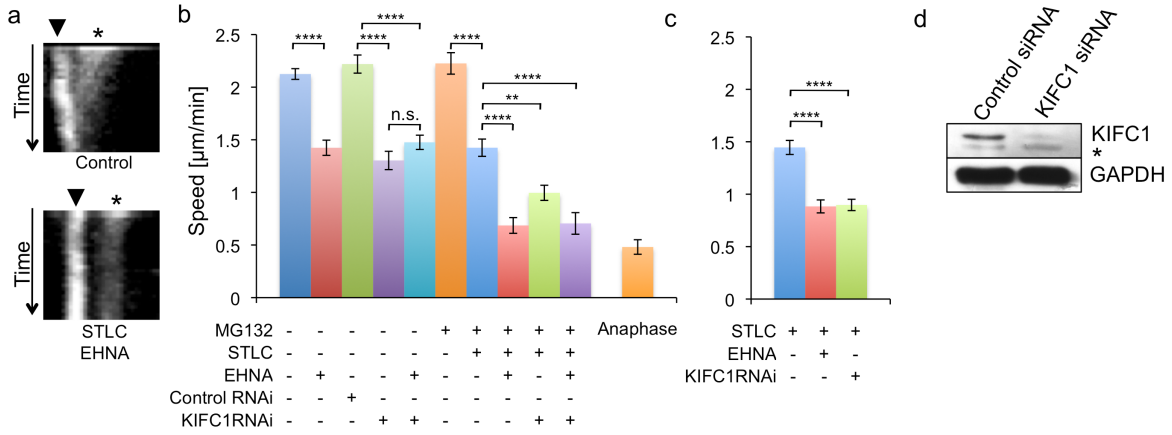

Figure 30. γ-tubulin poleward transport involves dynein, KIFC1 and KIF11 motors.

(a) Representative kymographs displaying poleward movement of γ-tubulin-paGFP fluorescence in a control cell and reduced movement in a cell after combined treatment with STLC to inhibit KIF11 and EHNA to inhibit dynein. The arrowhead indicates the position of the centrosome, the asterisk the position of laser activation. **(b)** The mean rates of poleward movement of γ-tubulin-paGFP fluorescence in half spindles of cells subjected to various treatments as indicated were quantified by kymograph analysis and plotted (error bars, SEM; 10-40 half-spindles per condition from at least two independent experiments; ** p<0.01, **** p<0.0001). **(c)** The mean rates of poleward movement of γ-tubulin-paGFP fluorescence in monopolar spindles of cells subjected to various treatments as indicated were quantified by kymograph analysis and plotted (error bars, SEM; 22-45 half-spindles per condition from at least two independent experiments; **** p<0.0001). **(d)** Cells were transfected with control or KIFC1 siRNA and analysed by western blotting with antibodies against KIFC1 and GAPDH as loading control. The asterisk indicates a non-specific band recognized by the KIFC1 antibody.

In this case combined motor inhibition led to additive effects; co-inhibition of KIF11 and dynein reduced the movement rate to 0.69 μm/min and combining inhibition of KIF11 with depletion of KIFC1 reduced the rate to 1 μm/min (Figure 30b, Table 1). Additive effects were also observed in monopolar spindles; in both cases I measured a speed of 0.88 μm/min (Figure 30c, Table 1).

1.3.5 A fraction of poleward-moving γ-tubulin is incorporated at the centrosome

Finally I asked if γTuRC complexes that accumulated at the pole in a microtubule minus end-dependent manner, also required microtubules to maintain pole association or were incorporated into the centrosomal PCM. To answer this question, I performed photoactivation in a line perpendicular to the spindle axis, and allowed γ-tubulin to be transported on microtubules towards the pole for two minutes. I then added a high concentration of nocodazole to rapidly and completely depolymerize microtubules (Figure 31a). Microtubule removal did not cause any reduction of the centrosomal signal intensity indicating that the γTuRC had been incorporated at the centrosomes (Figure 31a, b).

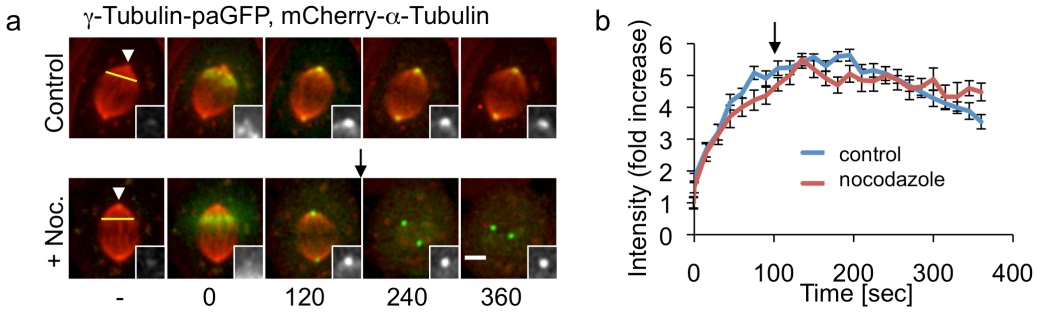

Figure 31. γTuRC are incorporated to the pole and no longer require minus end binding.

(**a**) Still images of a time-lapse recording of U2OS cells stably expressing γ-tubulin-paGFP and mCherry-α-tubulin. Shown is a merge of the channels for γ-tubulin-paGFP (green) and mCherry-α-tubulin (red). Numbers below images indicate time in seconds. Two minutes after photoactivation of γ-tubulin-paGFP in the spindle as in Figure 28**a** microtubules were depolymerized by addition of nocodazole (indicated by the black arrow). The white arrowheads indicate centrosomes where fluorescence intensity was measured. Scale bar, 5µm. **(b)** Quantifications of fluorescence intensity of γ-tubulin-paGFP at centrosomes in series of still images obtained from time lapse recordings of cells as in **a**. The black arrow indicates the time point of nocodazole addition. The mean intensity before photoactivation was set to one and the fold increase in intensity was plotted as a function of time (error bars, SEM; at least 10 centrosomes per condition from two independent experiments).

	Bipolar												Monopolar			Anaphase.
Speed (μm/min)	2.12	1.28	1.42	2.22	1.30	1.48	2.23	1.42	0.69	1.00	0.71	1.93	1.45	0.88	0.88	0.48
SEM	0.05	0.04	0.07	0.09	0.09	0.08	0.10	0.08	0.07	0.07	0.10	0.07	0.07	0.06	0.08	0.07
Number of half-spindles	40	41	22	10	25	24	13	30	19	32	13	13	45	22	28	10
(experiments)	(5)	(2)	(2)	(2)	(3)	(2)	(2)	(5)	(2)	(3)	(2)	(2)	(5)	(2)	(2)	(3)
MG132	-	+	-	-	-	-	+	+	+	+	+	-	-	-	-	-
STLC	-	-	-	-	-	-	-	+	+	+	+	-	+	+	+	-
Ciliobrevin D	-	+	-	-	-	-	-	-	-	-	-	-	-	-	-	-
EHNA	-	-	+	-	-	+	-	-	+	-	+	-	-	+	-	-
Control RNAi	-	-	-	+	-	-	-	-	-	-	-	-	-	-	-	-
KIFC1 RNAi	-	-	-	-	+	+	-	-	-	+	+	-	-	-	+	-
γ-tubulin RNAi + γ-Tubulin-paGFP	-	-	-	-	-	-	-	-	-	-	-	+	-	-	-	-

Table1. Measurement of the transport rate of γ-tubulin along the spindle under various conditions.

2. Mitotic spindle assembly and division in the absence of centrosomes

2.1 Laser ablation of centrosomes

In order to generate a model that would allow studying spindle assembly both in the presence and absence of centrosomes I decided to use laser ablation of centrosomes in pig LLC-PK cells. Previous work has demonstrated that laser ablation of centrosomes in prophase cells does not prevent normal spindle assembly and mitotic progression (Khodjakov et al. 2000). To rule out an important contribution of centrosomes to spindle assembly at prophase, I decided to ablate centrosomes prior to mitotic entry, in G2. Such cells have duplicated centrosomes and DNA, are ready to enter mitosis, but have not yet assembled any mitotic microtubule network.

I created a LLC-PK cell line stably expressing centrin-GFP to label the centrioles and mCherry-α-tubulin to label microtubules. Pulses with a 305nm laser was directed at the centrin-GFP signal to destroy centrosomes. This treatment led to a complete disappearance of the centrin-GFP signal (Figure 32).

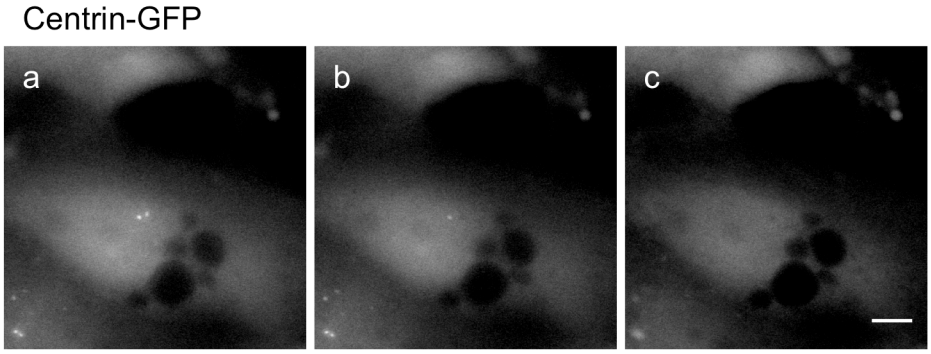

Figure 32. Laser ablation of centrosomes.

Seletcetd still images of a time-lapse recording of LLC-PK cells stably expressing centrin-GFP and mCherry-α-tubulin. Cells were subjected to laser-shots in regions corresponding to centrosomes. The first centrosome was destroy between **a** and **b**; and the second was destroy between **b** and **c**. Shown are still images of the channel for centrin-GFP. Scale bar, 5µm.

To confirm the complete destruction of the ablated centrosomes I fixed cells after laser ablation and stained for several centrosomal markers (pericentrin, γ-tubulin, NEDD1, centrin). The ablated cells did not display any centrosomal structure positive for these centrosomal proteins compared to adjacent, non-ablated cells or control cells that had been subjected to a laser pulse targeted at the cytoplasm (Figure 33a). A microtubule regrowth assay also showed that ablated cells did not present any microtubule nucleating center anymore. Whereas surrounding non-ablated cells formed robust microtubule asters at their centrosomes after one minute of regrowth, ablated cells did not form microtubule asters and only assembled a few disorganized microtubules in the cytoplasm (Figure 33b).

Together these results show that under the chosen conditions centrosomes were efficiently ablated.

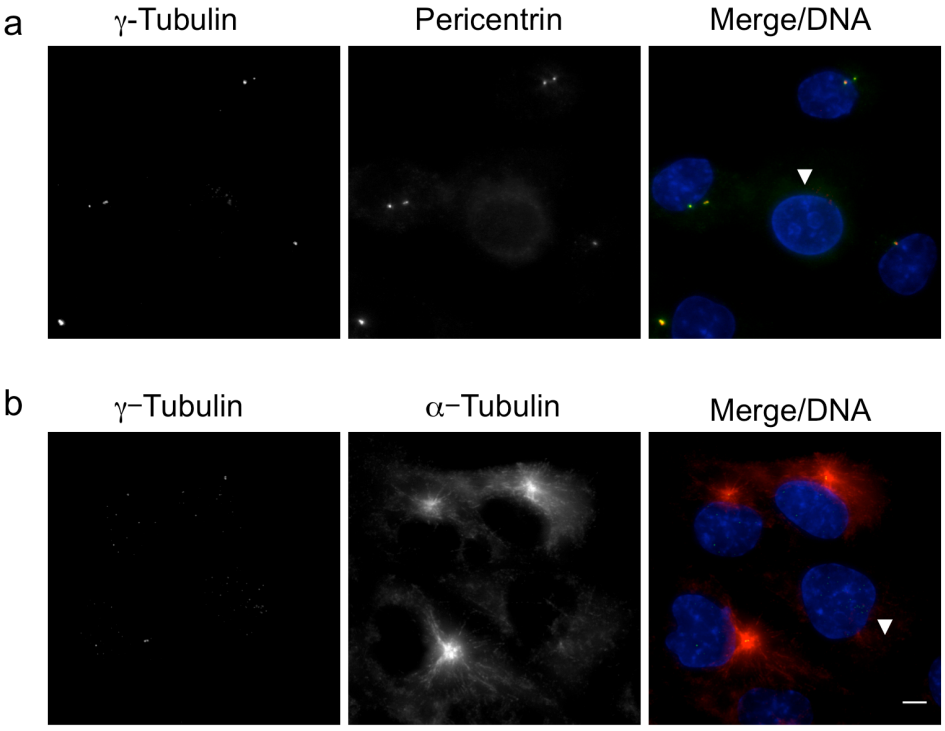

Figure 33. Laser ablation destroys centrosomes.

(a) LLC-PK cells stably expressing centrin-GFP and mCherry-α-tubulin were ablated as in Figure 32. After the ablation cells were fixed and stained with anti-γ-tubulin and anti-pericentrin antibodies; DAPI was used to label DNA. The white arrowhead indicates the ablated cell. Scale bar, 5 μm. **(b)** Cells were ablated as in Figure 32. After ablation a microtubule regrowth assay was performed. After one minute of regrowth cells were fixed and stained with anti- γ-tubulin and anti-α-tubulin antibodies. DAPI was used to label DNA. The white arrowhead indicates the ablated cell. Scale bar, 5 μm.

2.2 Cell cycle progression is independent of centrosome presence

To study mitotic spindle assembly in ablated cells I decided to image cells for 24 hours following ablation. Surprisingly, even though most of the ablated cells survived the treatment (80%), they did not enter mitosis during the recording time (21% of surviving cells entered mitosis). This cell cycle arrest was not observed for

non-ablated cells (Figure 34). To check whether cell cycle arrest was due to the absence of centrosomes or due to stress induced by laser treatment in combination with long-term imaging, I directed the laser pulse to a region in the cytoplasm not containing centrosomes. These control cells were then imaged under the same conditions as centrosome-ablated cells. As an additional control, centrosome or cytoplasm-ablated cells were imaged only with transmitted light to reduce imaging-induced stress. For each condition I determined the percentage of cells entering mitosis during the 24 hours period. This analysis revealed that laser ablation (directed either at the centrosome or at a random region in the cytoplasm) in combination with long-term fluorescence imaging were responsible for the observed cell cycle arrest, suggesting that laser ablation and light-induced cell stress, but not the presence or absence of centrosomes, prevented mitotic entry in many treated cells.

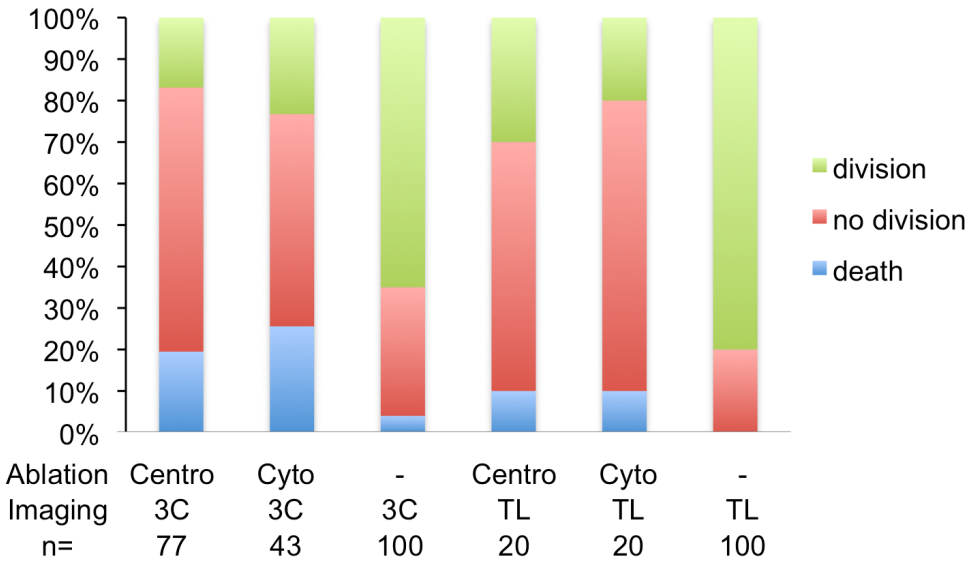

Figure 34. Centrsome absence does not prevent mitotic entry

LLC-PK cells stably expressing centrin-GFP and mCherry-α-tubulin were subjected to a laser shot directed to the centrosome (centro), in the cytoplasm (cyto) or none (-). Cells were imaged for 24 hours by transmitted light only (TL) or by transmitted light, green and red channels (3C). The survival, death and division of cells were counted. Numbers of cells are indicated.

2.3 Acentrosomal mitotic cells present transient multipolar spindles but divide bipolar.

Even though most ablated cells were cell cycle arrested, I could follow some cells undergoing acentrosomal mitosis (Figure 34). Non-ablated or cytoplasm-ablated cells assembled bipolar spindles and divided normally (Figure 35a). After nuclear envelope breakdown, robust microtubule asters were observed around the centrosomes. A bipolar spindle was rapidly set up and chromosomes aligned to form a metaphase plate. Shortly after this, cells entered into anaphase and sister chromatids moved to opposite poles. Finally, cytokinesis separated the two daughter cells. In contrast, cells lacking centrosomes (Figure 35b) did not display

microtubule asters but nucleated microtubules in a region corresponding to the location of the chromatin. In 77% of the cases these cells assembled multipolar spindles with 3 or 4 poles (23% assembled regular bipolar spindles). In these multipolar structures, two of the poles always appeared as “major” microtubule organizers. Unlike in cells with extra centrosomes (Kramer et al. 2011) the additional poles were not clustered before entry into anaphase. Surprisingly, these aberrant anaphases eventually led to a bipolar division resulting in two daughter cells. However, extended observation of the daughter cells showed that several died shortly after the division.

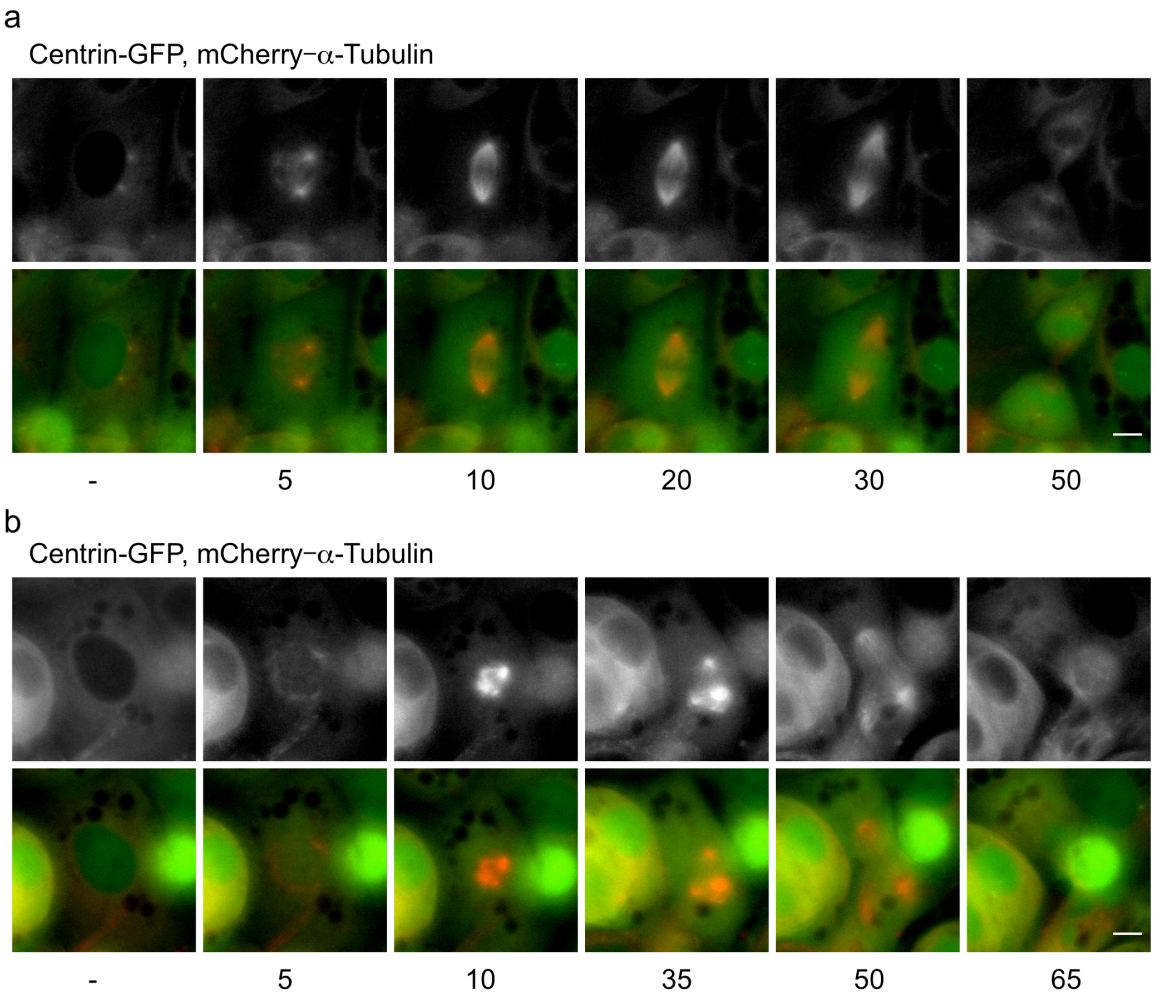

Figure 35. Acentrosomal cells assemble a multipolar spindle.

Still images of a time-lapse recording of a dividing LLC-PK cells stably expressing centrin-GFP and mCherry-α-tubulin not ablated **(a)** or centrosome ablated **(b).** Shown are still images of the channel for mCherry−α-tubulin- (grey scale) and a merge of the channels for centrin-GFP (green) and mCherry-α-tubulin (red). Numbers below images indicate time in minutes after NEB. Scale bar, 5µm.

2.4 *De novo* centriole formation

Cells in which centrosomes have been removed experimentally can generate centrioles *de novo*. In cells in which centrosomes were ablated at metaphase, centrioles re-appeared in the S phase of the next cycle (La Terra et al. 2005). These new centrioles are non-mature, cannot recruit pericentriolar material proteins and are not able to nucleate microtubules. Progression through mitosis is required for these centrioles to be able to build centrosomes (La Terra et al. 2005) (Wang et al. 2011). In my experiments, I observed de novo centriole formation in 21% of ablated cells (Figure 36, Table 2). Four out of sixteen of these cells entered mitosis; mitotic spindle assembly was similar to cells lacking centrioles; microtubule asters were absent and multipolarity was observed. Similar to previous studies (La Terra et al. 2005), the newly formed centrioles were somehow connected to spindle microtubules and were eventually located at one of the minor poles. However, the presence of these *de novo* centrioles could not rescue multipolarity and multipolar entry into anaphase.

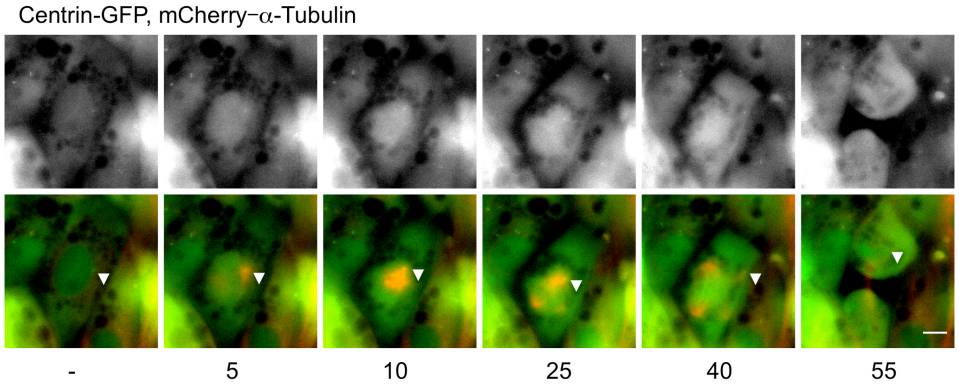

Figure 36. *De novo* centriole generation do not rescue the multipolar phenotype

Still images of a time-lapse recording of a dividing LLC-PK cells stably expressing centrin-GFP and mCherry-α-tubulin ablated for the centrosome as in Figure 32**.** Shown are still images of the channel for centrin-GFP (grey scale) and a merge of the channels for centrin-GFP (green) and mCherry-α-tubulin (red). Numbers below images indicate time in minutes after NEB. The white arrowhead indicates the *de novo* centriole that reappeared. Scale bar, 5µm

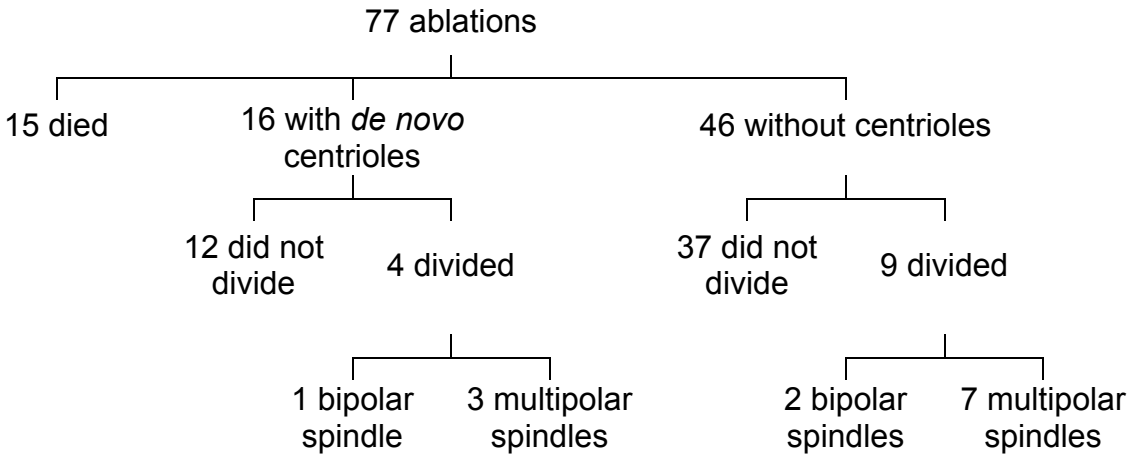

Table 2. Fates of centrosomes ablated cells.

Discussion

1. Sorting of non-centrosomal microtubules in the spindle

γTuRC as a minus end marker

The previously described architecture of the metaphase spindle with the minus ends of interpolar microtubules close to the poles raised the question what mechanism dynamically organizes the non-centrosomal microtubules during spindle assembly. Through their nucleation at the centrosome, centrosomal microtubules are already oriented and anchored with their minus ends facing the pole while the growing plus ends explore the cytoplasm. However, microtubules derived from other nucleation pathways such as microtubules generated by Ran-GTP-dependent nucleation, must be oriented and sorted to correctly integrate into the mitotic spindle. To analyze this mechanism, the analysis of microtubule minus end dynamics is crucial, but was previously not possible due to the lack of a suitable probe.

As a microtubule nucleator γTuRC is known to interact with microtubule minus ends. However, it has not been demonstrated previously that γTuRC is stably associated with minus ends of non-centrosomal microtubules in spindles. My distribution analysis of γTuRC components in the mitotic spindle revealed an accumulation in spindle regions close to the pole, which correlates with the previously described localization of minus ends of interpolar microtubules (Mastronarde et al. 1993) (Kamasaki et al. 2013). This result was consistent with the possibility that γTuRC might decorate minus ends within spindles.

I then generated and characterized a γ-tubulin mutant previously analyzed in fission yeast. The mutation of four residues at the surface of a region suspected to be at the interface of γ-tubulin with α-tubulin at the microtubule minus end did not perturb the formation of the γTuRC and its recruitment at the centrosomes, but

impaired its binding to microtubule minus ends. The use of this mutant allowed me to demonstrate the requirement of minus end binding for localization and sorting of γTuRC in the spindle.

Together my results indicate that the γTuRC is present at the minus ends of microtubules within spindles and can be used to study minus end dynamics.

The high density of microtubules in the spindle does not allow the direct visualization of individual minus ends by fluorescence microscopy. Therefore the ultimate proof of the presence of γTuRC at the minus ends of microtubules in spindles and a quantitative analysis of this property could potentially be revealed using electron microscopy (EM) techniques as previously described (Kamasaki et al. 2013). In this EM analysis of microtubule ends in metaphase spindles a large number of potential microtubule minus ends with a “closed” morphology have been revealed, suggesting the presence of some sort of capping structure such as γTuRC. However, due to the relatively large volume of the metaphase spindle such analyses are extremely challenging and time-consuming. Moreover, specific labeling/identification of γTuRC at microtubule ends in EM cryo sections poses an additional unsolved problem.

Requirement of γTuRC-HAUS interaction for proper distribution of the complexes within the spindle

Localization of γTuRC to the spindle is dependent on HAUS. To disturb interaction between the two complexes, I generated a specific mutant of NEDD1 that binds HAUS but not γTuRC (Y643A/S644A mutant) and took advantage of the previously described S418A mutant, which is not recruited by augmin to spindles. Expression

of these two mutants led to similar results: a reduction in spindle recruitment and lack of pole-proximal accumulation of γTuRC coupled to a mis-distribution of the HAUS complex; indeed even if the general amount of HAUS along the spindle was not strongly affected, the pole proximal fraction was strongly reduced while the amount of HAUS close to the central region was increased.

These results suggested that HAUS alone is able to interact with microtubules even in the absence of γTuRC binding. The accumulation of HAUS on microtubules close to the spindle center in the absence of interaction with the γTuRC indicates that HAUS alone is not correctly distributed along the spindle. However, it is not clear whether this abnormal redistribution is caused by preferential binding to microtubules near the chromatin or by the absence of a subset of spindle microtubules that might provide additional binding sites for HAUS.

The absence of S418A NEDD1 mutant along the spindle has been described previously. Surprisingly, the Y643A/S644A mutant, which lacks γTuRC binding, presented a similar behavior revealing that NEDD1 requires the γTuRC to correctly target and distribute along the spindle. These results suggest that the capacity of NEDD1 to interact with the HAUS complex is not sufficient to stabilize its recruitment to the spindle lattice and that γTuRC-dependent nucleation and or minus end-binding promote correct distribution.

γTuRC is preferentially loaded on pole-distal spindle microtubules

Our fixed cell analysis revealed an enrichment of γTuRC in the pole-proximal region whereas HAUS seemed to be more evenly distributed. The pole-proximal accumulation of γTuRC at steady state can be explained by several processes; one

possibility is that HAUS binds randomly along microtubules and decorates the entire spindle but γTuRC is preferentially recruited close to the pole leading to the observed distribution. Another possibility would be that HAUS recruits γTuRC everywhere along the spindle or in a pole distal region, and the nucleating complex is later transported to accumulate near the poles.

I addressed this issue by photoactivation of γTuRC in the cytoplasm, which showed that within a few seconds a fraction of these complexes is recruited to the spindle, preferentially to pole-distal sites. Over time, this distribution changed and γTuRC was eventually enriched near the poles, similar to what I observed in fixed cells.

Together these results indicate that HAUS, despite being distributed relatively evenly along the spindle, recruits γTuRC through the NEDD1 subunit preferentially at pole distal sites. This primary interaction might be weak but could be stabilized as soon as the γTuRC nucleates a microtubule(Figure 37a). Microtubule nucleation and stabilization of the γTuRC-spindle interaction through minus end binding could be triggered in the vicinity of the mitotic chromosomes by the presence of the Ran-GTP gradient and its activated effectors (TPX2, HURP, ch-Tog). However, my experiments could not distinguish between minus end binding following the nucleation of new microtubules and binding to pre-existing, free minus ends.

Microtubules minus ends are transported toward the pole through a molecular motor-dependent process

Based on the gradual re-distribution of γ-tubulin towards the poles that I observed after its initial preferential recruitment in the equatorial region I hypothesized that spindle-bound γTuRC was dynamic. I addressed this by performing photoactivation

of γ-tubulin on the mitotic spindle; the observation of poleward movement of the activated molecules confirmed my hypothesis. Utilization of the γ-tubulin 4A mutant in a similar experiment confirmed that the stable interaction of γTuRC with the spindle and poleward transport depend on the capacity of γTuRC to bind minus ends.

The strong reduction of the movement in the pole-proximal region can explain the distribution obtained in steady state experiments. The fast transport of non-centrosomal microtubules minus ends along the spindle coupled with this reduced rate close to the pole would lead to an accumulation of minus ends and associated γTuRC in this area.

Poleward transport can be driven by molecular motors or be the result of microtubule flux. The speed measured for the γ-tubulin transport (> 2 μm/min) was more consistent with faster motor-driven movement. Indeed, inhibition or depletion of molecular motors dynein, KIFC1 and KIF11 led to a movement rate decreased by 30% indicated their involvement in poleward transport.

The specificity of dynein inhibition by EHNA has been controversial. However, the observation of a similar reduced speed using another recently described, more specific inhibitor (Ciliobrevine D) confirmed the involvement of dynein in the transport.

Interestingly, simultaneous inhibition of dynein and KIFC1 motor activity did not have cumulative effects. This could indicate that the two motors provide two distinct functions that only together achieve effective movement, for example cross-linking/stabilization of microtubules and force generation. We could not determine if dynein and KIFC1 directly act on the γTuRC complex or on the bound microtubule, however it has been demonstrated that KIFC1 co-immunoprecipitates with two subunits of the γTuRC (γ-tubulin and GCP3) in Xenopus extract (Cai et al. 2010).

Slowing down of the transport in KIF11-inhibited monopolar and bipolar spindles demonstrated the importance of this motor in the transport. KIF11 could be used as an adaptator between the cargo (here γTuRC bound minus end) and dynein as described for TPX2 transport (Ma et al. 2010); Alternatively, through crosslinking of anti-parallel microtubule overlaps in the center of the spindle and plus end directed motor activity KIF11 could push interpolar microtubule minus ends towards the poles. Simultaneous inhibition of KIF11 with dynein or KIFC1, respectively, led to cumulative effects supporting the second hypothesis.

The residual transport rate (~0.7 μm/min) observed in double or triple inhibited cells could support the implication of microtubule flux in the transport, which has previously been determined to occur at a rate of ~0.5-0.6 μM/min in U2OS cells (Ganem et al. 2005) (Maffini et al. 2009). However, it could also be explained by the incomplete inhibition or depletion of the implicated motors.

The low rate measured in anaphase indicates that the transport does not occur at this stage of mitosis and is specific to prometaphase/metaphase. This observation is in agreement with the model that poleward sorting of non-centrosomal microtubule minus ends is particularly important for assembly and maturation of the bipolar spindle.

In summary, I propose that the recruited γTuRC in the center of the spindle, rapidly binds to interpolar microtubules minus ends, either by nucleation or directed interaction with pre-existing microtubules, and then is transported poleward by the simultaneous action of minus end-directed motors and the kinesin KIF11. Once cells enter anaphase, the poleward sorting ceases, potentially to promote relocalization of HAUS and γTuRC complexes into the central spindle (Cai et al. 2010), (Uehara & Goshima 2010). These results support the previously proposed “slide and cluster” model for spindle assembly (Burbank et al. 2007) to allow proper integration and orientation of interpolar microtubules (Figure 37b).

Centrosomal recruitment of γTuRC

I showed that centrosomal γ-tubulin is exchanged with γ-tubulin in the cytoplasm independently of microtubules, following previously published kinetics. However, I also discovered a novel microtubule-dependent centrosomal recruitment pathway that involves interaction of γTuRC with microtubule minus ends. My experiments suggest that γTuRC bound to minus ends of spindle microtubules transported along the spindle axis reaches and accumulates at the pole proximal region. The fact that microtubule depolymerization after pole proximal accumulation does not affect the quantity of γTuRC at the centrosome reveals that once it reaches the pole the nucleator complex is incorporated into the PCM and does not longer require minus end binding. Known interactors such as pericentrin or CDK5RAP2 could mediate this interaction. This result reveals a new mechanism of γTuRC recruitment at the centrosome in mitotic cells, which is microtubule-dependent and mediated by transport along the spindle, although a contribution mediated by astral microtubules could co-exist (Figure 37c). Future experiments in spindles without k-fibers (Nuf2 depletion) (DeLuca et al. 2002) or without astral microtubules (low doses of nocodazole) could provide additional information about the contribution of the different microtubule populations to this mechanism.

Significance of intra-spindle microtubule nucleation and sorting

Together my results suggest that augmin-γTuRC-dependent nucleation in pole-distal spindle regions is the source of interpolar microtubules. These acentrosomal microtubules are transported along pre-existing microtubules connected to the pole by mechanisms involving molecular motors. Pole proximal accumulation and

incorporation of these interpolar microtubules minus ends establish the cohesion between half spindles and reinforce the bipolarity (Figure 37). This function may be essential for acentrosomal spindles or spindles with abnormal number of centrosomes. Indeed, multiple poles derived from extra centrosomes have been shown to cluster, and depletion of HAUS or KIFC1 prevented the clustering of extra poles in cancer cells (Leber et al. 2010) (Kleylein-Sohn et al. 2013). The role of motor-dependent poleward sorting could be further tested by similar analyses in acentrosomal systems (see following paragraph), where depletion of augmin also causes multipolarity (Petry et al. 2011).

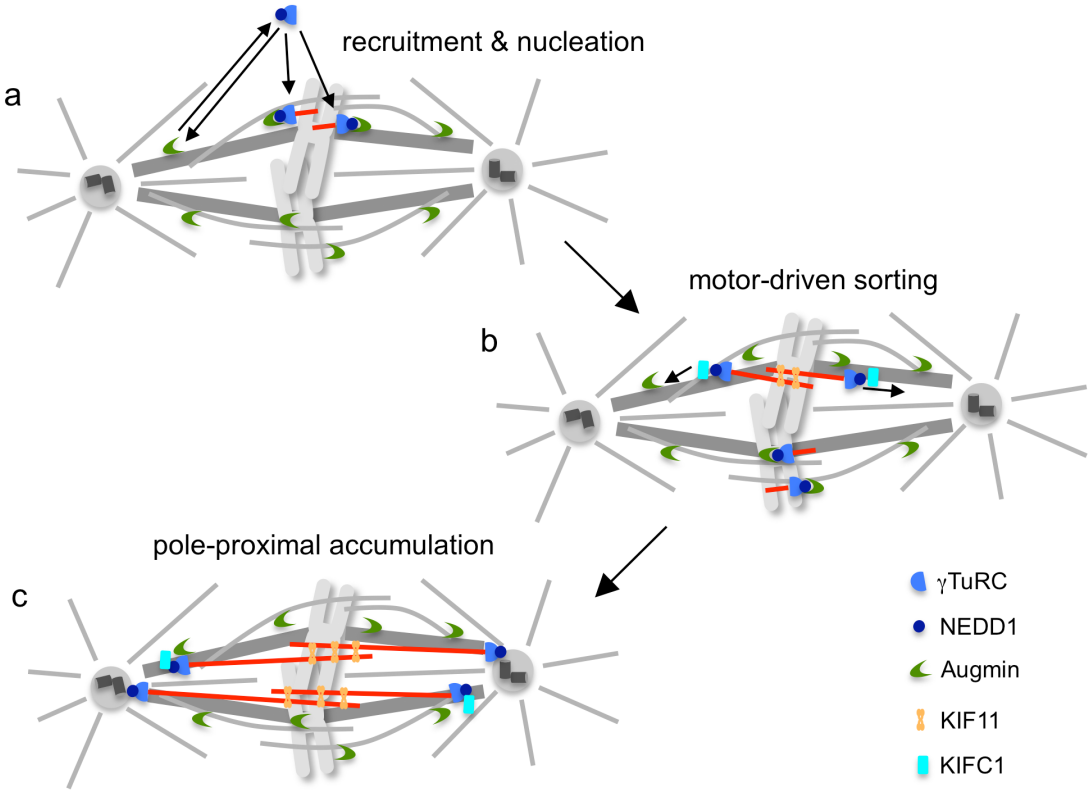

Figure 37. Model for intra-spindle nucleation and poleward sorting of minus ends of interpolar microtubules.

(a) γTuRC is recruited to spindle-bound augmin through its targeting subunit NEDD1. Nucleation and/or interaction with minus ends of previously nucleated microtubules allows γTuRC to stably associate with spindles. This occurs preferentially at pole-distal sites. **(b)** Plus ends of newly formed microtubules grow into the central spindle region, whereas minus ends with bound γTuRC are transported towards the poles. Poleward transport is driven by the kinesin KIF11, which slides antiparallel microtubules in the central spindle outwards, and by the minus end-directed motors dynein and KIFC1, which act more directly on minus ends, e.g. by binding to minus end-associated γTuRC (shown in the picture) and/or by lateral microtubule binding (not shown). **(c)** In pole-proximal regions poleward transport slows down, leading to accumulation of minus ends and of associated γTuRC. Some γTuRC reaches the poles and is incorporated at centrosomes. Extension of the plus ends and poleward-transport of the minus ends increase the extent of anti-parallel and parallel microtubule arrangements, respectively, which promotes protein-mediated crosslinking. In this way interpolar microtubules establish and maintain cohesion between half spindles that connect to chromosomes from opposite poles.

2. Acentrosomal microtubule nucleation in mitosis

The role of centrosomes in spindle bipolarity

The centrosome is the major microtubule nucleator in animal cells but the discovery of additional microtubule nucleation pathways raised the question about the contributions of these mechanisms to spindle assembly in the absence of centrosomes. Using centrosome laser ablation in interphase LLC-PK cells, I have demonstrated that chromatin-mediated microtubule nucleation can support spindle assembly and cell division as it has been described in other systems. However, I found that most acentrosomal LLC-PK cells assemble a multipolar mitotic spindle. Together these results indicate that in LLC-PK cells, the centrosomes are crucial for spindle bipolarity unlike in several other systems where bipolar spindles are assembled in absence of centrosomes. My observation of two “major” poles in acentrosomal multipolar spindles might indicate the presence of a weak “bipolar promoting” activity. It would be interesting to test in this acentrosomal system the role of the minus end poleward sorting mechanism that I identified in the first part of my thesis, for example by inhibition of KIFC1, KIF11, or dynein. In addition, specific disruption of other proteins involved in non-centrosomal microtubule nucleation could determine their importance in our model, similarly to the study carried in Drosophila embryos (Hayward et al. 2014).

In several ablated cells, I observed de novo formation of centrioles. Cells for ablation were chosen based on centriole configuration (two pairs of centrioles indicative of S/G2 phase) but the exact cell cycle stage could not be determined by this approach. Therefore these could be at a cell cycle stage still permissive for centriole duplication. However, as expected, centrioles appearing *de novo* could

not rescue the multipolarity phenotype, confirming that the centrosome needs to go through mitosis to complete its maturation process and function as microtubule organizer.

Bipolar division after spindle multipolarity

In cells with multiple centrosomes, multipolar poles can cluster to achieve bipolarity prior to anaphase onset (Kramer et al. 2011). In acentrosomal systems spindle microtubules self-organize into a bipolar configuration (Khodjakov et al. 2000) (Lecland et al. 2013). The absence of bipolarity in centrosome-ablated LLC-PK cells reveals that the known focusing factors are not strong enough in this system to establish bipolarity.

Multipolarity has been shown to frequently lead to defective kinetochore-microtubule interactions, in particular merotelic attachment. The spindle assembly checkpoint is active until resolution of abnormal kinetochore-microtubule interactions. However, merotelic attachment might not always be detected if chromosomes are bioriented.

LLC-PK cells present a normal SAC(Gorbsky et al. 1998), but in my centrosome-ablation experiments, the cells did not rescue their multipolarity before entering anaphase revealing that the checkpoint was not active. Surprisingly, LLC-PK cells without centrosomes eventually presented a bipolar division despite entering anaphase with multipolar spindles, indicating the possible presence of a mechanism enforcing bipolar division. Another possibility is that the presence of two “major” poles before anaphase could set up a semi-bipolarity that would be sufficient to satisfy the checkpoint and establish a single cleavage furrow in order to give birth to two daughter cells. It would be important in future studies to analyze

the checkpoint activity in these cells by staining kinetochores with antibodies directed against checkpoint proteins such as Mad2.

The death of several daughter cells after these abnormal divisions indicates a possible mis-segregation of the genetic material due to the multipolarity and probable merotelic attachment. Live imaging of such division with labeled chromosomes and analysis of the karyotype of daughter cells would be required to confirm this hypothesis.

Conclusions

- At steady state γTuRC in the mitotic spindle is enriched in pole-proximal regions where it is associated with microtubule minus ends
- HAUS recruits γTuRC preferentially to pole-distal spindle regions
- For stable spindle binding γTuRC needs to nucleate and/or interact with microtubule minus ends
- HAUS does not require γTuRC interaction for spindle binding but for correct distribution within the spindle
- Minus end-associated γTuRC is transported along other spindle microtubules towards the poles
- KIF11, KIFC1 and dynein are involved in the poleward transport of minus ends
- After reaching spindle poles minus end-bound γTuRC can be incorporated in the PCM
- Centrosomes are dispensable for mitotic spindle formation but ensure bipolarity
- LLCPK cells can enter anaphase with a multipolar spindle
- Cells entering anaphase with a multipolar spindle can still divide in a bipolar fashion
- Bipolar divisions following multipolar anaphase often leads to death

References

Akhmanova, A. & Hoogenraad, C.C., 2005. Microtubule plus-end-tracking proteins: mechanisms and functions. *Current Opinion in Cell Biology*, 17(1), pp.47–54.

Akhmanova, A. & Steinmetz, M.O., 2008. Tracking the ends: a dynamic protein network controls the fate of microtubule tips. *Nature reviews Molecular cell biology*, 9(4), pp.309–322.

Aldaz, H. et al., 2005. Insights into microtubule nucleation from the crystal structure of human gamma-tubulin. *Nature*, 435(7041), pp.523–527.

Allen, C. & Borisy, G.G., 1974. Structural polarity and directional growth of microtubules of Chlamydomonas flagella. *Journal of molecular biology*, 90(2), pp.381–402.

Anders, A. & Sawin, K.E., 2011. Microtubule stabilization in vivo by nucleation-incompetent gamma-tubulin complex. *Journal of Cell Science*, 124(Pt 8), pp.1207–1213.

Basto, R. et al., 2006. Flies without centrioles. *Cell*, 125(7), pp.1375–1386.

Bettencourt-Dias, M. & Glover, D.M., 2007. Centrosome biogenesis and function: centrosomics brings new understanding. *Nature reviews Molecular cell biology*, 8(6), pp.451–463.

Bobinnec, Y. et al., 1998. Centriole disassembly in vivo and its effect on centrosome structure and function in vertebrate cells. *The Journal of cell biology*, 143(6), pp.1575–1589.

Bornens, M., 2002. Centrosome composition and microtubule anchoring mechanisms. *Curr Opin Cell Biol*, 14(1), pp.25–34.

Bouissou, A. et al., 2009. {gamma}-Tubulin ring complexes regulate microtubule plus end dynamics. *The Journal of cell biology*, 187(3), pp.327–334.

Brust-Mascher, I. & Scholey, J.M., 2011. Mitotic motors and chromosome segregation: the mechanism of anaphase B. *Biochemical Society transactions*, 39(5), pp.1149–1153.

Bugnard, E., Zaal, K. & Ralston, E., 2005. Reorganization of microtubule nucleation during muscle differentiation. *Cell motility and the cytoskeleton*, 60(1), pp.1–13.

Bullitt, E. et al., 1997. The yeast spindle pole body is assembled around a central crystal of Spc42p. *Cell*, 89(7), pp.1077–1086.

Burbank, K.S. et al., 2006. A new method reveals microtubule minus ends

throughout the meiotic spindle. *The Journal of cell biology*, 175(3), pp.369–375.

Burbank, K.S., Mitchison, T.J. & Fisher, D.S., 2007. Slide-and-cluster models for spindle assembly. *Current biology : CB*, 17(16), pp.1373–1383.

Cai, S. et al., 2009. Kinesin-14 family proteins HSET/XCTK2 control spindle length by cross-linking and sliding microtubules. *Molecular biology of the cell*, 20(5), pp.1348–1359.

Cai, S. et al., 2010. Proper organization of microtubule minus ends is needed for midzone stability and cytokinesis. *Current biology : CB*, 20(9), pp.880–885.

Carazo-Salas, R.E. et al., 1999. Generation of GTP-bound Ran by RCC1 is required for chromatin-induced mitotic spindle formation. *Nature*, 400(6740), pp.178–181.

Chabin-Brion, K. et al., 2001. The Golgi complex is a microtubule-organizing organelle. *Molecular biology of the cell*, 12(7), pp.2047–2060.

Cheeseman, I.M. & Desai, A., 2008. Molecular architecture of the kinetochore-microtubule interface. *Nature reviews Molecular cell biology*, 9(1), pp.33–46.

Cho, C. & Vale, R.D., 2012. The mechanism of dynein motility: insight from crystal structures of the motor domain. *Biochimica et biophysica acta*, 1823(1), pp.182–191.

Chrétien, D., Fuller, S.D. & Karsenti, E., 1995. Structure of growing microtubule ends: two-dimensional sheets close into tubes at variable rates. *The Journal of cell biology*, 129(5), pp.1311–1328.

Cooper GM. The Cell: A Molecular Approach. 2nd edition. Sunderland, MA: Sinauer Associates; 2000.

Cunha-Ferreira, I., Bento, I. & Bettencourt-Dias, M., 2009. From zero to many: control of centriole number in development and disease. *Traffic*, 10(5), pp.482–498.

DeLuca, J. et al., 2002. hNuf2 inhibition blocks stable kinetochore-microtubule attachment and induces mitotic cell death in HeLa cells. *The Journal of cell biology*, 159(4), pp.549–555.

DeLuca, J.G. & Musacchio, A., 2012. Structural organization of the kinetochore-microtubule interface. *Curr Opin Cell Biol*, 24(1), pp.48–56.

Desai, A. & Mitchison, T.J., 1997. Microtubule polymerization dynamics. *Annu Rev Cell Dev Biol*, 13, pp.83–117.

Desai, A. & Mitchison, T.J., 1998. Tubulin and FtsZ structures: functional and therapeutic implications. *BioEssays : news and reviews in molecular, cellular and developmental biology*, 20(7), pp.523–527.

Downing, K.H. & Nogales, E., 1998. Tubulin structure: insights into microtubule properties and functions. *Curr Opin Struct Biol*, 8(6), pp.785–791.

Drechsel, D.N. et al., 1992. Modulation of the dynamic instability of tubulin assembly by the microtubule-associated protein tau. *Molecular biology of the cell*, 3(10), pp.1141–1154.

Duncan, T. & Wakefield, J.G., 2011. 50 ways to build a spindle: the complexity of microtubule generation during mitosis. *Chromosome research : an international journal on the molecular, supramolecular and evolutionary aspects of chromosome biology*, pp.1–13.

Dutcher, S.K., 2003. Long-lost relatives reappear: identification of new members of the tubulin superfamily. *Current opinion in microbiology*, 6(6), pp.634–640.

Ehrhardt, D. & Shaw, S., 2006. Microtubule dynamics and organization in the plant cortical array. *Annu Rev Plant Biol*, 57, pp.859–875.

Faulkner, N.E. et al., 2000. A role for the lissencephaly gene LIS1 in mitosis and cytoplasmic dynein function. *Nature cell biology*, 2(11), pp.784–791.

Ferenz, N.P., Gable, A. & Wadsworth, P., 2010. Mitotic functions of kinesin-5. *Semin Cell Dev Biol*, 21(3), pp.255–259.

Firestone, A.J. et al., 2012. Small-molecule inhibitors of the AAA+ ATPase motor cytoplasmic dynein. *Nature*, 484(7392), pp.125–129.

Foley, E.A. & Kapoor, T.M., 2013. Microtubule attachment and spindle assembly checkpoint signalling at the kinetochore. *Nature reviews Molecular cell biology*, 14(1), pp.25–37.

Fong, K.W. et al., 2008. CDK5RAP2 Is a Pericentriolar Protein That Functions in Centrosomal Attachment of the {gamma}-Tubulin Ring Complex. *Molecular biology of the cell*, 19(1), pp.115–125.

Fu, J. & Glover, D.M., 2012. Structured illumination of the interface between centriole and peri-centriolar material. *Open Biol*, 2(8), p.120104.

Ganem, N.J., Upton, K. & Compton, D.A., 2005. Efficient Mitosis in Human Cells Lacking Poleward Microtubule Flux. *Current Biology*, 15(20), pp.1827–1832.

Gorbsky, G.J., Chen, R.H. & Murray, A.W., 1998. Microinjection of antibody to

Mad2 protein into mammalian cells in mitosis induces premature anaphase. *The Journal of cell biology*, 141(5), pp.1193–1205.

Goshima, G. et al., 2008. Augmin: a protein complex required for centrosome-independent microtubule generation within the spindle. *The Journal of cell biology*, 181(3), pp.421–429.

Green, R.A., Paluch, E. & Oegema, K., 2012. Cytokinesis in animal cells. *Annu Rev Cell Dev Biol*, 28, pp.29–58.

Groen, A.C. et al., 2009. Functional overlap of microtubule assembly factors in chromatin-promoted spindle assembly. *Molecular biology of the cell*, 20(11), pp.2766–2773.

Gruss, O. et al., 2001. Ran induces spindle assembly by reversing the inhibitory effect of importin alpha on TPX2 activity. *Cell*, 104(1), pp.83–93.

Guerrero, A.A., Martínez-A, C. & van Wely, K.H., 2010. Merotelic attachments and non-homologous end joining are the basis of chromosomal instability. *Cell Div*, 5, p.13.

Guillet, V. et al., 2011. Crystal structure of γ-tubulin complex protein GCP4 provides insight into microtubule nucleation. *Nature structural & molecular biology*.

Gunawardane, R., Martin, O. & Zheng, Y., 2003. Characterization of a new gammaTuRC subunit with WD repeats. *Molecular biology of the cell*, 14(3), pp.1017–1026.

Hallen, M.A. et al., 2008. Fluorescence recovery kinetic analysis of gamma-tubulin binding to the mitotic spindle. *Biophys J*, 95(6), pp.3048–3058.

Haren, L. et al., 2006. NEDD1-dependent recruitment of the gamma-tubulin ring complex to the centrosome is necessary for centriole duplication and spindle assembly. *The Journal of cell biology*, 172(4), pp.505–515.

Haren, L. et al., 2009. NuMA is required for proper spindle assembly and chromosome alignment in prometaphase. *BMC Res Notes*, 2, p.64.

Hayward, D. et al., 2014. Synergy between Multiple Microtubule-Generating Pathways Confers Robustness to Centrosome-Driven Mitotic Spindle Formation. *Developmental Cell*, 28(1), pp.81–93.

Heald, R. et al., 1996. Self-organization of microtubules into bipolar spindles around artificial chromosomes in Xenopus egg extracts. *Nature*, 382(6590), pp.420–425.

Heald, R. & Walczak C. The Kinetochore:From Molecular Discoveries to Cancer Therapy. chapter 8. De Wulf P. & Earnshaw W.; 2008.

Hendrickson, T.W. et al., 2001. Conditional mutations in gamma-tubulin reveal its involvement in chromosome segregation and cytokinesis. *Molecular biology of the cell*, 12(8), pp.2469–2481.

Horio, T. & Oakley, B.R., 1994. Human gamma-tubulin functions in fission yeast. *The Journal of cell biology*, 126(6), pp.1465–1473.

Howell, B. et al., 1999. Dissociation of the tubulin-sequestering and microtubule catastrophe-promoting activities of oncoprotein 18/stathmin. *Molecular biology of the cell*, 10(1), pp.105–118.

Hunter, A.W. et al., 2003. The kinesin-related protein MCAK is a microtubule depolymerase that forms an ATP-hydrolyzing complex at microtubule ends. *Mol Cell*, 11(2), pp.445–457.

Hutchins, J.R.A. et al., 2010. Systematic analysis of human protein complexes identifies chromosome segregation proteins. *Science (New York, NY)*, 328(5978), pp.593–599.

Janke, C. & Bulinski, J.C., 2011. Post-translational regulation of the microtubule cytoskeleton: mechanisms and functions. *Nature reviews Molecular cell biology*, 12(12), pp.773–786.

Janski, N. et al., 2012. The GCP3-Interacting Proteins GIP1 and GIP2 Are Required for gamma-Tubulin Complex Protein Localization, Spindle Integrity, and Chromosomal Stability. *THE PLANT CELL ONLINE*.

Jaspersen, S.L. & Winey, M., 2004. The budding yeast spindle pole body: structure, duplication, and function. *Annu Rev Cell Dev Biol*, 20, pp.1–28.

Johmura, Y. et al., 2011. Regulation of microtubule-based microtubule nucleation by mammalian polo-like kinase 1. *Proceedings of the National Academy of Sciences of the United States of America*, 108(28), pp.11446–11451.

Kaláb, P. et al., 2006. Analysis of a RanGTP-regulated gradient in mitotic somatic cells. *Nature*, 440(7084), pp.697–701.

Kaláb, P., Weis, K. & Heald, R., 2002. Visualization of a Ran-GTP gradient in interphase and mitotic Xenopus egg extracts. *Science (New York, NY)*, 295(5564), pp.2452–2456.

Kamasaki, T. et al., 2013. Augmin-dependent microtubule nucleation at microtubule walls in the spindle. *The Journal of cell biology*, 102(1), p.263.

Kapitein, L.C. et al., 2005. The bipolar mitotic kinesin Eg5 moves on both microtubules that it crosslinks. *Nature*, 435(7038), pp.114–118.

Khodjakov, A. & Rieder, C.L., 1999. The sudden recruitment of gamma-tubulin to the centrosome at the onset of mitosis and its dynamic exchange throughout the cell cycle, do not require microtubules. *The Journal of cell biology*, 146(3), pp.585–596.

Khodjakov, A. et al., 2000. Centrosome-independent mitotic spindle formation in vertebrates. *Current biology : CB*, 10(2), pp.59–67.

Kirschner, M. & Mitchison, T., 1986. Beyond self-assembly: from microtubules to morphogenesis. *Cell*, 45(3), pp.329–342.

Kleylein-Sohn, J. et al., 2013. Acentrosomal spindle organization renders cancer cells dependent on the kinesin HSET. *Journal of Cell Science*, 125(22), pp.5391–5402.

Knop, M. & Schiebel, E., 1998. Receptors determine the cellular localization of a gamma-tubulin complex and thereby the site of microtubule formation. *The EMBO Journal*, 17(14), pp.3952–3967.

Knop, M. & Schiebel, E., 1997. Spc98p and Spc97p of the yeast gamma-tubulin complex mediate binding to the spindle pole body via their interaction with Spc110p. *The EMBO Journal*, 16(23), pp.6985–6995.

Kollman, J.M. et al., 2011. Microtubule nucleation by γ-tubulin complexes. *Nature reviews Molecular cell biology*.

Kollman, J.M. et al., 2008. The Structure of the {gamma}-Tubulin Small Complex: Implications of Its Architecture and Flexibility for Microtubule Nucleation. *Molecular biology of the cell*, 19(1), pp.207–215.

Kotak, S., Busso, C. & Gönczy, P., 2012. Cortical dynein is critical for proper spindle positioning in human cells. *The Journal of cell biology*, 199(1), pp.97–110.

Kramer, A., Maier, B. & Bartek, J., 2011. Centrosome clustering and chromosomal (in)stability: a matter of life and death. *Mol Oncol*, 5(4), pp.324–335.

La Terra, S. et al., 2005. The de novo centriole assembly pathway in HeLa cells: cell cycle progression and centriole assembly/maturation. *The Journal of cell biology*, 168(5), pp.713–722.

Lajoie-Mazenc, I. et al., 1994. Recruitment of antigenic gamma-tubulin during mitosis in animal cells: presence of gamma-tubulin in the mitotic spindle.

Journal of Cell Science, 107 (Pt 10), pp.2825–2837.

Lawo, S.H.M.G.G.D.P.L., 2012. Sub-diffraction imaging of centrosomes reveals higher-order organizational features of pericentriolar material. *Nature cell biology*, 14.

Leask, A., Obrietan, K. & Stearns, T., 1997. Synaptically coupled central nervous system neurons lack centrosomal gamma-tubulin. *Neuroscience letters*, 229(1), pp.17–20.

Leber, B. et al., 2010. Proteins Required for Centrosome Clustering in Cancer Cells. *Science Translational Medicine*, 2(33), pp.33ra38–33ra38.

Lecland, N. et al., 2013. Establishment and mitotic characterization of new Drosophila acentriolar cell lines from DSas-4 mutant. *Biology Open*, 2(3), pp.314–323.

Löwe, J. et al., 2001. Refined structure of alpha beta-tubulin at 3.5 A resolution. *Journal of molecular biology*, 313(5), pp.1045–1057.

Lüders, J., 2012. The amorphous pericentriolar cloud takes shape. *Nature cell biology*, 14(11), pp.1126–1128.

Lüders, J., Patel, U.K. & Stearns, T., 2006. GCP-WD is a gamma-tubulin targeting factor required for centrosomal and chromatin-mediated microtubule nucleation. *Nature cell biology*, 8(2), pp.137–147.

Ma, N. et al., 2010. Poleward transport of TPX2 in the mammalian mitotic spindle requires dynein, Eg5, and microtubule flux. *Molecular biology of the cell*, 21(6), pp.979–988.

Maffini, S. et al., 2009. Motor-Independent Targeting of CLASPs to Kinetochores by CENP-E Promotes Microtubule Turnover and Poleward Flux. *Current Biology*, 19(18), pp.1566–1572.

Maia, A.R.R. et al., 2013. Modulation of Golgi-associated microtubule nucleation throughout the cell cycle. *Cytoskeleton (Hoboken, N.J.)*, 70(1), pp.32–43.

Maiato, H., Rieder, C.L. & Khodjakov, A., 2004. Kinetochore-driven formation of kinetochore fibers contributes to spindle assembly during animal mitosis. *The Journal of cell biology*, 167(5), pp.831–840.

Manning, J.A. et al., 2010. A direct interaction with NEDD1 regulates gamma-tubulin recruitment to the centrosome. *PloS one*, 5(3), p.e9618.

Margolis, R.L. & Wilson, L., 1978. Opposite end assembly and disassembly of

microtubules at steady state in vitro. *Cell*, 13(1), pp.1–8.

Maro, B., Howlett, S.K. & Webb, M., 1985. Non-spindle microtubule organizing centers in metaphase II-arrested mouse oocytes. *The Journal of cell biology*, 101(5 Pt 1), pp.1665–1672.

Mastronarde, D.N. et al., 1993. Interpolar spindle microtubules in PTK cells. *The Journal of cell biology*, 123(6 Pt 1), pp.1475–1489.

McDonald, H.B., Stewart, R.J. & Goldstein, L.S., 1990. The kinesin-like ncd protein of Drosophila is a minus end-directed microtubule motor. *Cell*, 63(6), pp.1159–1165.

Megraw, T.L., Kao, L.R. & Kaufman, T.C., 2001. Zygotic development without functional mitotic centrosomes. *Current biology : CB*, 11(2), pp.116–120.

Mennella, V. et al., 2012. Sub-diffraction-resolution fluorescence microscopy reveals a domain of the centrosome critical for pericentriolar material organization. *Nature cell biology*, 14.

Merdes, A. et al., 1996. A complex of NuMA and cytoplasmic dynein is essential for mitotic spindle assembly. *Cell*, 87(3), pp.447–458.

Meunier, S. & Vernos, I., 2012. Microtubule assembly during mitosis - from distinct origins to distinct functions? *Journal of Cell Science*, 125(Pt 12), pp.2805–2814.

Mishra, R.K. et al., 2010. The Nup107-160 complex and gamma-TuRC regulate microtubule polymerization at kinetochores. *Nature cell biology*, 12(2), pp.164–169.

Mitchison, T. & Kirschner, M., 1984. Dynamic instability of microtubule growth. *Nature*, 312(5991), pp.237–242.

Mitchison, T.J., 1993. Localization of an exchangeable GTP binding site at the plus end of microtubules. *Science (New York, NY)*, 261(5124), pp.1044–1047.

Mogensen, M., 1999. Microtubule release and capture in epithelial cells. *Biology of the cell / under the auspices of the European Cell Biology Organization*, 91(4-5), pp.331–341.

Moritz, M. et al., 2000. Structure of the gamma-tubulin ring complex: a template for microtubule nucleation. *Nature cell biology*, 2(6), pp.365–370.

Moudjou, M. et al., 1996. gamma-Tubulin in mammalian cells: the centrosomal and the cytosolic forms. *J Cell Sci*, 109 (Pt 4), pp.875–887.

Moutinho-Pereira, S. et al., 2013. Genes involved in centrosome-independent mitotic spindle assembly in Drosophila S2 cells. *Proceedings of the National Academy of Sciences of the United States of America*, 110(49), pp.19808–19813.

Moutinho-Pereira, S., Debec, A. & Maiato, H., 2009. Microtubule cytoskeleton remodeling by acentriolar microtubule-organizing centers at the entry and exit from mitosis in Drosophila somatic cells. *Molecular biology of the cell*, 20(11), pp.2796–2808.

Murata, T. et al., 2005. Microtubule-dependent microtubule nucleation based on recruitment of γ-tubulin in higher plants. *Nature cell biology*, 7(10), pp.961–968.

Musa, H. et al., 2003. Microtubule assembly in cultured myoblasts and myotubes following nocodazole induced microtubule depolymerisation. *J Muscle Res Cell Motil*, 24(4-6), pp.301–308.

Nachury, M. et al., 2001. Importin beta is a mitotic target of the small GTPase Ran in spindle assembly. *Cell*, 104(1), pp.95–106.

Nakamura, M. et al., 2012. Arabidopsis GCP3-INTERACTING PROTEIN 1/MOZART1 is an integral component of the gamma-tubulin-containing microtubule nucleating complex. *The Plant journal : for cell and molecular biology*.

Nogales, E., Wolf, S.G. & Downing, K.H., 1998. Structure of the alpha beta tubulin dimer by electron crystallography. *Nature*, 391(6663), pp.199–203.

O'Toole, E.T., Winey, M. & McIntosh, J.R., 1999. High-voltage electron tomography of spindle pole bodies and early mitotic spindles in the yeast Saccharomyces cerevisiae. *Molecular biology of the cell*, 10(6), pp.2017–2031.

Oakley, C. & Oakley, B., 1989. Identification of gamma-tubulin, a new member of the tubulin superfamily encoded by mipA gene of Aspergillus nidulans. *Nature*, 338(6217), pp.662–664.

Oegema, K. et al., 1999. Characterization of two related Drosophila gamma-tubulin complexes that differ in their ability to nucleate microtubules. *The Journal of cell biology*, 144(4), pp.721–733.

Ookata, K. et al., 1995. Cyclin B interaction with microtubule-associated protein 4 (MAP4) targets p34cdc2 kinase to microtubules and is a potential regulator of M-phase microtubule dynamics. *The Journal of cell biology*, 128(5), pp.849–862.

Petry, S. et al., 2011. Augmin promotes meiotic spindle formation and bipolarity in

Xenopus egg extracts. *Proceedings of the National Academy of Sciences of the United States of America*, 108(35), pp.14473–14478.

Petry, S. et al., 2013. Branching Microtubule Nucleation in Xenopus Egg Extracts Mediated by Augmin and TPX2. *Cell*, 152(4), pp.768–777.

Piehl, M. et al., 2004. Centrosome maturation: measurement of microtubule nucleation throughout the cell cycle by using GFP-tagged EB1. *Proc Natl Acad Sci U S A*, 101(6), pp.1584–1588.

Raaijmakers, J.A. et al., 2012. Nuclear envelope-associated dynein drives prophase centrosome separation and enables Eg5-independent bipolar spindle formation. *The EMBO Journal*, 31(21), pp.4179–4190.

Rath, O. & Kozielski, F., 2012. Kinesins and cancer. *Nature Reviews Cancer*, 12(8), pp.527–539.

Rebollo, E. et al., 2004. Contribution of noncentrosomal microtubules to spindle assembly in Drosophila spermatocytes. *PLoS Biology*, 2(1), p.E8.

Reilein, A. & Nelson, W.J., 2005. APC is a component of an organizing template for cortical microtubule networks. *Nature cell biology*, 7(5), pp.463–473.

Rice, L.M., Montabana, E.A. & Agard, D.A., 2008. The lattice as allosteric effector: structural studies of alphabeta- and gamma-tubulin clarify the role of GTP in microtubule assembly. *Proceedings of the National Academy of Sciences of the United States of America*, 105(14), pp.5378–5383.

Rios, R. et al., 2004. GMAP-210 recruits gamma-tubulin complexes to cis-Golgi membranes and is required for Golgi ribbon formation. *Cell*, 118(3), pp.323–335.

Rogers, G.C. et al., 2008. A multicomponent assembly pathway contributes to the formation of acentrosomal microtubule arrays in interphase Drosophila cells. *Molecular biology of the cell*, 19(7), pp.3163–3178.

Sampath, S.C. et al., 2004. The chromosomal passenger complex is required for chromatin-induced microtubule stabilization and spindle assembly. *Cell*, 118(2), pp.187–202.

Schuh, M. & Ellenberg, J., 2007. Self-organization of MTOCs replaces centrosome function during acentrosomal spindle assembly in live mouse oocytes. *Cell*, 130(3), pp.484–498.

Sillje, H.H. et al., 2006. HURP is a Ran-importin beta-regulated protein that stabilizes kinetochore microtubules in the vicinity of chromosomes. *Current*

biology : CB, 16(8), pp.731–742.

Sonnen, K.F. et al., 2012. 3D-structured illumination microscopy provides novel insight into architecture of human centrosomes. *Biology Open*.

Srsen, V. et al., 2009. Centrosome proteins form an insoluble perinuclear matrix during muscle cell differentiation. *BMC Cell Biol*, 10, p.28.

Starr, D.A. et al., 1998. ZW10 helps recruit dynactin and dynein to the kinetochore. *The Journal of cell biology*, 142(3), pp.763–774.

Stiess, M. et al., 2010. Axon extension occurs independently of centrosomal microtubule nucleation. *Science (New York, NY)*, 327(5966), pp.704–707.

Sumigray, K.D., Chen, H. & Lechler, T., 2011. Lis1 is essential for cortical microtubule organization and desmosome stability in the epidermis. *The Journal of cell biology*, 194(4), pp.631–642.

Szollosi, D., Calarco, P. & Donahue, R.P., 1972. Absence of centrioles in the first and second meiotic spindles of mouse oocytes. *J Cell Sci*, 11(2), pp.521–541.

Tai, C.-Y. et al., 2002. Role of dynein, dynactin, and CLIP-170 interactions in LIS1 kinetochore function. *The Journal of cell biology*, 156(6), pp.959–968.

Tassin, A.M., Maro, B. & Bornens, M., 1985. Fate of microtubule-organizing centers during myogenesis in vitro. *The Journal of cell biology*, 100(1), pp.35–46.

Teixidó-Travesa, N. et al., 2010. The gammaTuRC revisited: a comparative analysis of interphase and mitotic human gammaTuRC redefines the set of core components and identifies the novel subunit GCP8. *Molecular biology of the cell*, 21(22), pp.3963–3972.

Teixidó-Travesa, N., Roig, J. & Lüders, J., 2012. The where, when and how of microtubule nucleation - one ring to rule them all. *Journal of Cell Science*, 125(Pt 19), pp.4445–4456.

Tilney, L.G. et al., 1973. Microtubules: evidence for 13 protofilaments. *The Journal of cell biology*, 59(2 Pt 1), pp.267–275.

Torosantucci, L. et al., 2008. Localized RanGTP accumulation promotes microtubule nucleation at kinetochores in somatic mammalian cells. *Molecular biology of the cell*, 19(5), pp.1873–1882.

Tseng, B.S. et al., 2010. Dual detection of chromosomes and microtubules by the chromosomal passenger complex drives spindle assembly. *Developmental*

Cell, 18(6), pp.903–912.

Tulu, U.S. et al., 2006. Molecular requirements for kinetochore-associated microtubule formation in mammalian cells. *Current biology : CB*, 16(5), pp.536–541.

Tulu, U.S., Rusan, N.M. & Wadsworth, P., 2003. Peripheral, non-centrosome-associated microtubules contribute to spindle formation in centrosome-containing cells. *Current biology : CB*, 13(21), pp.1894–1899.

Uehara, R. & Goshima, G., 2010. Functional central spindle assembly requires de novo microtubule generation in the interchromosomal region during anaphase. *The Journal of cell biology*, 191(2), pp.259–267.

Uehara, R. et al., 2009. The augmin complex plays a critical role in spindle microtubule generation for mitotic progression and cytokinesis in human cells. *Proceedings of the National Academy of Sciences of the United States of America*, 106(17), pp.6998–7003.

Uetake, Y. & Sluder, G., 2007. Cell-cycle progression without an intact microtuble cytoskeleton. *Current biology : CB*, 17(23), pp.2081–2086.

Vallee, R.B., Tai, C. & Faulkner, N.E., 2001. LIS1: cellular function of a disease-causing gene. *Trends in cell biology*, 11(4), pp.155–160.

Vinopal, S. et al., 2012. gamma-Tubulin 2 nucleates microtubules and is downregulated in mouse early embryogenesis. *PloS one*, 7(1), p.e29919.

Wang, W.-J. et al., 2011. The conversion of centrioles to centrosomes: essential coupling of duplication with segregation. *The Journal of cell biology*, 193(4), pp.727–739.

Wiese, C. & Zheng, Y., 2000. A new function for the gamma-tubulin ring complex as a microtubule minus-end cap. *Nature cell biology*, 2(6), pp.358–364.

Wiese, C. et al., 2001. Role of importin-beta in coupling Ran to downstream targets in microtubule assembly. *Science (New York, NY)*, 291(5504), pp.653–656.

Witt, P., Ris, H. & Borisy, G., 1980. Origin of kinetochore microtubules in Chinese hamster ovary cells. *Chromosoma*, 81(3), pp.483–505.

Wittmann, T. et al., 2000. TPX2, A novel xenopus MAP involved in spindle pole organization. *The Journal of cell biology*, 149(7), pp.1405–1418.

Wollman, R. et al., 2005. Efficient chromosome capture requires a bias in the “search-and-capture” process during mitotic-spindle assembly. *Current biology*

: CB, 15(9), pp.828–832.

Wu, G. et al., 2008. Hice1, a novel microtubule-associated protein required for maintenance of spindle integrity and chromosomal stability in human cells. *Molecular and cellular biology*, 28(11), pp.3652–3662.

Xiong, Y. & Oakley, B.R., 2009. In vivo analysis of the functions of gamma-tubulin-complex proteins. *Journal of Cell Science*, 122(Pt 22), pp.4218–4227.

Zhang, D. et al., 2007. Three microtubule severing enzymes contribute to the "Pacman-flux" machinery that moves chromosomes. *The Journal of cell biology*, 177(2), pp.231–242.

Zhang, H. & Dawe, R.K., 2011. Mechanisms of plant spindle formation. *Chromosome research : an international journal on the molecular, supramolecular and evolutionary aspects of chromosome biology*, 19(3), pp.335–344.

Zheng, Y. et al., 1995. Nucleation of microtubule assembly by a gamma-tubulin-containing ring complex. *Nature*, 378(6557), pp.578–583.

Zhu, H. et al., 2008. FAM29A promotes microtubule amplification via recruitment of the NEDD1-gamma-tubulin complex to the mitotic spindle. *The Journal of cell biology*, 183(5), pp.835–848.

Zimmerman, W.C. et al., 2004. Mitosis-specific anchoring of gamma tubulin complexes by pericentrin controls spindle organization and mitotic entry. *Molecular biology of the cell*, 15(8), pp.3642–3657.